THE APPLICATION OF EXPANSION FOAM ON LIQUEFIED NATURAL GAS (LNG) TO SUPPRESS LNG VAPOR AND LNG POOL FIRE THERMAL RADIATION

A Dissertation

by

JAFFEE ARIZON SUARDIN

Submitted to the Office of Graduate Studies of
Texas A&M University
in partial fulfillment of the requirements for the degree of

DOCTOR OF PHILOSOPHY

August 2008

Major Subject: Chemical Engineering

THE APPLICATION OF EXPANSION FOAM ON LIQUEFIED NATURAL GAS (LNG) TO SUPPRESS LNG VAPOR AND LNG POOL FIRE THERMAL RADIATION

A Dissertation

by

JAFFEE ARIZON SUARDIN

Submitted to the Office of Graduate Studies of
Texas A&M University
in partial fulfillment of the requirements for the degree of

DOCTOR OF PHILOSOPHY

Approved by:

Chair of Committee,	M. Sam Mannan
Committee Members,	Mahmoud El-Halwagi
	Kenneth R. Hall
	N.K. Anand
Head of Department,	Michael Pishko

August 2008

Major Subject: Chemical Engineering

ABSTRACT

The Application of Expansion Foam on Liquefied Natural Gas (LNG) to Suppress LNG Vapor and LNG Pool Fire Thermal Radiation. (August 2008)

Jaffee Arizon Suardin, B.S., Institut Teknologi Bandung, Indonesia;

M.S., Texas A&M University

Chair of Advisory Committee: Dr. M. Sam Mannan

Liquefied Natural Gas (LNG) hazards include LNG flammable vapor dispersion and LNG pool fire thermal radiation. A large LNG pool fire emits high thermal radiation thus preventing fire fighters from approaching and extinguishing the fire. One of the strategies used in the LNG industry and recommended by federal regulation National Fire Protection Association (NFPA) 59A is to use expansion foam to suppress LNG vapors and to control LNG fire by reducing the fire size.

In its application, expansion foam effectiveness heavily depends on application rate, generator location, and LNG containment pit design. Complicated phenomena involved and previous studies have not completely filled the gaps increases the needs for LNG field experiments involving expansion foam. In addition, alternative LNG vapor dispersion and pool fire suppression methodology, Foamglas® pool fire suppression (PFS), is investigated as well.

This dissertation details the research and experiment development. Results regarding important phenomena are presented and discussed. Foamglas® PFS effectiveness is described. Recommendations for advancing current guidelines in LNG vapor dispersion and pool fire suppression methods are developed. The gaps are presented as the future work and recommendation on how to do the experiment better in the future. This will benefit LNG industries to enhance its safety system and to make LNG facilities safer.

DEDICATION

To Mama and Daddy. You told me education is the best gift for children and I think I have benefitted from it. Being separated half way around the world does not make me feel any less of the love and support you gave me.

To Anisa, for long hours, days and nights I spent studying…for each and every minute of her love, patience and support. Finally, we did it.

To Ibu and Bapak, for their support and making Anis into the woman I love; the way she was, she is, and she will be.

To Uni, Erwin, Lucille, Adjie, and Adit for all of their love, support, and encouragement.

ACKNOWLEDGMENTS

I would like to express great gratitude to my advisor and mentor, Dr. Mannan. His guidance and wise advice in both academic and personal issues has led to my degree completion and also prepared me for future challenge. His help in several life-changing events will never be forgotten.

I thank Dr. El-Halwagi, Dr. Hall, and Dr. Anand for being my committee members and helping me throughout my research. I thank Dr. Laird for being at my defense.

I would also like to thank BP Global Gas Plc for the research funding. Special appreciation goes to Robin Passmore and Benedict Ho for their personal and technical attention throughout the progress of my research. Their interest and help in advancing LNG safety knowledge are very beneficial to me as a student and for LNG industries.

I would also like to express my gratitude to Pittsburgh Corning Corporation (PCC), especially to Brandon Stambaugh and Neal Waaks for their support in expanding knowledge in alternative methods in suppressing LNG pool fires. Their attention to progress input and help in moving the experiment forward are greatly appreciated.

Much gratitude goes to Dr. Benjamin Cormier and Morshed Rana. Without them this research would have been difficult to accomplish. Thanks to Dr. Yingchun Zhang, Geunwoong Yun, and Ruifeng Qi for their hard work and support.

Thanks also to all members and staff of the Mary Kay O’Connor Process Safety Center (MKOPSC). Valerie Green, Mary Cass, and Donna Startz were very helpful in taking care of administrative matters throughout my involvement in the MKOPSC. Thanks to all the students who have been like a second family here at the MKOPSC. I hope our interaction will continue far into the future.

I greatly appreciate Kirk Richardson and the firefighter team at Brayton Fire Training Field at TEEX. Work at the fire school for so many months, including the field experiment itself, would have been impossible without the guidance, help, and teamwork from Kirk and his team. I really appreciate them.

Thanks also goes to Phani Raj, for having discussions regarding LNG pool fire and lending me radiometers that helped me obtain good LNG pool fire radiant heat data.

For others that I did not mention, I would like to thank you all.

NOMENCLATURE

C_p	=	Specific heat of LNG	(J/kg k)
D	=	LNG pool fire base diameter	(m)
E	=	Flame surface emissive power	(W/m^2)
E_∞	=	Surface emissivity	(W/m^2)
h_{0T}	=	Initial foam height	(m)
h_0	=	Foam height after drained	(m)
h_0	=	Initial height of dispersed expansion foam	(m)
h_1	=	Height of dispersed expansion foam	(m)
h_2	=	Thickness of frozen expansion foam	(m)
$\dot{h}_r$	=	Rate of height decrease	(m/s)
H_f	=	Heat of solidification of water	(J/kg)
k_m	=	Coefficient of absorptivity	(m^{-1})
L	=	Initial foam front length	(m)
L_T	=	Foam front length after drained	(m)
L	=	Flame length	(m)
$\dot{m}_w$	=	Water evaporated	(kg/m^2 s)
$\dot{m}_d$	=	Water loss due to drainage	(kg/m^2 s)
$\dot{m}_{dr}$	=	Additional water drainage due to radiation	(kg/m^2 s)
q_r	=	Heat radiation	(kW/m^2)
q	=	Heat radiation	(kW/m^2)
q	=	Total heat flux	(kW/m^2 s)
q''	=	LNG pool fire heat flux	(kW/m^2)
Q_A	=	Heat transfer from foam to vaporized gas	(J/m^2)
Q_B	=	Change in latent heat of foam layer	(J/m^2)

Q_C	=	Heat transfer from bottom side of foam to LNG	(J/m^2)
Q_D	=	Heat transfer from ambient air	(J/m^2)
Q_E	=	Heat transfer from ambient air by radiation	(J/m^2)
S	=	Foam expansion ratio	(kg/m^2 s)
S	=	Distance between object and the center of the fire	(m)
T_0	=	Initial temperature of expansion foam	(^oC)
T_f	=	Solidification point of water	(^oC)
T_l	=	Boiling point of LNG	(^oC)
t	=	Duration of temperature increase	(s)
$\Delta\overline{T}$	=	Temperature increase of vaporized gas	(^oC)
$U_0(t)$	=	Initial foam velocity	(m/s)
$\dot{\omega}$	=	Vaporization rate of LNG	(kg/m^2 s)
$\dot{v}$	=	Initial volumetric flow rate	(m^3/min)
τ_f	=	Friction shear stress	(dimensionless)
ρ	=	Expansion foam local density	(kg/m^3)
β	=	Friction parameter	(dimensionless)
σ	=	Stefan-Boltzmann constant	($J\ K^{-4}\ m^{-2}\ s^{-1}$)
τ	=	Atmospheric transmissivity	(dimensionless)
θ	=	Tilted angle	(degree)

TABLE OF CONTENTS

Page

ABSTRACT iii

DEDICATION iv

ACKNOWLEDGMENTS v

NOMENCLATURE vii

TABLE OF CONTENTS ix

LIST OF FIGURES xii

LIST OF TABLES xvi

1 INTRODUCTION: THE APPLICATION OF HIGH EXPANSION FOAM ON LNG 1

- 1.1 Introduction to LNG 1
- 1.2 High Expansion Foam Background 3
- 1.3 Research Framework 5
  - 1.3.1 Research Objectives 5
  - 1.3.2 Experiment Scope 6
- 1.4 Statement of Problem and Significance 6
- 1.5 Organization of the Dissertation 8

2 HIGH EXPANSION FOAM APPLICATION ON LNG - REVIEW 10

- 2.1 Introduction 10
- 2.2 Foam 10
- 2.3 LNG Pool Fire Characteristics 12
- 2.4 Expansion Foam System 14
- 2.5 HEX Application 16
  - 2.5.1 Applications on Non-LNG 16
  - 2.5.2 Applications on LNG 17
- 2.6 HEX Important Parameters 20
  - 2.6.1 Application Rate 21
  - 2.6.2 Expansion Foam Spreading 22
  - 2.6.3 Heat Transfer and Expansion Foam Temperature Profile 26
- 2.7 HEX Previous Study and Experiments 28
  - 2.7.1 LNG Vapor Dispersion Suppressions 28
  - 2.7.2 LNG Pool Fire Suppressions 38
  - 2.7.3 Combined Application with Dry Chemical 39

Page

2.8 Gaps from the Past 39

3 ALTERNATIVE METHOD: FOAMGLAS APPLICATION AS AN ALTERNATIVE - REVIEW 42

3.1 Introduction 42
3.2 What is Foamglas® 43
3.3 Foamglas® PFS System 44
3.4 Foamglas Application Previous Experiments 45
3.5 Important Parameters, Identified Gaps, and Future Study 47

4 EXPERIMENTAL DEVELOPMENT 48

4.1 Facilities 48
4.2 HEX Application Rate and Containment Pit Design – Test 1 to Test 4 53
4.3 Expansion Foam Temperature Profile – Test 5 to Test 7 54
4.4 Foamglas® PFS – Test 8A/B 59
4.5 Data Collection System and Equipment 65
4.5.1 Introduction 65
4.5.2 Gas Concentration Measurement 66
4.5.3 Point Gas Detectors 66
4.5.4 Portable Gas Detector 68
4.5.5 High Speed Camera 68
4.5.6 Hydrocarbon Imaging Camera(s) 69
4.5.7 Thermocouples 70
4.5.8 Radiometer(s) 71
4.5.9 Data Collection Equipment 72
4.5.10 Flow Meter 72
4.5.11 LNG Volumetric Flow Measurement 72
4.5.12 Non-cryogenic Liquid Volumetric Flow Measurement 73
4.5.13 Wind Speed Measurement 73
4.5.14 Weather Stations 74
4.5.15 Pressure Measurement 74
4.5.16 Bunker Gear(s) 76
4.5.17 Other Logistics 76

5 EXPANSION FOAM FINDINGS/RESULTS 77

5.1 Introduction – Purpose of the Study 77
5.2 HEX Application Rate and Containment Pit Effect 78
5.2.1 HEX Application Rate 80
5.2.2 Application Rate of 3.5 L/min/m^2 in the 65 m^2 Pit 81
5.2.3 Application Rate of 7 L/min/m^2 in the 65 m^2 Pit 82
5.2.4 Application Rate of 10 L/min/m^2 in the 65 m^2 Pit – Test 4A 84
5.2.5 Application Rate of 10 L/min/m^2 in the 65 m^2 Pit – Test 4B 85

Page
5.2.6 Experiment on the 45 m^2 Pit 87
5.2.7 LNG Pool Fire Characteristics on Different Types of LNG Spill Containment Pit 89
5.3 Expansion Foam 93
5.3.1 Temperature Profile 94
5.3.2 Evaporation Rate 107
5.3.3 Gas Concentration 109
5.3.4 Heat Flux 110

6 FOAMGLAS®PFS RESULTS AND FINDINGS 114

6.1 Foamglas® PFS Application on LNG Pool Fire 116
6.1.1 Foamglas Temperature Profile 116
6.1.2 Temperature Profile at Different Locations in Visible Fire 120
6.1.3 View Factor 122
6.2 Foamglas® PFS Application during LNG Vapor Dispersion 124
6.2.1 Temperature Profile with Foamglas®PFS Application 124
6.2.2 Comparison with Unmitigated Continuous Spill 129
6.2.3 Comparison with Expansion Foam 130
6.2.4 Hydrocarbon Camera 131
6.2.5 Gas Concentration 134

7 CONCLUSIONS AND RECOMMENDATIONS 139

7.1 HEX Application Rate and Containment Pit Effect 139
7.2 Expansion Foam 141
7.3 Foamglas® PFS 142
7.4 Future Works 143

REFERENCES 146

VITA 149

LIST OF FIGURES

Page

Figure 1. Energy source in the US 2
Figure 2. Fire zones 13
Figure 3. Fire characteristics 14
Figure 4. Foam tetrahedron 15
Figure 5. Foam delivery system 15
Figure 6. Foam creation 16
Figure 7. Angus Turbex Foam Generator on LNG liquid and pool fire 19
Figure 8. The HEX spreading phenomena 22
Figure 9. Foam layer exposed to heat radiation from fire 25
Figure 10. Heat transfer between HEX and LNG 27
Figure 11. Concentration reduction during HEX application 29
Figure 12. HEX experimental setup 1 31
Figure 13. Evaporation rate experiment setup 32
Figure 14. Temperature above the LNG spill before and after HEX application 33
Figure 15. HEX temperature profile experiment results 35
Figure 16. Heat transfer balance modeling system 36
Figure 17. Evaporation rate 37
Figure 18. Expansion ratio effect on LNG pool fire radiant heat 39
Figure 19. Foamglas block 44
Figure 20. Foamglas(R) PFS installation in a containment dike 45
Figure 21. Foamglas experiment results 46
Figure 22. LNG props at TEEX's Brayton Fire Training Field 48
Figure 23. Experiment layout for the 65 m^2 pit 49
Figure 24. The 65 m^2 LNG Pit 50
Figure 25. Experiment layout for the 45 m^2 pit 50
Figure 26. Side view of the pit 51

Page

Figure 27. Texas A&M University Brayton Fire Training Field 52
Figure 28. Test 5 setup 2 55
Figure 29. Test 5 - thermocouples and foam generator setup 56
Figure 30. Test 6 setup 57
Figure 31. Gas detector location on test 6 57
Figure 32. Test 7A/B experimental setup 58
Figure 33. Placement of equipment in the pit 60
Figure 34. Gas detectors and thermocouples placement 61
Figure 35. LNG pit layout and equipment placement 62
Figure 36. Foamglas® PFS experimental setup - top view 63
Figure 37. Foamglas® PFS experimental procedures 64
Figure 38. Gas detector closed and air tight chamber 67
Figure 39. High speed camera connection 69
Figure 40. Radiometers placement on portable tripod – example 71
Figure 41. Weather station 74
Figure 42. LNG pool level measurement with differential pressure transmitter 75
Figure 43. LNG pool fire control time (90% heat flux reduction) at tested application rate. 80
Figure 44. Fire control time for pool fire in the 65 m^2 pit with foam application rate of 3.5 $L/min/m^2$ 82
Figure 45. Pool fire on the 65 m^2 pit before and after foam application rate of 7 $L/min/m^2$ 83
Figure 46. Fire control time for pool fire in the 65 m^2 pit with foam application rate of 7 $L/min/m^2$ 84
Figure 47. Test 4A - fire control time for pool fire in the 65 m^2 pit with foam application rate of 10 $L/min/m^2$ 85
Figure 48. Fire at 65m^2 pit 86

Page

Figure 49. Test 4B - fire control time for pool fire in the 65 m^2 pit with foam application rate of 10 L/min/m^2 – Test 4B 87
Figure 50. Fire at 45 m^2 pit 88
Figure 51. Fire control time for pool fire in the 45 m^2 pit with foam application rate of 10 L/min/m^2 – test 1 89
Figure 52. Flame drag at below the ground pit 91
Figure 53. Fire turbulence at 45 m^2 containment pit 92
Figure 54. LNG fire phenomena in the 45 m^2 pit 93
Figure 55. Foam temperature profile during vapor dispersion on test 6 96
Figure 56. LNG vapor density reduction during expansion foam application – test 6 97
Figure 57. LNG vapor dispersion shown by hydrocarbon camera before expansion foam application during test 6 98
Figure 58. LNG vapor dispersion shown by hydrocarbon camera after expansion foam application during test 6 98
Figure 59. Temperature profile during vapor dispersion on test 7 measure by level thermocouple 1 99
Figure 60. Temperature profile during vapor dispersion on test 7 measure by level thermocouple 2 100
Figure 61. LNG pool fire with foam – test 6 101
Figure 62. Temperature profile during fire in test 6 103
Figure 63. Temperature profile during fire in test 7 104
Figure 64. Test 5 temperature profiles during fire occurrence 105
Figure 65. Temperature profile during fire on test 7 measure by level thermocouple 1 106
Figure 66. Temperature profile during fire on test 7 measure by level thermocouple 2 106
Figure 67. Pit condition after expansion foam application – test 5 107
Figure 68. Evaporation rate based on pressure differential measurement on test 7 108

Page

Figure 69. LNG evaporation rate based on heat transfer calculation 109
Figure 70. Gas concentration reduction shown during test 7 110
Figure 71. Heat flux measurement from test 7B 111
Figure 72. Heat flux at several distances before and after HEX application on test 7... 112
Figure 73. Heat flux at 35ft with its associated HEX temperature profile – test 7 113
Figure 74. FOAMGLAS® PFS block 115
Figure 75. Fire temperature profile (A), fire and thermocouple location (B), and fire illustration (C) during Foamglas® PFS application 118
Figure 76. LNG pool fire during Foamglas® PFS application 119
Figure 77. Foamglas condition after the experiment 119
Figure 78. Temperature profile : Foamglas(R) PFS and expansion foam application... 121
Figure 79. View factor 123
Figure 80. T average temperature profile at 240 seconds average 126
Figure 81. Gas movement in the pit - illustration 127
Figure 82. Expansion foam experiment 128
Figure 83. Temperature (average) comparison: Foamglas®PFS vs expansion foam 130
Figure 84. LNG vapor density reduction during expansion foam application 131
Figure 85. Un-mitigated continuous spill - hydrocarbon camera snapshots 133
Figure 86. Foamglas hydrocarbon camera snapshots 134
Figure 87. Methane cloud characteristics - no suppression and with expansion foam .. 134
Figure 88. Methane concentration profile in the 65m^2 pit during Foamglas®PFS application 136
Figure 89. Methane concentration profile inside the 65m^2 pit during Foamglas®PFS application 137
Figure 90. Foamglas maximum concentration contour at several gas detectors 138

LIST OF TABLES

Page
Table 1. Expansion foam according to NFPA 11 11
Table 2. Gas concentration reduction 29
Table 3. Shell Research Foamglas experiment results summary 46
Table 4. Experiment condition 53
Table 5. List of equipment 65
Table 6. Test summary 77
Table 7. Foam application experiment on LNG pool fire in 2005 and 2006 79
Table 8. Heat flux reduction during HEX application on test 7 112

1 INTRODUCTION: THE APPLICATION OF HIGH EXPANSION FOAM ON LNG

1.1 Introduction to LNG

Liquefied natural gas (LNG) is natural gas that is liquefied to -162.2°C. It commonly consists of 85%-98% methane with combination of nitrogen, carbon dioxide, ethane, propane, and other heavier hydrocarbon gases as the remainder. It is highly flammable within a concentration range of 4.4% and 16.4 % volume by volume concentration in the air.

As illustrated in Figure 1, the natural gas accounts for 24% of the energy consumption in US. US Department of Energy predicted that the demand and supply gap will be 21% by 2030 [1]. This demand can be met by large supplies of natural gas worldwide thus importing it is one option to fill the natural gas supply gap. In 2005, US Department of Energy stated that 2.8% of natural gas was supplied by LNG while by 2030, 16% of it will be supplied by LNG [1]. While there are currently five US LNG facilities and one in Puerto Rico that can handle LNG import, those are not enough and US needs to develop more LNG import terminals [1].

This dissertation follows the style of Journal of Hazardous Materials.

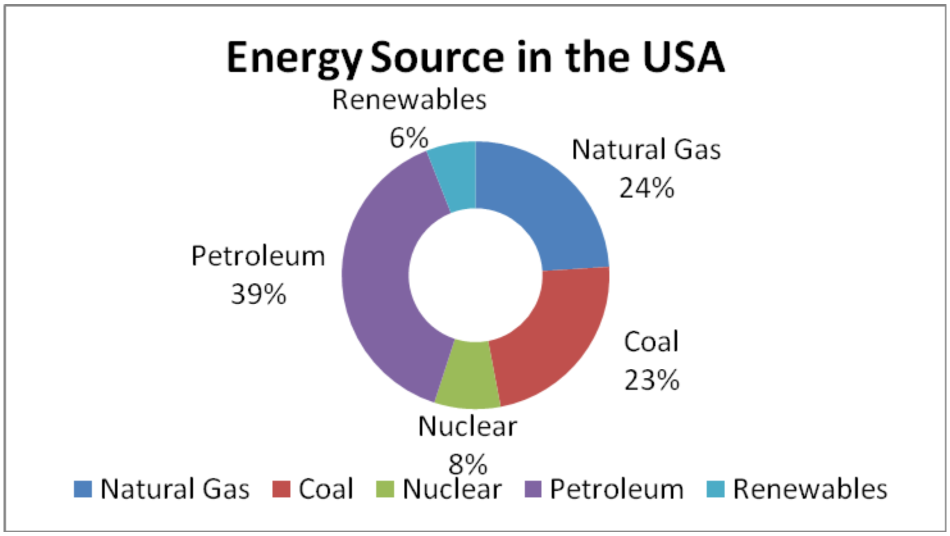

Source: [1]

Figure 1. Energy source in the US

There are several potential hazards that could arise from an LNG spill and have been identified as follows:

- Cryogenic hazards

  LNG is stored and transported at its boiling point of -162.2°C, which is a cryogenic temperature. Cryogenic hazards come from the low temperature that includes the freezing of living tissue as a result of direct contact with very cold liquid. In addition, cryogenic liquid can cause the embrittlement that leads to a failure of containment and/or structure material when in direct contact. Thus careful handling of LNG that involve human and the selection of process equipment material are very important in the LNG industries.

- Vapor cloud flash fire

  As LNG will evaporate upon releasing, the LNG vapor generated will start to mix with the surrounding air and will be dispersed downwind by and with the air. The cold vapor has density lower than air density, thus called heavier than air or dense gas. Once the LNG vapor is warm enough, it will become positively buoyant when vapor density becomes lesser than air density. When this flammable vapor meets ignition source, the vapor cloud may ignite. The flame might then travels back to the LNG pool through the vapor. This type of hazards is dangerous because of the flame will be in contact with everything along the vapor path. Human and equipments can be injured and damaged. Damage to equipment will generally be limited, since the time of exposure to the fire will be relatively short [2].

- Pool fire

  Once the vapor flash fire travels back to the LNG pool, then pool fire is formed. Compared to a vapor cloud fire, the effects are more localized, but of longer duration [2, 3].

- Rapid phase transition (flameless explosion)

  Rapid phase transition happens during LNG spill on water. Fast evaporation creates the explosion without any ignition source.

1.2 High Expansion Foam Background

Liquefied Natural Gas (LNG) has been associated with LNG vapor dispersion and LNG pool fire thermal radiation as its hazards. Based on its characteristics, LNG spill creates LNG liquid pool and LNG vapor that is able to disperse covering a wide downwind area. Between 5% and 15% in volume concentration, the vapor becomes flammable. Once it ignites, fire occurs and flashes back to the vapor source creating pool fire. Large LNG pool fire emits high thermal radiation thus preventing fire fighter from coming closer and extinguishing the fire while increasing the risk of damage and additional LNG spill from nearby equipment or storage. One of the strategies used in LNG industry and recommended by federal regulation National Fire Protection Association (NFPA) 59A is to use high expansion foam (HEX) to suppress LNG vapor dispersion and to control LNG fire by reducing the fire size and heat radiation allowing fire fighters to approach the pool fire and be able extinguish it with dry chemical [4].

In its application, HEX effectiveness heavily depends on HEX application rate, generator location, and LNG containment pit design. While theoretical study of the effects of HEX application on LNG vapor and fires is important, the complicated phenomena involved increases the needs for medium to large LNG experiment. This also leads to the fact that previous studies completed in the past have not covered and quantified all the necessary and important parameters.

NFPA 11 A.8.20.3 suggests HEX application on LNG should be established by specific test under controlled environment [5]. To inline with that, this proposed research attempts to investigate HEX application on LNG through comprehensive and novel medium scale LNG experiments. It suggests to conduct six (6) small and medium experiments and to analyze the data obtained together with 2 other previous experimental data that have never been analyzed before. The experiment covers LNG experiment with HEX in 3 different types of LNG containment pit, different HEX application rates, HEX 3-D temperature profile with and without fire occurrences, and HEX spreading on LNG pool surface. In addition, Foamglas, another alternative method in suppressing LNG vapor and thermal radiation is investigated and its effectiveness will be compared to HEX's. An attempt to match the real LNG facilities is prepared by conducting the experiments at Brayton Fire Training Field where the containment pit is specifically designed to have similar characteristics to the ones installed at LNG facilities. Additionally, commercial HEX system is utilized while all measurements are performed with research grade or modified industrial equipment.

3-D temperature profile associated with the HEX application rate, depth and spreading rate, different types of pits and methane concentration at different downwind distances and heights are studied. 3-D temperature profile correlated to fire occurrence and pool fire thermal radiation reductions are investigated. Finally, the effectiveness of Foamglas as alternative method is explored and compared with HEX's.

The proposed research is intended to provide knowledge for improving guidelines for LNG vapor dispersion and LNG pool fire thermal radiation suppression. HEX depth, HEX application time, type of pit used for LNG spill containment and HEX generator location can be effectively predicted with the assistance of novel knowledge obtained in this proposed research.

1.3 Research Framework

1.3.1 Research Objectives

High Expansion Foam Application on LNG suppress LNG vapor and pool fire thermal radiation is objected to:

1. To study the effectiveness of HEX (500:1 expansion ratio) in controlling LNG pool fire in two different LNG containment pits.
2. To validate the effectiveness the recommended HEX application rate of 10L/min/m^2 by testing it and benchmarking it with other application rate of 3.5 L/min/m^2 and 7L/min/m^2. This is also to find the feasibility of having more economic HEX application rate while still considering safety factor during the real world application.
3. To examine 3-D temperature profile in relation with LNG vapor concentration along downwind distance and LNG vapor cloud size when HEX contacts with LNG at a cryogenic temperature with medium scale LNG experiment.
4. To study the 3-D temperature profile during fire occurrence in relation with thermal radiation reduction, LNG burning rate with medium scale LNG experiment.
5. To investigate the HEX spreading behaviors on LNG pool surface in order to predict the time to fill containment pit with HEX.

Foamglas Application on LNG to suppress LNG vapor and pool fire thermal radiation is objected to:

1. To examine the effectiveness of Foamglas in suppressing LNG vapor dispersion by investigating the gas temperature profile, gas cloud size, and LNG vapor downwind concentration with medium scale experiment.
2. To confirm Foamglas ability to suppress LNG pool fire thermal radiation with medium scale experiment.
3. To benchmark the HEX effectiveness compared to alternative method, such as Foamglas.

1.3.2 Experiment Scope

The scope of this experiment includes the following:

- The experiment was designed to investigate the effectiveness Foamglas® PFS on suppressing LNG pool fire and LNG vapor dispersion of LNG spill on concrete.
- This experiment was part of a series of LNG field tests conducted by MKOPSC, thus, the data of free LNG vapor dispersion and burns were obtained from the experiments conducted the previous day.
- The findings of this experiment were based on experimental conditions, thus, any practice should be adjusted to the varying conditions.

1.4 Statement of Problem and Significance

Previous experiments and studies have provided LNG industries with very useful knowledge of HEX application on LNG. However, those studies have been focusing on methane concentration and thermal radiation reduction while the detail phenomena in the pit were observed qualitatively only, even though it is obvious that the pit is the source of the LNG vapor and pool fire and where HEX is applied [6, 7]. In addition, most of the studies were conducted back in 70-80's where the containment pit used in the experiment does not represent the different types of pit in real LNG facilities [6, 7]. Laboratory experiment studying foam (not particularly HEX) heat transfer on cryogenic liquid was also conducted with nitrogen and artificial heat producer instead of utilizing LNG and its pool fire [8]. Foam spreading phenomena on liquid has been studied in

FOAMSPEX [9] project but only non-cryogenic liquid and different types of containment pit were used. The gaps that are not covered by previous studies should be filled in order to improve LNG vapor dispersion and pool fire thermal radiation suppression.

This research is proposed to obtain novel and innovative understanding of the detail and quantitative phenomena in the pit, especially temperature changes with and without fire occurrence, associated with gas concentration, gas temperature outside the pit, and thermal radiation reduction. The behavior of HEX application on LNG at different types of pits is also investigated. One alternative method, Foamglas, is also explored to understand how it is effective and can be used in real application and to be compared with HEX.

One of the most critical factors is HEX spreading on LNG. The ability to predict HEX spreading on LNG gives valuable information as basis of HEX system design as well as fire fighting tactics. The only foam, not HEX, spreading experiment was done in 2002 in the Foamspex Projects where the foam spreading onto water, lube oil and fuel oil were studied [9]. Novel understanding and data obtained from this research will be very useful in improving the strategy and guidelines in suppressing LNG vapor and pool fire thermal radiation.

The last test was made on the late 1970's where Foamglas was tested to suppress pool fire [10]. However, the ability to suppress LNG vapor was not tested and there has been no continuation on the HEX research and application on LNG hazards.

To summarize, the problem in the HEX application on LNG is the fact that several gaps mentioned above need to be filled in order to improve strategy and guidelines in suppressing LNG vapor and pool fire thermal radiation. This research attempts to fill those gaps by performing novel small and medium experiments with the LNG, using containment pit representing real LNG facilities, and utilizing commercial/industrial type HEX system while all measurement are using research grade and state-of-the-art equipment that offers higher accuracy compared to industrial grade.

1.5 Organization of the Dissertation

This dissertation presents the application of expansion foam on suppressing both LNG vapor dispersion and LNG pool fire. In addition, an alternative suppression methodology is also investigated to ensure the safety of LNG facilities on-land.

Therefore, this dissertation is arranged to meet its objectives. Section 1 provides the introduction of this research. Information regarding LNG and its associated hazards, and expansion foam systems and applications are described in this section. In addition, the frameworks of the research are also explained and include the research objectives, scopes, statement of problem, and research significance.

Section 2 describes the literature review of expansion foam application on LNG as well as LNG pool fire characteristics. This section provides background knowledge to support the understanding of this research, especially data analysis/discussion part. The basic knowledge of expansion foam, its application on LNG vapor dispersion and pool fire, and identification of pertinent parameters that affects its performances. Moreover, previous studies and experiments are explained and compared with the pertinent parameters. This is to identify the gaps and to ensure this research is part of an attempt to fill the identified-gaps.

Section 3 explains the one alternative method for suppressing LNG pool fires, Foamglas® PFS. This provides background information to understand the reason behind its ability to become alternative method. Similar approach to Section 2 is taken in this section. The only available previous study is explained and gaps are identified.

Once the gaps for both expansion foam and Foamglas® PFS are recognized, experiment plan was developed to meet the research objectives. Section 4 illustrates the experiment development. Each of the experiment was conducted in sequence with improvement in between one experiment to another. Equipment and sensors played important roles in this research. Thus, all equipments, data acquisition system, and its setup are illustrated in Section 4.

Section 5 discusses the experiment results related to the expansion foam while Section 6 discusses the Foamglas® PFS experimental results. The discussion is arranged according to the research objectives.

This dissertation is completed by Section 7 and Section 8, where all conclusions, limitation, and recommendations, and future researches are presented.

2 HIGH EXPANSION FOAM APPLICATION ON LNG - REVIEW*

2.1 Introduction

As mentioned in the previous section, generally, incidental LNG spill releases LNG at its boiling point which receives energy from the surrounding to create LNG a flammable vapor cloud. Once the vapor is ignited, LNG pool fire is formed. Due to the rising demand of LNG, especially in the US, the quest to find effective methodology in suppressing both LNG vapor dispersion and pool fire has never been stopped. Several previous researches have been considering high expansion foam (HEX) with expansion ratio of 500:1 as one effective methodology in suppressing both LNG vapor dispersion and LNG pool fire. This section is to describe the HEX suppression system, previous researches, important parameters, and how to move forward and fill the current knowledge gap.

2.2 Foam

There are several important foam terminologies that are commonly used when dealing with foam, which include [7, 11]:

- Foam concentrate, which is the concentrated liquid foaming agent received from the manufacturer. Several types of foam concentrate include [11]:
    - Regular protein foam
    - Fluoroprotein foam
    - Film forming fluoroprotein foam
    - Aqueous film forming foam
    - Alcohol resistant aqueous film forming foams (AR-AFFF)
    - Vapor mitigating foam

---

*Reprinted with permission from "*Liquefied Natural Gas: New Research: Development of Design and Safety Specifications for LNG Facilities Based on Experimental and Theoretical Research*", by Cormier, B., J. Suardin, M. Rana, Y. Zhang, M.S. Mannan., Nova Science Publishers Inc, Hauppauge NY. Copyright by Nova Science Publishers Inc. Accepted.

  - Emulsifiers
  - HEX

- Foam solution, which represents the mixture of water and foam liquid concentrate in a proper mixing ratio.
- Foam expansion ratio, which is the ratio of the expanded bubble volume to the foam solution volume. Expansion ratio depends largely on the type of foam concentrate used, proportioning of water and foam concentrate, foam concentrate quality (how much foaming chemical contained), and aeration method. Foam concentrates can be categorized into 3 types: low-expansion, medium-expansion, and high expansion. National Fire Protection Association (NFPA) 11 describes these types as shown in Table 1. The difference between these types of expansion foam is the final product, which depends mainly on the aeration process. HEX was firstly developed for coal mining fire [12]. This type of expansion foam is usually proportioned at 1% to 2 %.

Table 1. Expansion foam according to NFPA 11

Source: adapted from [11]

Expansion foam types	**Expansion ratio (air/solution ratio)**
Low	20 : 1
Medium	20 : 1 to 200 : 1
High	200 : 1 to 1,000 : 1

- Foam drainage, which refers to the quality and stability of expansion foam during its application. It represents the time required for the 25% of the expansion foam to breakdown into liquid solution. It is also commonly called quarter-drain time, 25-percent drainage time, or quarter life. Longer quarter-drain time corresponds to the foam capability to hold water and provide insulation for a longer period of time before the water releases. Fuel temperature, radiant heat from fire, size of flame front, ambient temperature, and wind play important roles in the drainage process.

- Application rate or foam discharge rate per unit area which refers to expanded foam volumetric flow rate per LNG surface area, e.g. Liter/min m^2 [5].

Foam concentrate in its liquid form or vapor might pose minimal risk to the emergency responder [11]. It can be irritating to the skin and harmful when ingested or swallowed, thus material safety data sheet (MSDS) should be consulted before using particular foam concentrate. Fred et al. [11] described that when dealing with environmental impact, the main issue is the biodegradability after foam is used. This determine by the rate of foam broken down or degraded or dissolved by environmental bacteria and how much oxygen involved in the degradation process. Less oxygen required in the degradation process is preferred due to the fact that the fish and other habitat in the water have to compete in order to obtain oxygen.

2.3 LNG Pool Fire Characteristics

One of the LNG hazards is LNG pool fires. The fire is formed on the top of the LNG pool, as shown in Figure 2, and continue to exists until the fuel from the LNG pool below are all burnt away. McCaffrey, as explained by Raj [13], separates pool fire into three different zones. The first zone, vapor rich zone, is where the LNG vapor is at maximum amount from boiling liquid LNG pool. Unburned LNG vapor in the first zone, due to the lack of oxygen, will move upward and create the second zone, which is where the flame is still anchored to the flame base and flame pulsating exists. The pulsating is also caused by the entrained air and large eddies from the atmosphere. The third zone is the where the rest of unburned LNG vapor moves. Depending on the amount oxygen available, the pulsating will occur and can be seen as peeled-off blobs of fuel burn in irregular clumps [13].

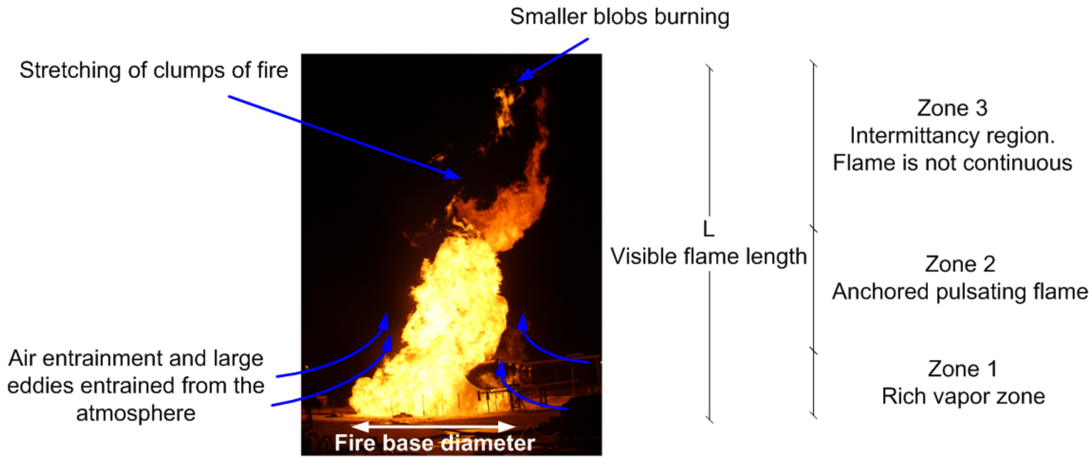

Source: modified from Raj [13]

Figure 2. Fire zones

LNG pool fire can be represented as the circular cylindrical shape with fire diameter is equal to the base diameter, as suggested in solid flame model [14]. There are two effects of wind on LNG pool fire, flame tilt and flame drag. Figure 3 illustrates the LNG pool fire at 65m^2 concrete pit tilted by the wind speed of 2.2 m/s. The length of the flame is the length of the fire measured from fire base to the last visible top part.

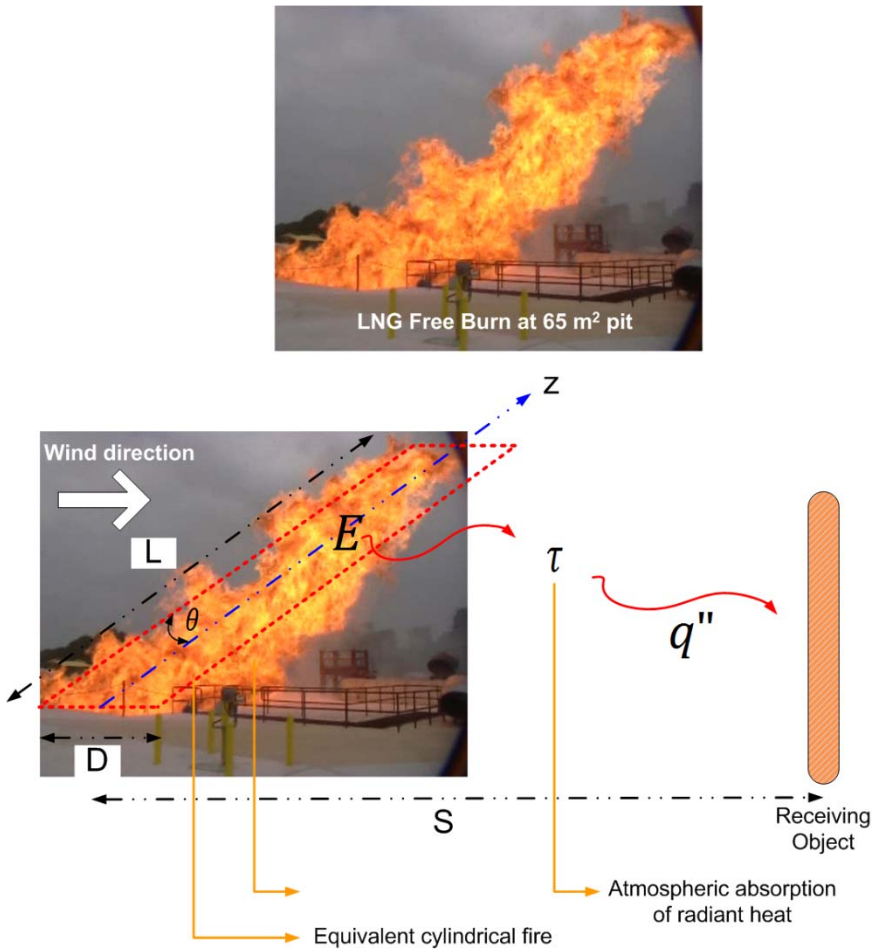

Source: Modified from Raj [13]

Figure 3. Fire characteristics

2.4 Expansion Foam System

Foam development has to follow foam tetrahedron, as illustrated in Figure 4. Water, foam concentrate, air and mechanical agitation must be available in a proportional ratio. Otherwise, no foam or low quality foam will be produced. Foam delivery system consists of four primary elements, water, foam concentrate, proportioner, and delivery device, as demonstrated in Figure 5.

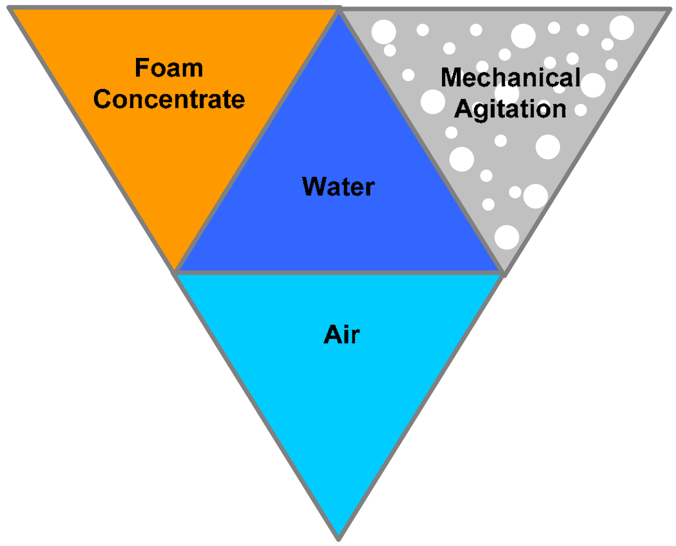

adapted from [11] with permission from Principles of Foam Fire Fighting/IFSTA

Figure 4. Foam tetrahedron

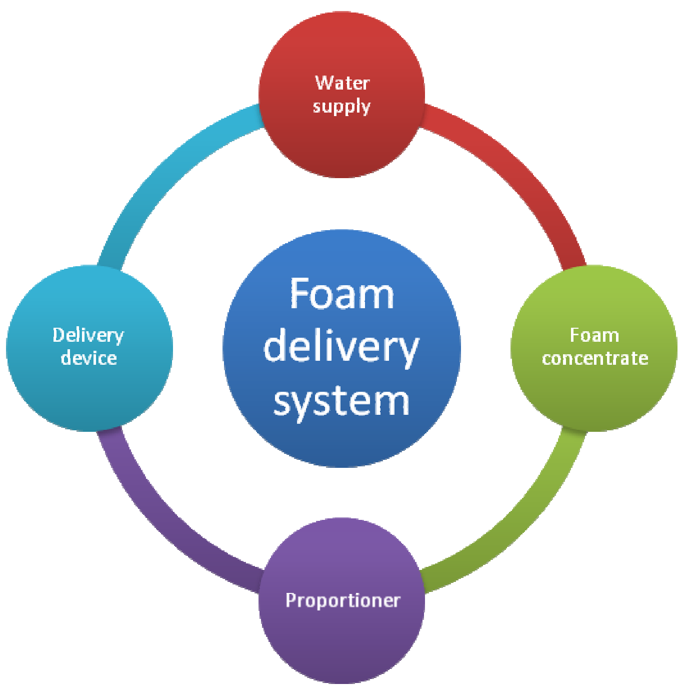

adapted from [11] with permission from Principles of Foam Fire Fighting/IFSTA

Figure 5. Foam delivery system

The water generally comes from pressurized water from a water pump. The proportioner helps mixing the foam concentrate with water in a proper ratio. The delivery device for HEX is a mechanical blower [11]. The foam solution is sprayed by nozzle in a fine spray into the mechanical blower which has a screen or a series of screen that breaks up the foam and mixes it with air. This creates foam with high content of air, as illustrated in Figure 6.

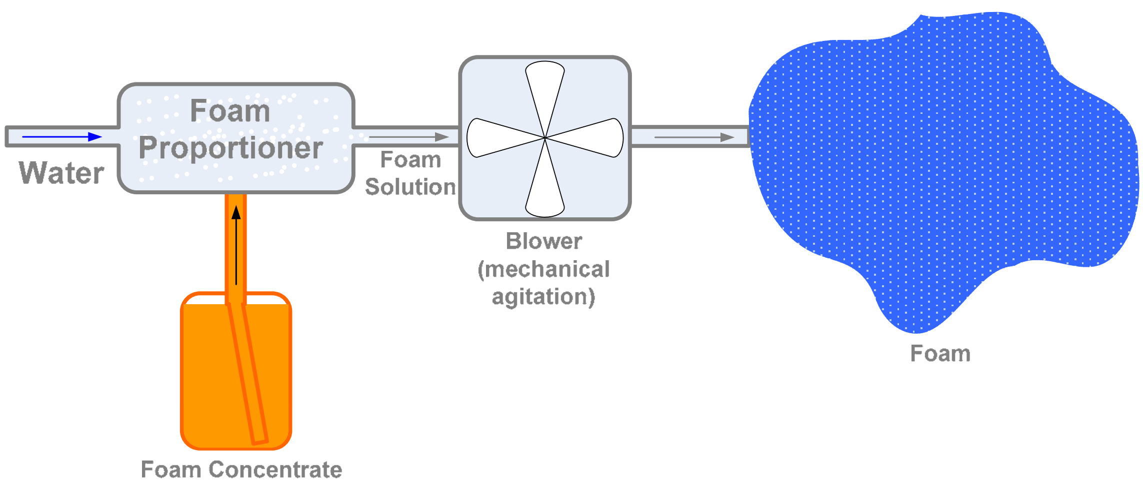

adapted from [11] with permission Principles of Foam Fire Fighting/IFSTA

Figure 6. Foam creation

2.5 HEX Application

2.5.1 Applications on Non-LNG

HEX applications for non-LNG include [11, 12]:

- Covered area such as basement compartment, coal mines, shipboard compartment, etc.
- Fixed-extinguishing system for specific industrial uses such as rolled or bulk paper storage
- Class A fire application

- Sulfur trioxide (SO_3). HEX through chemical reaction will convert SO_3 vapors into less hazardous sulfuric acid mists (H_2SO_4).
- Fire extinguishment where extinguishment is important and minimal runoff is preferable. Examples include pesticides and herbicides fires.

2.5.2 Applications on LNG

While LNG has had a good record for the last 45 years and no LNG tanker or land-based facility has experienced large accidental releases, the development of new LNG facilities have generated public concern [15]. This is due to the fact that although with the protection systems available in LNG facilities, it is important to be prepared for the consequence of the spill. While large spill is less likely to happen, the small spill could also develop into large spill if not properly handled [16].

Generally, LNG facilities are divided into four different types as follows [16]:

- Gathering and liquefaction plants. This is where the natural gas is liquefied, sold, and shipped with LNG tanker.
- Base load terminals. This is where the shipped LNG is received, stored, vaporized, and send to gas pipelines to consumer at a normal rate.
- Peak shaving plants. This is where the extra amount of the available gas (usually during warm weather) is intentionally liquefied, stored and will be used only during peak season where the normal LNG distribution rate is not sufficient. The LNG is re-vaporized and send convert extra gas to meet the future demand.
- Satellite facilities. This is similar to the peak shaving plant but without the liquefaction unit. LNG is shipped and stored in smaller quantities with LNG truck or barge. The location is usually in remote location where the peak shaving facility is not available.

Since LNG vaporizes when released to the atmosphere, it is important to limit the area of the spill to limit the spill size and reduce the associated vapor cloud on the above facilities. This may be achieved by having the following [16]:

- Diking and sub-diking surrounding the potential spill area.
- Deep sump at critical pump to trap spilled liquid.
- Insulating the dike or containment to reduce heat transfer to LNG to reduce evaporation rate.
- LNG spill limitation system to limit the flow during emergency situation.

However, the vapor cloud produced by the limited LNG pool could create a significant size of vapor cloud. Thus, there is a need to have mitigation system to help reducing LNG vapor dispersion in conjunction with the available dike or containment pit.

HEX is well known that its dispersion over LNG pool surface results in decreasing the vaporization rate by reducing the radiative and convective heat transferred to the surface of the pool. When HEXs are applied to the boiling LNG pool surface the HEX provides some of its heat to the pool while the drained water from the foam forming a frozen blanket of foam over the surface. The frozen layer of foam just above the liquid surface acts as a layer of insulation. While LNG vapor begins its travel upwards as a heavier than air gas, as the vapor move up through the foam layers, they absorb heat from the foam and become more buoyant where the vapor density is lower. If heated sufficiently the LNG vapors become less dense than air and tend to disperse upwards thereby reducing the concentration of vapors downwind of the spill. These phenomena are illustrated in Figure 7.

There are three ways as how HEX can be effective in suppressing LNG vapor dispersion and fire [10]:

- Reduces the radiative and convective heat input from surroundings to the LNG pool surface.

- Reduces the LNG vapor density by increasing its temperature while penetrating through HEX.
- Reduces the fire growth by lowering the oxygen concentration or flow to the burning LNG pool.

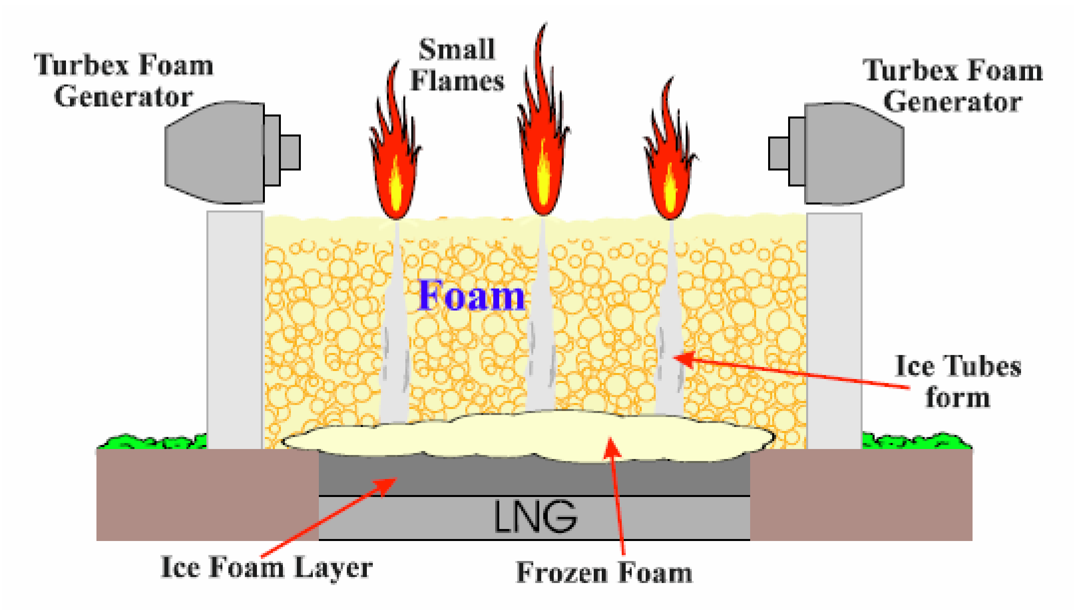

Reprinted with permission from Angus Fire

Figure 7. Angus Turbex Foam Generator on LNG liquid and pool fire (Copyright retained)

Both HEX and dry chemical can be used together to fight LNG pool fire Zuber [16] and White [17]. High expansion is objected to reduce the radiant heat to a level where the LNG pool fire is being controlled and firefighters could approach the fire. Dry chemical that is used to extinguish the controlled LNG pool fire may include sodium bicarbonate NaHCO3 (ordinary), potassium bicarbonate KHCO3, or mono-ammonium phosphate (multipurpose).

Dry chemical has several limitation, which are described by Nolan[18]:

- The fire can re-ignite even after being suppressed initially. This happens when an ignition source (such as hot surface) is still available. This can be avoided by having the right application strategy and sufficient amount of dry chemical applied.
- Dry chemical is in form of white cloud which is spread under pressure. Thus, it reduces visibility and poses breathing hazards.
- Dry chemical must be applied as soon as practicable to prevent the surrounding equipment to become too hot and be an ignition source for the re-ignition.

Based on previous researches, HEX application on LNG is summarized by Wesson et al. [19] as follows:

- HEX reduces the radiant heat of LNG pool fire thus provides adequate control.
- The optimum expansion ratio is 500:1 where it showed superior results to expansion ratio of 750:1 and 1,000:1.
- The 500:1 HEX provides heat, especially at the initial foam dispersion. Thus, LNG vapor is warmed while creating induced buoyancy at the same time. This effect will help reducing downwind ground level LNG vapor concentration.
- HEX controls the LNG pool fire and help dry chemical extinguishing the LNG pool fire.

2.6 HEX Important Parameters

HEX application is a well known methodology to control LNG vapor dispersion and LNG pool fire heat radiation. Much of experiment has been done dealing with different types of HEXs and different application rates at different types of dikes or bunds. In addition, According to National Fire Protection Association (NFPA) 11 which provides guideline for “Standard for Low-, Medium-, and high-expansion foam 2002 edition [20], some of the important points are:

- HEX is effective in controlling LNG spill test fires and reducing downwind vapor concentration for unignited LNG spill test up to $111m^2$.
- System design is dependent on each individual site analysis and discharge rate should be determined by test and include additional necessary factor. The targeted discharge rate should be able to reduce radiant heat within time limit provided in the analysis. The test conducted should provide the minimum discharge rate thus additional factor of 3 to 5 can be provided.
- Consider radiant heat exposure to the surrounding
- HEX is not normally extinguishing the fire but rather to reduce the radiant heat by blocking radiation back to the LNG surface.
- HEX is able to reduce downwind vapor ground level concentration by warming the vapor that is passing through the foam creating induced buoyancy.
- Minimum foam depth should be between 0.45 m to 1.5 m within the time established in the analysis.
- All discussions refer to the data obtained during the LNG experiment sponsored by American Gas Association (AGA).

While NFPA 11 provides some guidance in general, it is not simple and practical to apply it to the large LNG facilities as there is no adequate guidance of the design of the foam system except that experiment or test could be used as the reference. Therefore, with the purpose of finding the best guidance for HEX system design, it is necessary first to identify the important parameters in the application of HEX to suppress LNG vapor dispersion and pool fires, as described in the following section.

2.6.1 Application Rate

Application rate is generally the volumetric flow rate of the foam solution per LNG surface area. This parameter is closely related to how fast HEX could provide total blanket/insulation on top of LNG surface and arrive at the required foam depth as soon as practicably possible. While the higher application rate is desired, finding the minimum application rate is also important as well. As mentioned above, NFPA 11 suggested that the design application rate should be 3 to 5 times of the minimum application rate obtained from the test [20].

2.6.2 Expansion Foam Spreading

One of the most critical factors is foam spreading on LNG. The ability to predict foam spreading on LNG gives valuable information as basis of HEX system design as well as fire fighting tactics. The latest foam spreading experiment was done in 2002 in the Foamspex Projects where the foam spreading onto water, lube oil and fuel oil were studied [21].

The spreading of HEX over a cryogenic liquid surface is illustrated in Figure 8. To achieve an effective suppression, it is crucial for the HEX to shield the LNG pool surface and develop the required effective HEX depth as fast as possible. The friction force provided by the liquid surface, which is different from one liquid to another, is one of the factors that against the spreading. The nature of cryogenic liquid will add more complication to this phenomenon due to the formation of frozen layer in the HEX.

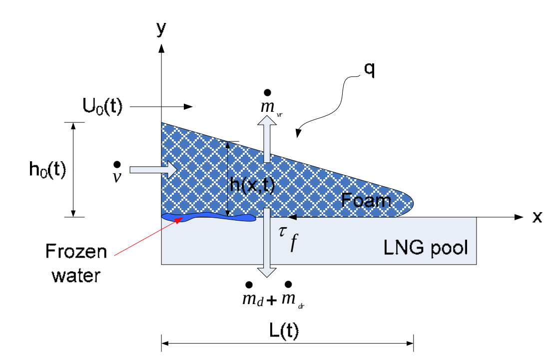

Foam spreading on LNG liquid pool surface. Foam is applied from the left with constant volume rate and the spread is opposed by a friction shear stress. The foam is exposed to heat radiation from fire causing an evaporation mass loss and a radiation-induces drainage in addition to the conventional drainage. Drained water will form ice due to cryogenic temperature of LNG liquid pool (adapted from FOAMSPEX report)

Adapted from [21] with permission from SP Technical Research Institute of Sweden

Figure 8. The HEX spreading phenomena

Since there is no HEX spreading research focuses on the cryogenic liquid, the best available simple foam (not specific to HEX) spreading modeling is analogous to the spreading of oil slicks on water [21]. The phenomena are assumed dominated by quasi steady balance between the gravity as the driving force and viscous friction as the resisting force while the inertial effects are neglected. The HEX is considered as a pure volume flow with a constant mean density where the mass transfer caused by drainage and evaporation is neglected. The current model should be broaden by including mass loss, inertia, and the bulk density in order to predict the ability of HEX in blocking the vapor to diffuse through the HEX. The viscosity of HEX is several orders of magnitudes larger than hydrocarbons [21]. Thus the velocity gradient in the HEX is smaller compared to the one in the liquid. Therefore, it assumed that the HEX layers have constant velocity.

There are two models available for generic foam, the foam spreading without and with radiant heat. The foam spreading without fire starts with the continuity equation of foam flow and can be expressed as in equations below [21].

$$\frac{\partial}{\partial t}(\rho h)+\frac{\partial}{\partial t}(\rho u h)=-G(x,t)$$

$$-G(x,t)=\dot{m}d+\dot{m}dr+\dot{m}vr$$

With ρ symbolizes the HEX local density and the function $G(x,t))$ represents the mass loss due to both drainage and evaporation as shown in equation 15. The $\dot{m}d$ denotes the mass loss due to drainage, $\dot{m}dr$ identifies the additional drainage due to the radiation and $\dot{m}vr$ stands for the mass loss due to the vaporization. The variation of bulk density including the mass loss can be taken into account by equation below:

$$h\ \left(\frac{D\rho}{Dt}\right)=h\ \left(\frac{\partial\rho}{\partial t}+u\ \ \frac{\partial\rho}{\partial x}\right)=-G(x,t)$$

This simplifies the continuation equation into equation below.

$$\frac{\partial h}{\partial t}+\frac{\partial}{\partial x}(u\,h) = 0$$

As mentioned above, the foam spreading is considered to be quasi steady balance thus the simple momentum balance can be stated as in equation below [21].

$$\tau_f = -\rho g \left(1-\frac{1}{S}\right) h \frac{\partial h}{\partial x}$$

Where S represents the foam expansion ratio, τ_f symbolizes friction force, h stands for the heights of HEX. Some of the boundary conditions used to solve the mathematical expressions are provided in equations below [21].

$$h_0\ L = 2\ \dot{V}\ t$$

$$u_0 = \beta\ \frac{h_0^2}{L}$$

$$u_0\ h_0 = \dot{V}$$

Where β is the friction parameter, $\dot{V}$ represents constant volume flow, and u_0 symbolizes the foam velocity. The final solution of this model can be expressed in the form shown in equations 22 and 23 as the following [21]:

$$h_0 = \left(\frac{4\dot{V}^2}{\beta}\right)^{1/4} t^{1/4}$$

$$L = \left(4\beta\dot{V}^2\right)^{1/4} t^{3/4}$$

The models provided above have not been compared with experimental results thus further analysis and validation should be accomplished if it is applied to the case of LNG. When the foam is spreading in flames, it is exposed to the fire radiant heat. The phenomenon is shown in Figure 9. Previous research shows that radiant heat causes water to drain and evaporate at the same time thus the reduction of foam thickness is prescribed as a function of radiant heat flux and can be assumed being independent of the rate mass loss [21]. Introduced is the term of the effective rate of decrease, $\dot{h}_r$, which is assumed constant. This is the decrease of the thickness of the HEX layer until the layer cannot block the fuel vapors and the vapor may re-ignite.

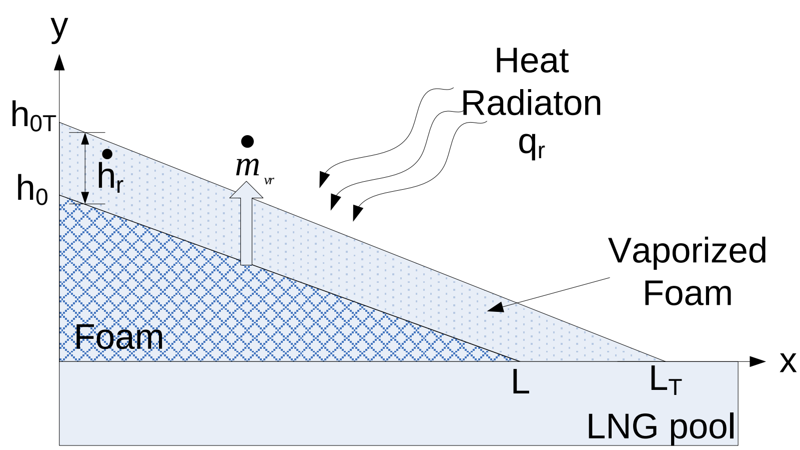

Adapted from [21] with permission from SP Technical Research Institute of Sweden

Figure 9. Foam layer exposed to heat radiation from fire

The relation between L and h_0 is represented by equation below while the expression for h_0 and L as a function of $\dot{h}_r$ are shown in equations below [21].

$$L = \frac{\beta}{\dot{V}} h_0{}^3$$

$$h_0 = h_{0T} - \frac{2}{7} h_r\, t$$

$$L = \frac{\beta}{\dot{V}} (h_{0T} - \frac{2}{7} h_r\, t)^3$$

The foam layer is growing over time until it reaches the critical time, which is where the foam growth is stopped by the fire radiant heat, and the foam length will reach the critical foam extension, given by equations below [21].

$$t_{cr} = 1.05\left[\frac{\dot{V}^2}{\beta h r^4}\right]^{1/3}$$

$$L_{cr} = 0.74\frac{\dot{V}}{h_r}$$

Based on this modeling, the maximum length covered by the foam is not influenced by the friction force but rather by volumetric flow rate and the foam consumption rate.

2.6.3 Heat Transfer and Expansion Foam Temperature Profile

The fire size depends on the LNG evaporation rate since evaporation provides the fuel of the fire. Therefore, it is necessary to study the driving force for LNG evaporation. In the past, it is qualitatively understood that there is heat exchange between foam and LNG pool and between foam, fire, and LNG pool during the occurrence of fire. A better understanding of heat transfer phenomenon will provide insight in how the HEX mitigates LNG vapor and fire. The total heat balance between surroundings, HEX, and cryogenic liquid has been studied at a small scale experiment by using nitrogen, as shown in Figure 10 [21].

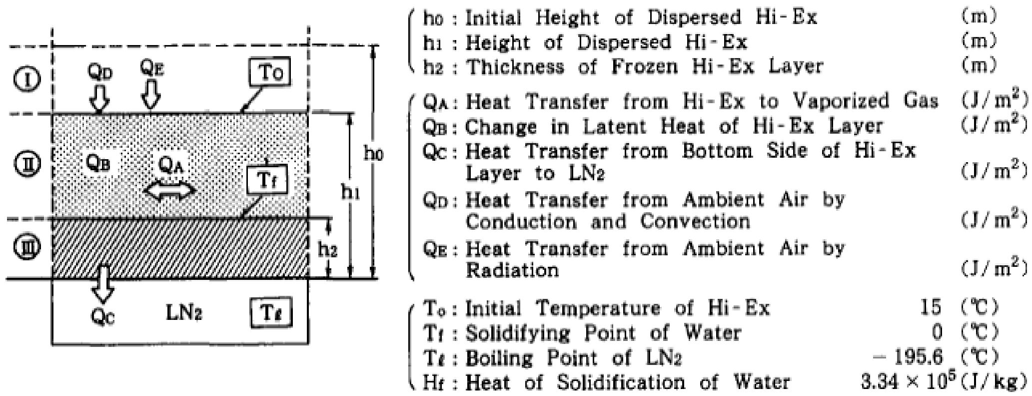

Reprinted with permission from Elsevier

Figure 10. Heat transfer between HEX and LNG

Since HEX consists of mostly water and air, the heat transfer is dominated by heat transfer phenomena of water and air and should be considered separately. Based on the diagram provided in Figure 10, the change of latent heat of HEX layer (Q_B) is shown in Equation below [8].

$$Q_B = q_1 + q_2 + q_3 + q_4 + q_5$$

Where q_1 and q_2 are the air temperature decrease in the region I and III and they can be expressed as in Equations below [8].

$$q_1 = (h_1 - h_2)\, C_{pg}\ \rho g\ (T_O - \frac{T_O + T_f}{2})$$

$$q_2 = h_2\, C_{pg}\ \rho g\ (T_O - \frac{T_O + T_f}{2}))$$

Water experiences not only temperature decrease but also undergoes a solidification process. The whole phenomena can be stated as in Equations below [8].

q_3 (water temperature decrease in the region II) :

$$q_3 = (h_1 - h_2)\frac{1}{B} C_{pl}\ \rho_l\ (T_o - \frac{T_o + T_f}{2})$$

q_4 (water temperature decrease in the region I and III):

$$q_4 = \{(h_0 - h_1) + h_2\}\frac{1}{B} C_{pl}\ \rho_g\ (T_o - \frac{T_o + T_f}{2})$$

q_5 (solidification of water in the region II and III):

$$q_5 = \{(h_0 - h_1) + h_2\}\frac{1}{B}\ \rho_l\ H_f\ (T_o - \frac{T_o + T_f}{2})$$

The total heat required for temperature change of vaporized gas Q_A can be represented by Equation below [8]:

$$Q_A = \dot{\omega} C_p\ \Delta\overline{T}\, t\ \ (J/m^2)$$

2.7 HEX Previous Study and Experiments

2.7.1 LNG Vapor Dispersion Suppressions

2.7.1.1 Gas Concentration Reduction

University Engineers in 1971, sponsored by Philadelphia Gas Works and American Gas Association [16], conducted a large series of LNG fire control and fire extinguishment tests. The experiment was performed with LNG in a 9.1 m by 12.2 m pit with one series of thermocouples were placed at 23 cm (TC-1) and 78 (TC-2) cm above the pit bottom. HEX with expansion ratio of 500:1 was dispersed to reach 0.61 m depth. The main objective of the experiment was to study the effects of HEX on the dispersion of LNG vapors and to obtain initial data on radiant heat flux from LNG fire [22].

Gas detectors to measure methane concentration were placed at 3 m and 45.7 m downwind distance from the edge of the pit. As shown in Figure 11 and summarized in

Table 2, HEX helped reducing methane concentration.

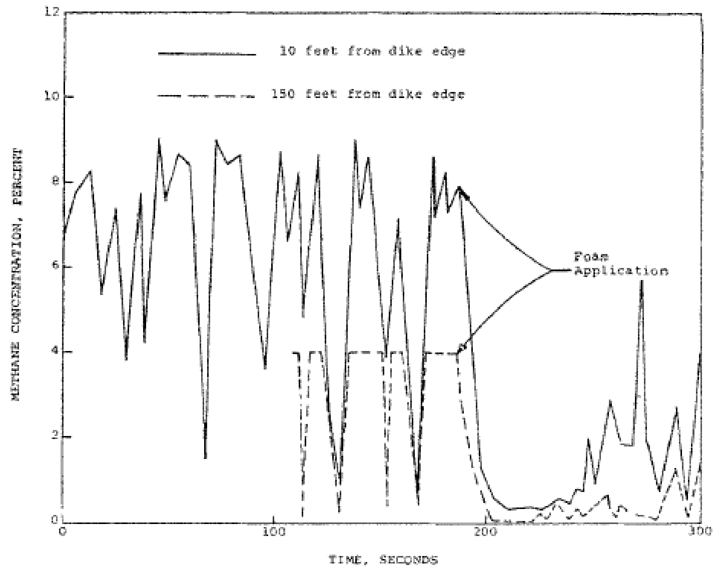

Reprinted with permission from Springer

Figure 11. Concentration reduction during HEX application

Table 2. Gas concentration reduction

Source: [16]

<table>
<tr><th rowspan="2">Gas detectors distance from edge of pit [22]</th><th colspan="2">Maximum methane concentration (%)[23]</th><th rowspan="2">Remarks</th></tr>
<tr><th>Before HEX</th><th>After HEX</th></tr>
<tr><td>3 meter</td><td>> 9</td><td>≈ 0</td><td rowspan="2">Fluctuation due to wind changes affected concentration changes but not more than 1 % [22]</td></tr>
<tr><td>45.7 meter</td><td>> 4</td><td>≈ 0</td></tr>
</table>

2.7.1.2 Foam Temperature Profile

There are several previous studies conducted in studying the characteristics of foam when in contact with cryogenic such as LNG. Although both experiment yielded in similar results, it is important to understand how the experiments were conducted and what phenomena observed and investigated.

One part of the experiment conducted by University Engineers (explained above in gas concentration section) was the temperature profile investigation. HEX with ratio of 500:1 was used. To see the HEX application affecting the LNG liquid pool, temperature before and after HEX application was observed.

Takeno et al. [8] performed the second experiment separately to test the temperature profile inside the HEX (HEX) with expansion ratio of 500:1. The experiment was specifically objected to study the following problems by using liquid nitrogen in simulating LNG [8]:

- The flow path (ice channels in the HEX) effect on the vapor temperature changes.
- Temperature profile and its variation according to time during evaporation and the raising of the gas through the HEX.
- Heat transfer and balance to determine the optimum dispersion rate.
- Evaporation rate measurement of the liquid with and without HEX application.

There were two types of experiments were conducted by Takeno [8]:

- The study of temperature increase of the vaporized gas during the application of HEX. The experiment was performed in a 3 m x 3 m x 0.5 m polyurethane-insulated vessel and used liquid nitrogen as the cryogenic liquid. Thermocouples were placed vertically on a rod to measure the liquid level reduction and temperature in the foam. Controlled-heat to evaporate the liquid was provided by electric heater. HEX with expansion ratio of 500:1 was dispersed onto the 2 m^2

area of liquid nitrogen surface up to 2 m height. There were two ways of HEX dispersion methodologies, single and re-topping dispersion. Single dispersion was that HEX was applied at the beginning until it reached 2 m height with no re-topping whenever the height was changing. The re-topping methods referred an attempt to maintain 1.5 m in height of HEX whenever HES level is decreasing to less than 1 m due to the foam drainage or break. The experimental setup is illustrated in Figure 12.

- The investigation of evaporation changes during HEX application. This was conducted in a small scale test experiment where the evaporation rate was estimated by measuring the weight of the liquid lost when HEX was applied. This setup is described in Figure 13.

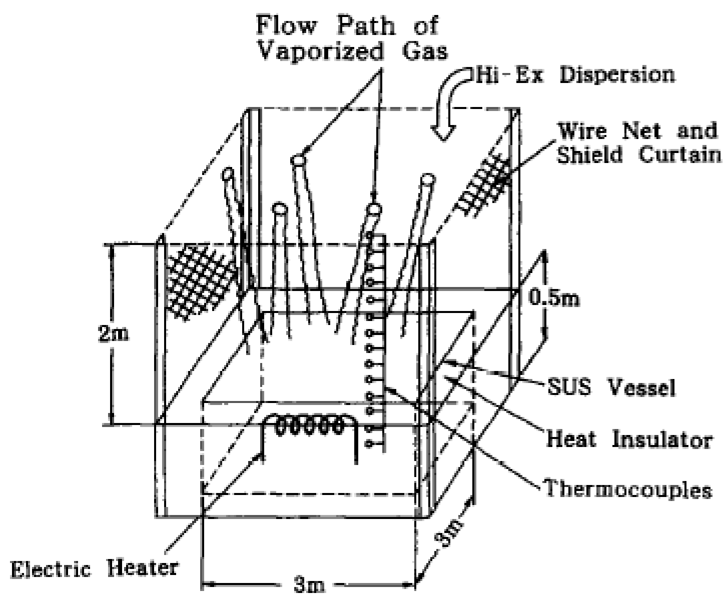

Reprinted with permission from Elsevier

Figure 12. HEX experimental setup 1

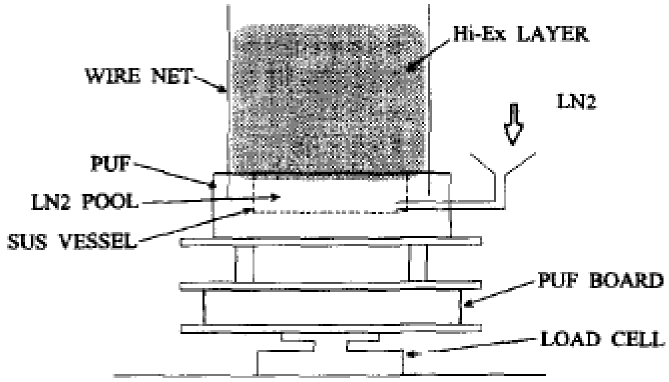

Reprinted with permission from Elsevier

Figure 13. Evaporation rate experiment setup

Main observation was focused on how the HEX affected the vaporized gas from a cryogenic pool. As explained by Zuber [16], University engineers observed that when the LNG was spilled, the TC-1 showed a temperature reduction down to -162 C while TC-2 showed a temperature range of -6.7 C to 1.1 C. Once the HEX was applied, TC-1 showed a temperature increase up to -128 C while TC-2 showed an increase up to about ambient temperature before going down to the water solidification temperature. This phenomenon is clearly illustrated in Figure 14 where temperature above the spill before and after HEX application was shown. Frozen layer and the reduction of the visible vapor cloud were also observed [16]. Several inches of frozen HEX layer occurred at the LNG pool-HEX interface, the foam above the frozen remained liquid and no uniform LNG vapor penetration was observed [23].

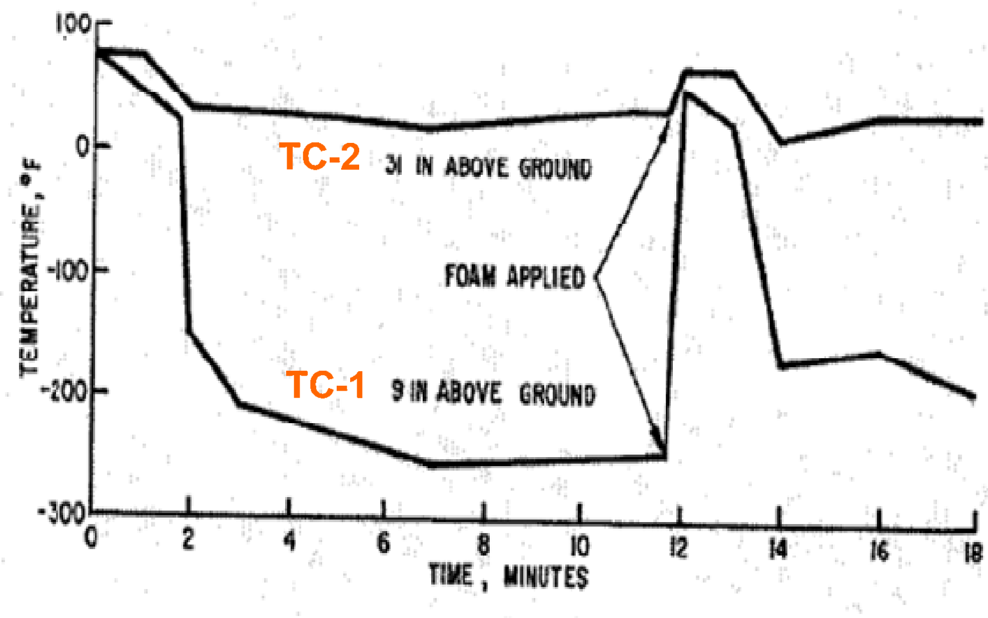

Reprinted and modified with permission from Hydrocarbon Processing

Figure 14. Temperature above the LNG spill before and after HEX application

Another experiment was conducted by University Engineers in 1972 in collaboration with the Ansul company, the Mearl corporation, Rockwood, Safety First Products Corp, Walter Kidde & Co Inc, and American Gas Association [7]. The experiment was conducted on 36.8 m^2 and 110 m^2 LNG pool area. The objectives of the experiment were to study the effect of foam blanket in LNG vapor dispersion.

Similar results was observed by Takeno [8]. It was observed that the vaporized gases were flowing out from the foam and created un-uniform holes on the top part of the HEX. After 15 minutes, this was measured that there were seven to nine holes per square meter of liquid nitrogen area. The diameters of the holes were increasing from 100-200 mm at 20 minutes after HEX dispersion to 300-400 mm at 45 minutes after HEX dispersion. Interior conditions were also investigated by Takeno [8]. HEX layer were floating on the liquid nitrogen surface and its bottom part was frozen creating honeycomb-like frozen ice layer with gas passages inside.

In addition, Takeno [8] also discovered that after 20 minutes, temperature at the first 150 mm of HEX decreased to about -80 C while temperature at 300 mm stayed at 0 C (water freezing point). Vaporized gas temperature was increased to 0-5 C at 1 minute and slightly reduced to -20 to 5 C after 20 minutes. Maintaining Hex height in the range of 1 meter to 1.5 meters did not change the phenomena. Additional Hex dispersion provided additional heat while the temperature range is maintained at -20 to 5 C. This phenomenon is shown in Figure 15.

Moreover, heat balance was also investigated by Takeno [8]. The system is illustrated in Figure 16 while the modeling procedures and calculations are shown Figure 17. The heat transfers are considered as convection of drained water (water traveling downward as a result from foam drained/broken) and thermal conduction through HEX layer. Heat balanced is achieved by the heating of vaporized gas, the cooling of both air and water in the foam, and the solidification of water (drained and in the foam). Ice formation was observed during the experiment. At 5 cm above nitrogen liquid, ice density was 300-350 kg/m^3 while at 20 cm the density was 200-250 kg/m^3 and lowered to 10-12 kg/m^3 at 50 cm. Takeno [8] estimated that 92% of the heat provided by dispersed HEX was consumed by the heating of vaporized gas moving upward while the remaining 8% was consumed by the evaporation of the liquid. In addition, the heat required to increase vaporized gas temperature was balanced with heat released by the dispersed HEX to freeze.

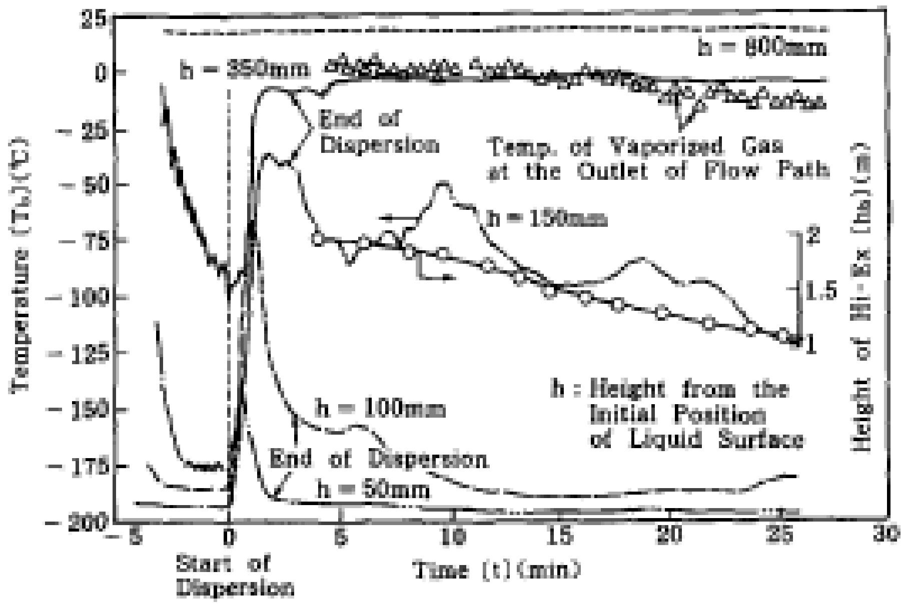

Reprinted with permission from Elsevier

Figure 15. HEX temperature profile experiment results

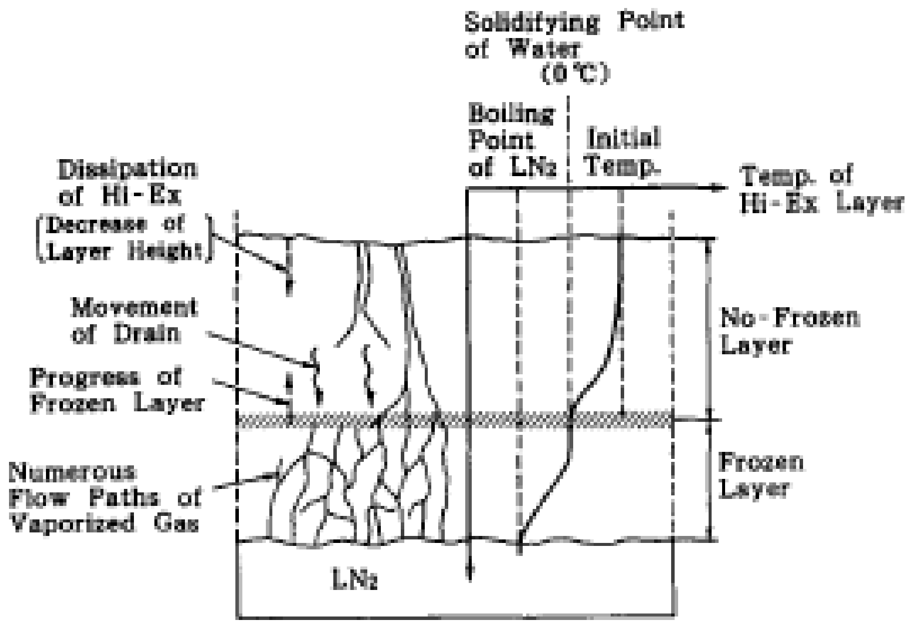

Reprinted with permission from Elsevier

Figure 16. Heat transfer balance modeling system

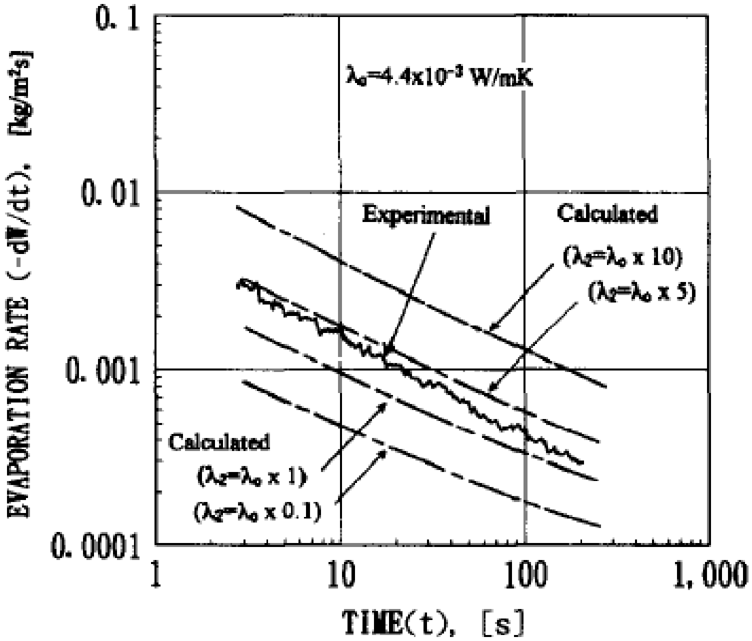

Reprinted with permission from Elsevier [8]

Figure 17. Evaporation rate

2.7.1.3 Other Tests

The first attempt to find LNG vapor dispersion and LNG pool fire suppression method was conducted at Lake Charles, La in 1960-1961 [19]. Low expansion foam with expansion ratio of 8:1 was utilized on 0.5 m by 0.5 m LNG pool fires. It was found that this type of foam was ineffective [19]. HEX with expansion ratio of 1,000:1 was reportedly effective and used in LNG facilities in Japan and France. These test found that [19]:

- High expansion ratio of 500:1 was seen to be the optimum expansion ratio.
- The foam quickly frozen and create a 2 inches of ice at the foam/LNG interface. However, the ice was still light enough to float on the LNG surface even when an additional HEX was dispersed.
- Three to six feet appeared to be a good HEX depth for controlling LNG pool fires.

- Several feet of HEX would help reducing the evaporation rate as it is blocking the heat from atmosphere from reaching the LNG pool surface.

2.7.2 LNG Pool Fire Suppressions

During the course of it dispersion, there is a possibility that the LNG vapor meets ignition source and LNG vapor will be ignited to create LNG pool fire. Water curtain and direct water sprays have been used to protect surrounding equipment and/or structures by reducing the radiant heat to tolerable zone. An estimated of 30,000 to 50,000 GPM of water would be required in major LNG spill or tank fire. The following section discusses the previous investigations of LNG pool fire suppression.

2.7.2.1 Radiant Heat Reduction

Experiment by University Engineers [22] (explained in the vapor dispersion section) was also conducting LNG fire control using high expansion test which includes:

- HEX effectiveness in suppressing LNG pool fire.
- The comparison of HEX effectiveness with water curtain.

By measuring radiant heat flux at one-diameter distance, the LNG fire test on $7m^2$ and $111m^2$ LNG fire showed that a radiant heat reduction up to 95 % was able to be provided by HEX. However, as expected, while HEX reduces a significant amount for radiant heat, HEX does not have the capability to extinguish the fire.

University Engineers [22] observed that HEX provided higher radiant heat reduction with less pressure and water flow rate compared with water curtain system. The same water system (pressure and water flow) employed to HEX system; the water curtain provided a reduction of 30 % radiant heat.

Experiments towards finding the optimum foam expansion ratio were conducted on 0.13 m and 0.26 m diameter pits with expansion ratio of 500:1, 750:1 and 1,000:1. As described in Figure 18, foam expansion ratio of 500:1 provides both higher radiant heat reduction and faster fire control time [19].

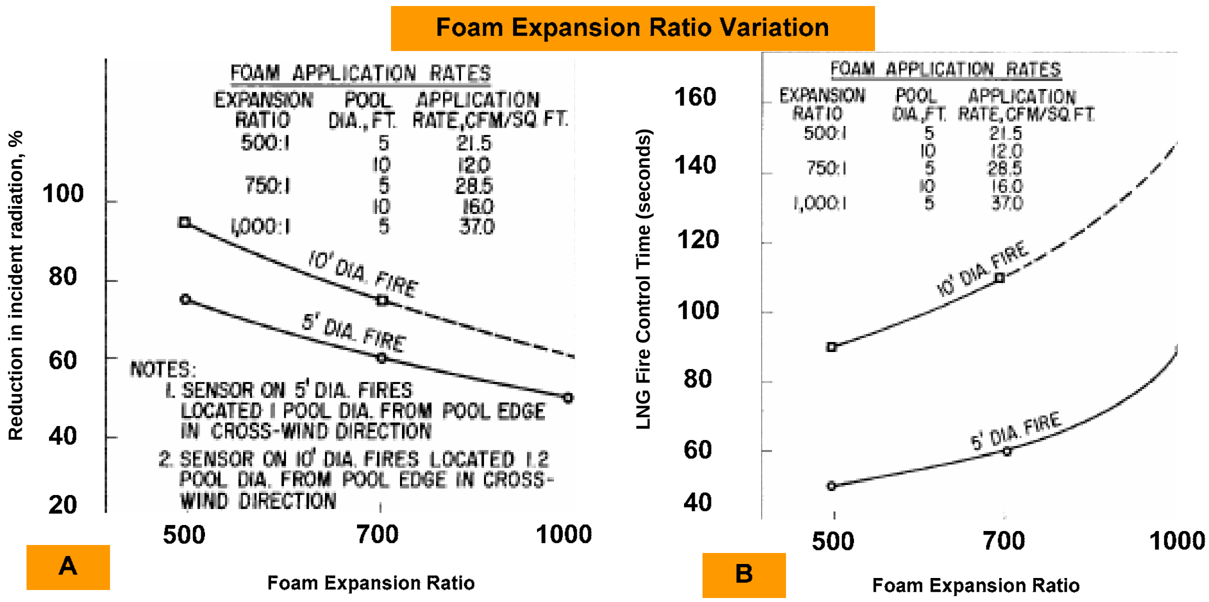

Adapted from [19]

Figure 18. Expansion ratio effect on LNG pool fire radiant heat

2.7.3 Combined Application with Dry Chemical

Following the experiment of foam expansion foam ratio mentioned above, the dry chemical was applied to study the extinguishment ability provided by dry chemical. After being controlled by HEX of 500:1, the controlled ten feet diameter pool fire was able to be extinguished using 30lb P-K dry chemical without recharging, twice.

2.8 Gaps from the Past

Previous researches have provided great fundamental knowledge on HEX application on LNG. However, while NFPA 11 and NFPA 59A are regarding those researches in developing recommendation, the regulations or the researches do not provide more detail design guidelines. Identifying knowledge gaps will help improving and/or developing HEX application guidelines. Based on the important parameters and the previous researches, knowledge gaps can be identified, as follows:

- Three dimensional temperature profile of HEX while suppressing LNG vapor dispersion and pool fire. While experiment conducted by University Engineers and Takeno studied temperature profile, there were not 3 dimensional and using liquid nitrogen to simulate LNG. Scaling up could be problem as well. Thus, medium to large LNG experiment should be conducted.
- HEX spreading on LNG surface: Foam spreading determines how fast HEX to cover the LNG surface and create the required insulation depth. While from the experiment the HEX spreads in short amount of time, the importance of spreading becomes more obvious when dealing with large release into a large containment pit or bund. Knowing the spreading and surface friction will help determining the strategy of HEX generator placement around the pit.
- Heat transfer modeling: While previous experiment by Takeno [8] shows the modeling, it has not been validated by a larger scale of LNG experiment. In addition, it did not account for foam breakdown, and water drainage movement (convection). This type of information assists in predicting the HEX depth requirement as a dependent to the LNG pool area and the spill amount on a large scale.
- Evaporation rate and burning rate measurement LNG: Evaporation rate during HEX application has been studied in small experiment using liquid nitrogen by Takeno [8]. Validation with a larger scale with LNG should be done as well.
- Shelf life of high expansion: As an active system, it is necessary to keep HEX concentrate ready when needed during incidental spill. Therefore, recognizing the shelf life time might be very helpful as part of the maintenance of the system.
- Computational Fluid Dynamics (CFD): CFD has been used in many applications including in the LNG safety area. HEX application in an open and wide application might be easier to predict compared to the application with

obstructions where there is no study or data to support the analysis. CFD could help predicting the behavior and the effectiveness of the HEX when obstructed. In addition, the evaporation rate and/or burning rate, the temperature and methane gas concentration profile when leaving HEX, and methane concentration and radiant heat reduction could be applied as an input to CFD, as part of the source modeling. The ability to simulate the LNG safety with and without mitigation system provides better understanding.

3 ALTERNATIVE METHOD: FOAMGLAS APPLICATION AS AN ALTERNATIVE - REVIEW *

3.1 Introduction

Foamglas or Cellular glass is available as scrap in many different countries. The cellular glass can be shaped into a variety of forms and sizes thus provided a wide range of application as insulation. While Foamglas® is widely applicable as a nonflammable, load-bearing insulating material, its new application on LNG pool fire is an attempt to avoid the imperfection of the conventional LNG fire fighting methods such as [10]:

a) The need for a vast dry chemical amount and smart strategy to ensure a complete extinction of large LNG fires, even after being controlled by HEX. Incomplete application or failed strategy might lead to the re-establishment of pool fire.
b) The unsuitability of the low expansion foam to fight LNG fires because of its high water content and hence the increased LNG evaporation increasing the fire size.
c) Only some kinds of foams such as HEX are suitable to control LNG fires on a larger scale. However, HEX is deteriorated by the fire and creates a necessity to replace the broken foam with new one which means continuous application is required. This type of application requires a large system to provide large amount of water and foam solution. In addition, as an active system, HEX system involves an activation system that might offer a delay during application.

---

* Reprinted with permission from "*Liquefied Natural Gas: New Research: Development of Design and Safety Specifications for LNG Facilities Based on Experimental and Theoretical Research*", by Cormier, B., J. Suardin, M. Rana, Y. Zhang, M.S. Mannan., Nova Science Publishers Inc, Hauppauge NY.

3.2 What is Foamglas®

The application of Foamglas® as an alternative method in LNG pool fire suppression has been presented by Shell research [10]. Although Foamglas® has been used as insulation in pipelines and in storage tanks (e.g. inner LNG storage tank bottom), industrial application experience has been limited in the area of suppressing LNG vapor and pool fire suppression. The following are several important characteristics of Foamglas® PFS that builds confidence in having Foamglas® PFS as a potential alternative for LNG fire mitigation [10]:

- It is “solid foam” that acts as a floating barrier to insulate a burning liquid surface.
- It is a nonflammable material.
- Its density is less than one third of LNG’s density (Foamglas® PFS’s density is 130kg/m^3), and thus floats on LNG pool surfaces when LNG spills. It remains independent of the amount of LNG pool depth, and creates constant coverage during the spill when applied correctly. Current Foamglas®PFS technology is able to reduce the density to less than 120kg/m^3 without compromising the performance.
- It has a completely closed-cell structure; as a result, no LNG liquid is absorbed during contact.
- Its softening temperature is 730 °C hence the structure is stable at flame temperature, and the effectiveness is not reduced; thus, no re-application or further coverage maintenance is required.
- It is waterproof, impervious to water vapor, acid resistant, and is easily cut to shape. It has high compressive strength, and is also dimensionally stable.

Foamglas® PFS can be easily arranged to take the shape of the spill containment pit. Generally, it is packed as block within a UV-resistant polyethylene bag to facilitate installation and protect the Foamglas® PFS from various weather conditions, as shown in Figure 19. When the LNG pool fire starts, the polyethylene cover is burned, and small cubes are distributed to cover the liquid surface. A LNG pit, bund, or trench can be fully covered by Foamglas® PFS.

3.3 Foamglas® PFS System

Currently, Foamglas® is advertised as Foamglas® PFS with PFS stands for "Pool Fire Suppression". It is basically a 125 small cubes forming a 0.2 m by 0.2 m by 0.2 cube enveloped by polyethylene ultraviolet protection shown as the green bag in Figure 19. The setup in the pit is illustrated in Figure 20. As a passive mitigation system, all Foamglas® PFS green cubes are piled and arranged in the pit before the incidental release. Supporting metal should be provided in between the pit bottom and Foamglas® PFS to provide space for rain water and any other material that could go into the containment pit. As mentioned above, since Foamglas® PFS density is only a third of LNG density, it floats on LNG surface. Once the LNG vapor is ignited, the green bag will burn at the beginning of the LNG pool fire then releasing all of the 125 cubes providing insulation in between LNG and pool fires.

Figure 19. Foamglas block

Figure 20. Foamglas(R) PFS installation in a containment dike

3.4 Foamglas Application Previous Experiments

There has been only one previous experiment with Foamglas® for suppression of LNG pool fires, which was performed by Shell Research [10]. As shown in Table 3, two experiments were conducted where radiant heat was measured for both experiments.

The more detail test results are shown in Figure 21. It is clearly seen that Foamglas® provided the good insulation from the beginning the of fire starts. Shell research [10] concluded that Foamglas is able to be used to control LNG bund fires. It provided fast and continuous protection without additional procedure or task (manual or automatic) during protection.

Table 3. Shell Research Foamglas experiment results summary

Source: [10]

Experiment	Pool Fire Size (m2)	Foamglas®	Measurement	Burning rate and Radiant Heat	
				Free burn	With Foamglas
1	1.8 m in diameter 320-mm LNG depth	200-mm layer	Evaporation rate Total radiation at 2 and 5 pool diameters crosswind and downwind of fire.	0.049 kg/m^2 s < 0.6 kW/m^2	0.59 kg/m^2 s 20-25 kW/m^2
2	6 m x 6 m clay bund 250-mm LNG depth	90-100-mm layer	Radiant heat from 27 m from the bund	9 kW/m^2	<0.5 kW/m2 (27 m) – 95% reduction

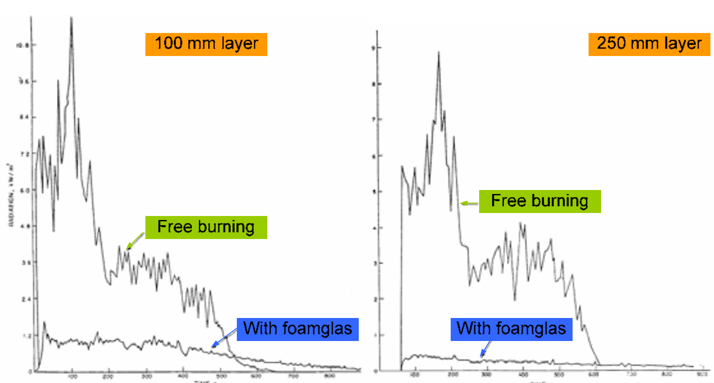

Reprinted with permission and adapted from Lev [10]

Figure 21. Foamglas experiment results

3.5 Important Parameters, Identified Gaps, and Future Study

In order to maintain its effectiveness, there are several important parameters that should be looked at, as follows:

- Radiant heat reduction, including the reduction of hazardous distance of 5 kW/m^2 (hazardous distance for human exposure)
- The number of Foamglas® PFS layer(s)
- Lifetime under LNG flame temperature
- Fire size to be controlled
- Time required for dry chemical to extinguish the Foamglas® PFS-controlled LNG pool fire

While Shell Research Inc [10] have identified the Foamglas® PFS capabilities in suppressing LNG pool fire, not all of the parameters above are identified. In addition, the MKOPSC has been collaborating with Pittsburgh Corning Corporation (Foamglas® PFS manufacturer) and Brayton Fire Training Field as part of MKOPSC/BP partnership in LNG research. The collaboration includes the experiment to assess the Foamglas® PFS effectiveness in suppressing LNG pool fires.

While current knowledge might be enough to predict Foamglas® PFS capability in suppressing LNG pool fire, some of the additional parameters should be identified to advance its application. The detail results in finding the "5 kW/m^2" distance should be experimentally identified. The variation of Foamglas® PFS layers could also be investigated along with the variation of LNG fire size to be controlled. This is to ensure that Foamglas® PFS could maintain its ability in suppressing larger-than-experiment LNG pool fire even during bad weather (rain, etc). In addition, the Foamglas® PFS lifetime under the flame temperature can be investigated as well.

4 EXPERIMENTAL DEVELOPMENT

4.1 Facilities

A Liquefied Natural Gas (LNG) emergency response training facility has been constructed as the BP Global Gas Plc's LNG emergency responses program sponsorship to Texas A&M University (TAMU) Emergency Services Training Institute (ESTI), as shown in Figure 22.

1. Small pit : 3.05 m x 3.05 m x 1.22 m
2. Large pit (65 m2 pit) : 10.06 m x 6.71 m x 1.22 m
3. L-Trench
4. Small pit : 6.71 m x 6.71 m x 2.44 m

Source: Modified from TEEX

Figure 22. LNG props at TEEX's Brayton Fire Training Field

The facility is located at Texas Engineering Extension Services (TEEX) Brayton Fire Training Field where emergency responses training and researches have been conducted. In line with that effort, BP Global Gas Plc has also joined forces with the Mary Kay O'Connor Process Safety Center of Texas A&M University to perform research on LNG safety and mitigation system. One of the main focuses is to study the expansion foam application to suppress LNG vapor and LNG pool fire heat radiation. Fire fighters at Brayton Fire Training Field (BFTF) helped and provided supervision to ensure the safety of the experiment.

Two LNG containment concrete pits (dikes) were used to simulate industrial LNG spills. The large pit is called the "65 m^2" pit, as shown in Figure 22 (number 2), Figure 23, and Figure 24 while the smaller one is the "45 m^2 pit" or "marine pit", as shown in Figure 22 (number 4) and in Figure 25. The main differences between the two types are the surface area and wall height and location. The 65 m^2 pit has four feet deep (1.2m) underground wall while the 45 m^2 pit has eight feet deep (2.4m) with four feet of the wall height above ground as illustrated in Figure 26.

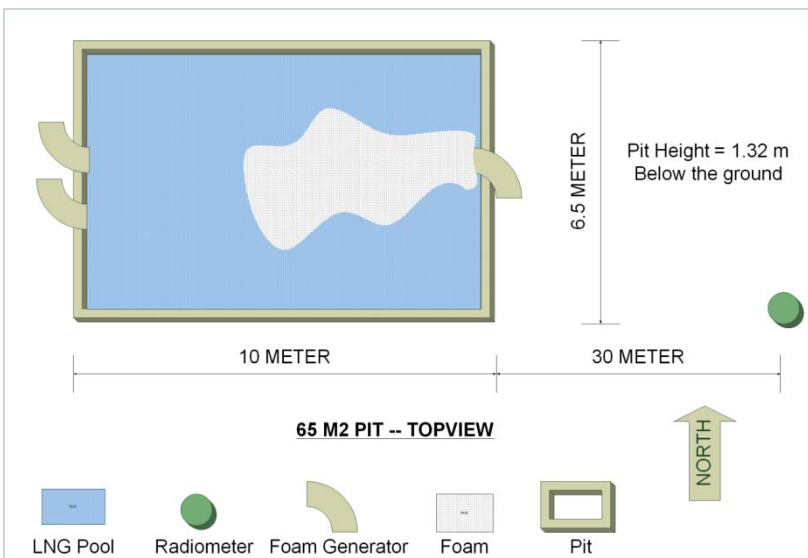

Figure 23. Experiment layout for the 65 m^2 pit

Figure 24. The 65 m^2 LNG Pit

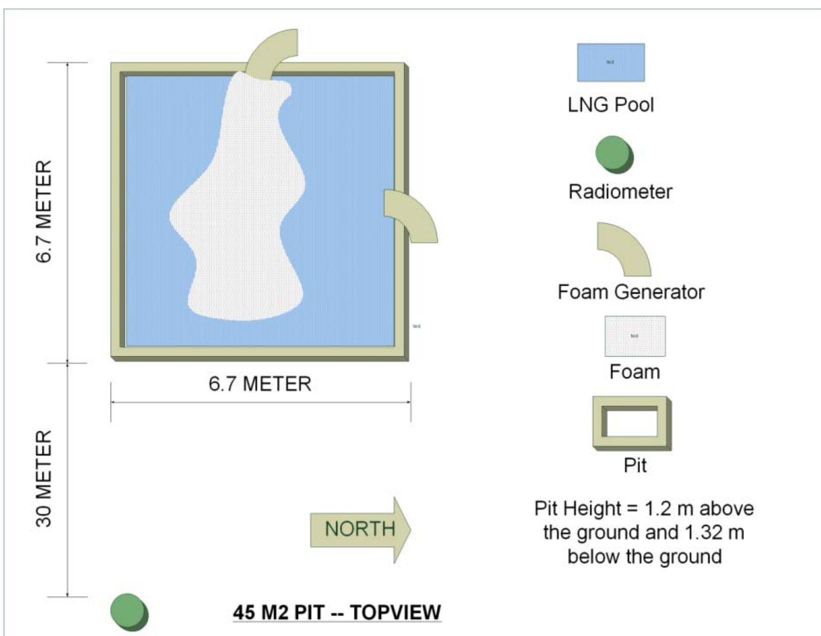

Figure 25. Experiment layout for the 45 m^2 pit

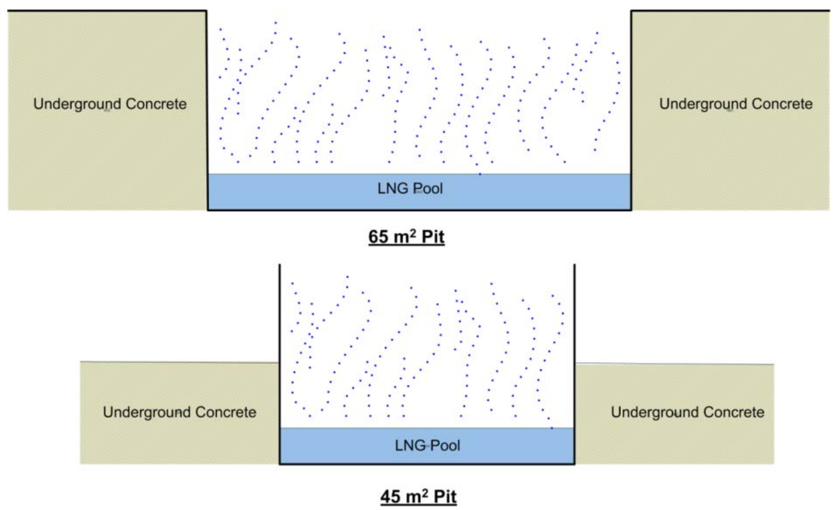

Figure 26. Side view of the pit

The experiment was performed at the Texas A&M University Brayton Fire Training Field (BFTF) located in College Station, Texas as part of the Texas A&M University System (TAMUS). One of the primary missions of the BFTF is to educate firefighters on LNG behavior. An LNG training facility covering three LNG concrete containment-pits, and one L-trench, was sponsored by BP to train firefighters around the world. The facility area is shown in Figure 27:

- An L-shaped trench used to simulate the trenches whose purpose is to divert any LNG spills into the containment pits.
- Two four-foot deep pits below the ground with areas of 3 m x 3 m (10 ft x 10 ft) and 10 m x 6.7 m (33 ft x 22 ft), called pit one and two respectively.
- A total of an 8 ft deep pit (4 ft below the ground and 4 ft above the ground) with an area of 6.7 m x 6.7 m (22 ft x 22 ft) called pit three. This pit includes a high dike wall, typical of the containment facilities used during LNG offloading.

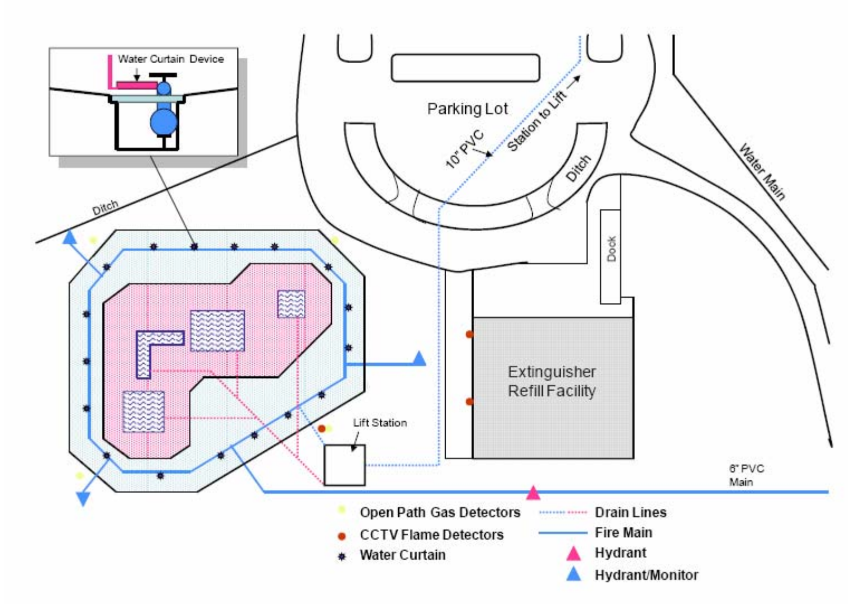

Source: Texas Engineering Extension Service (TEEX)

Figure 27. Texas A&M University Brayton Fire Training Field

To ensure safety within the facility, there are four open path detectors to detect a methane cloud when it is dispersed outside the perimeter. The location is shown in Figure 27. Around the site, a series of water curtains were installed to control the dispersion of spilled LNG. The water supply is available at four locations around the site. The cryogenic spill system is composed of a spill line that is 53 meters long and a 3 inch NPT. A tanker is connected on one side away from the site area, and the LNG volume carried by the LNG truck is approximately 41 m^3 (11,000 gallons). Liquid flow is determined by the gravity in the truck. Normal practice is to increase pressure by a few psi in order to increase the LNG discharge flow rate. The added pressure is obtained by boiling off LNG inside the tanker. The ground is sloped towards the pits to prevent any LNG from escaping offsite. More detail on the cryogenic spill system is available through MKOPSC.

The LNG spill during the experiment is controlled by the valve at the bottom of the truck. When the release is ordered, the truck opens the valve, and LNG cools the pipeline. The size of the discharge pipe is three inches in diameter and positioned at a 45 degree angle.

4.2 HEX Application Rate and Containment Pit Design – Test 1 to Test 4

Five experiments have been conducted during October 2005 and April 2006. The summary of the experiment parameters are provided in Table 4.

Table 4. Experiment condition

Test ID	**1**	**2**	**3**	**4A**	**4B**
Pit size (meter)	45	65	65	65	65
HEX Application rate (L/minutes m^2)	10	3.5	7	10	10
Radiometer location for pit edge (meter)	30	30	30	30	27
Initial LNG pool depth (meter)	0.13	NA	0.10	0.15	0.15
Average wind speed (meter/second)	3.7	NA	1.2	2.2	3.7
Air temperature (^{o}C)	15.8	NA	26.7	24.5	28.7
Relative humidity (%)	83	NA	74.8	81.3	71

There are four scenarios performed on the 65 m^2 pit in 2005 and 2006 with application rates of 3.5, 7, and 10 L/min/m^2. The 10 L/min/m^2 is the recommended foam application rate for modern facilities to give an adequate safety margin for the unexpected in the event of a real incident like rain storms or cooling water entering the containment pit which intensifies the LNG fire and makes it more difficult to control, so early control is crucial for success and the minimizing of danger to personnel and site disruption. Consequently in both years experiment with 10 L/min/m^2 were tested to ensure consistency of results. The experimental layout is shown in Figure 23.

Based on data from the 65m^2 pit a further experiment was conducted for 45 m^2 pit to determine whether pit design had an influence on control, so this was also conducted using foam application rate of 10 L/min/m^2. It was performed on April 20th 2006. The experiment layout is presented in Figure 25.

4.3 Expansion Foam Temperature Profile – Test 5 to Test 7

There are three experiments conducted in studying expansion foam temperature profile. The experiments were conducted in three separate times. In between experiment, data and experimental setup/procedures were analyzed to improve the next experiment. However, all experiments share the main experimental procedures (with modification) which were:

- Place 4ft walls around the containment to have a total of 8ft of walls during vapor dispersion experiment.
- Spill the LNG onto the concrete bottom until it reaches 6 inches of LNG and then the flow is stopped. This part is considered as the continuous spill section of the experiment. The data is recorded throughout the spill.
- Once the spill is ended, the section becomes unmitigated free spill. For several minutes, the LNG is let evaporates while the data is recorded.
- Apply expansion foam until the pit is overfilled with foam and record the data for several minutes. One data recording is finished, this part indicates the completion of LNG vapor dispersion part of the experiment and preparation of LNG pool fire experiment begins. Data acquisition is continuously recording data.

- All walls are removed from the pit and place them at safe locations. Gas detectors and cables that were not used during LNG pool fire experiment were also moved to a safe distance.
- LNG is ignited using small portable flare to create LNG pool fire.
- LNG free burn occurs for 40 seconds.
- Apply expansion foam to the fire for several minutes (it is hard to overfilled the pit).
- Extinguish the fire using dry chemical that is already prepared. This part designates the end of the experiment.

The first experiment (test 5) was conducted on October 2007. This experiment was planned to be a pre-test in order to test experimental procedures and equipment on small pit before performing the larger experiment. It was conducted on 9.3m^2 pit with expansion foam with 51 thermocouples that was attached to the metal structures as shown in Figure 28 .

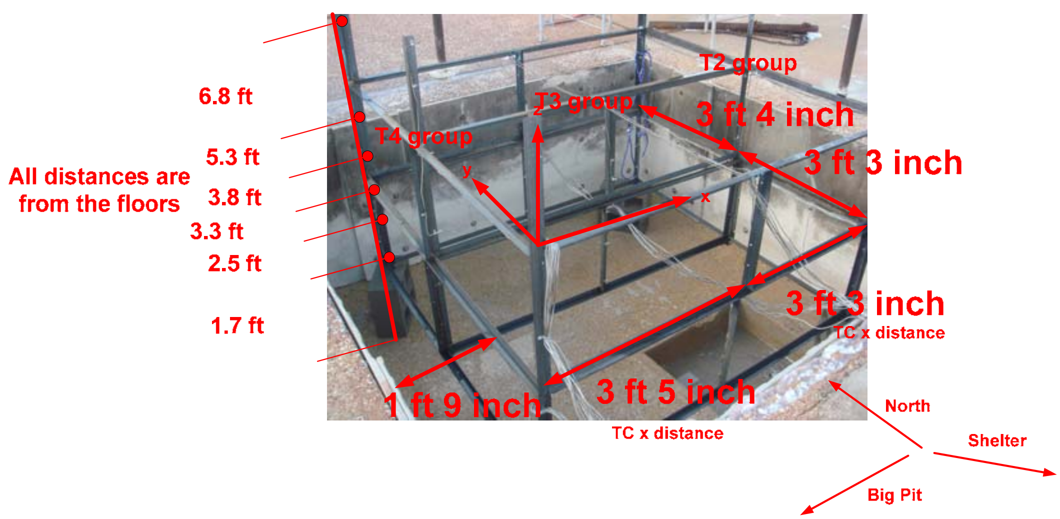

Figure 28. Test 5 setup 2

One Angus Fire turbex foam generator was used and placed 4 feet above the top part of the containment pit, as shown in Figure 29 below. Gas detectors were not used during this test thus there was no gas concentration data.

Figure 29. Test 5 - thermocouples and foam generator setup

The second test (test 6) was performed on November 2007 on $65m^2$ pit. This was a larger test with improved equipment and sensors. The following is the experiment condition:

- Foam Expansion Ratio : 227 : 1
- LNG flow rate: ≈ 100 gpm
- LNG liquid height: 6 inch
- Water flow rate: ≈ 160 gpm
- Solution flow rate: ≈ 3 gpm
- Solution ratio: ≈ 2 %

The detail setup is shown in Figure 30 while the gas detectors placement is shown in Figure 31. The improvement in this test includes the usage of large pit and gas detectors.

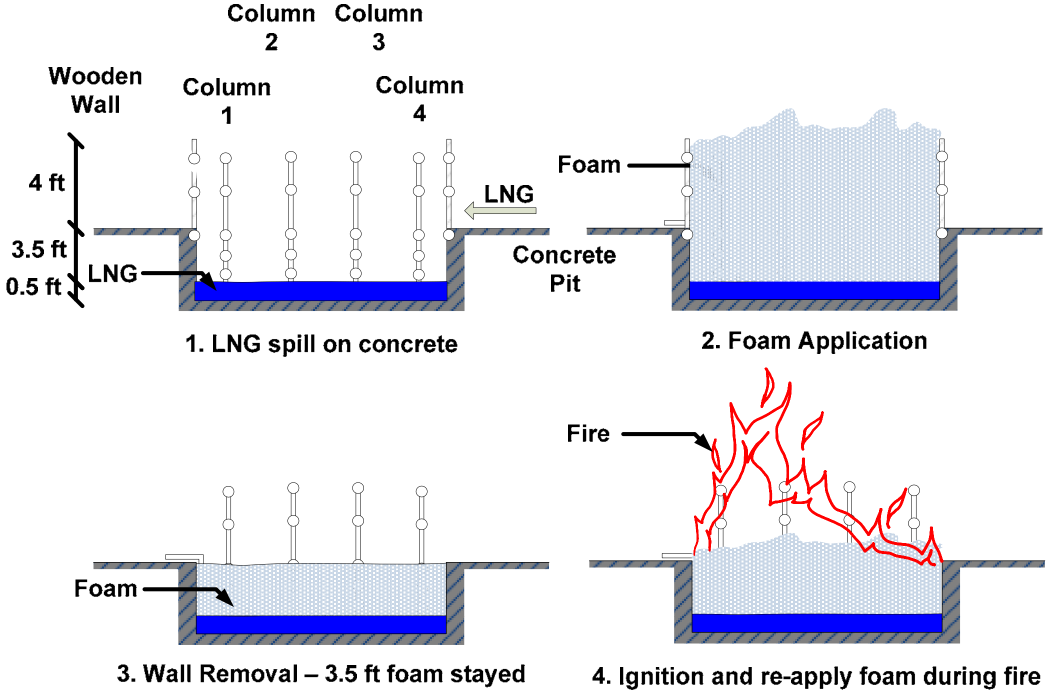

Figure 30. Test 6 setup

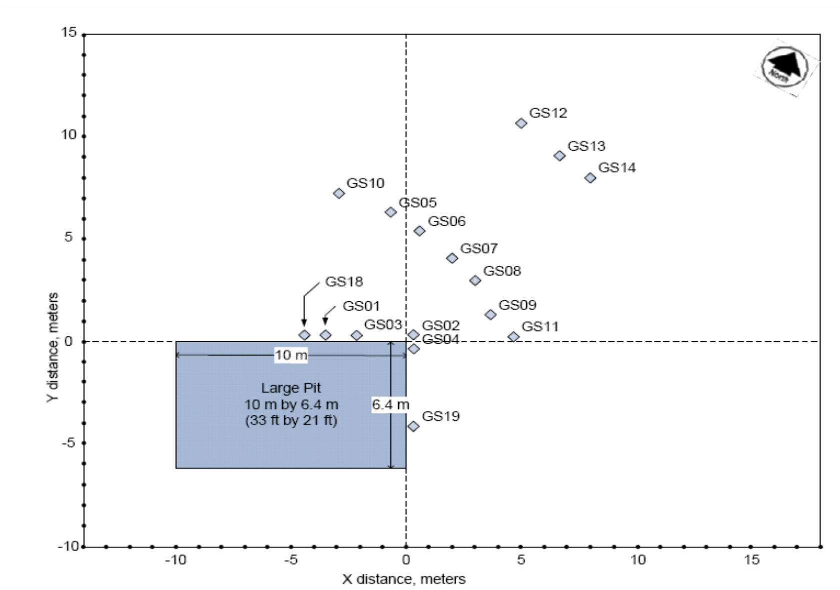

Figure 31. Gas detector location on test 6

The third experiment (test 7) was conducted on March 25, 2008 on $65m^2$ pit as the last test. The setup is shown in Figure 32. The improvement includes the usage of the following:

- High expansion foam was used instead of expansion foam used in test 5 and test 6
- Radiometers (heat flux transducer)
- Pressure differential measurement
- Level measurement with thermocouples
- Gas detectors and thermocouples above the containment pit and above the top part of expansion foam

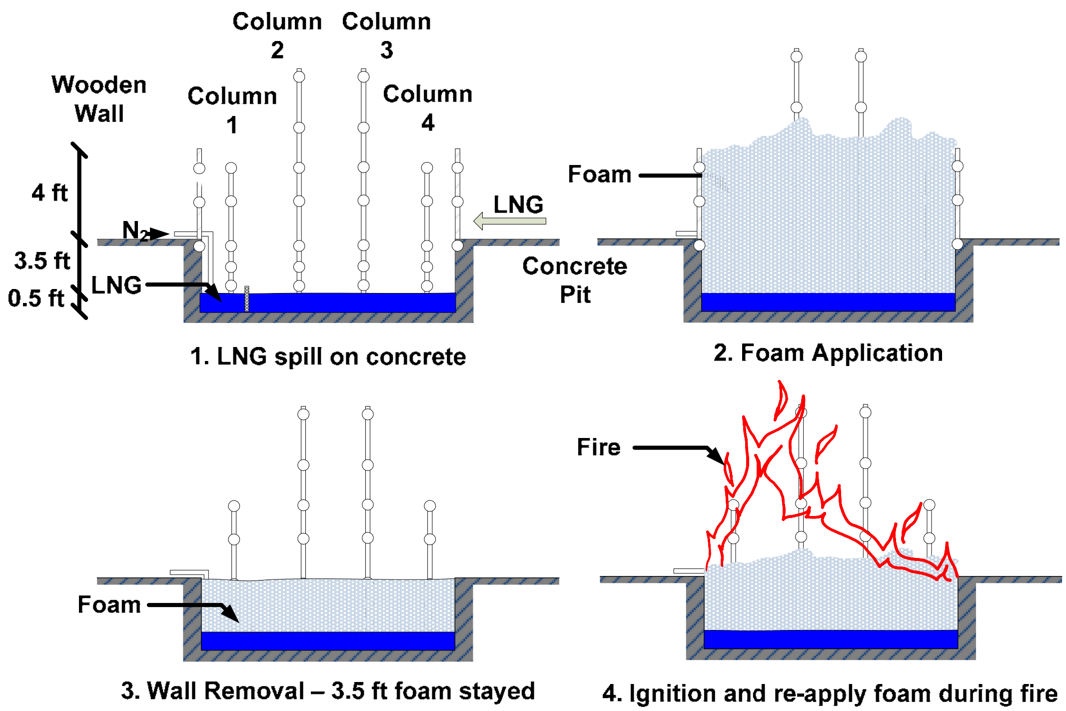

Figure 32. Test 7A/B experimental setup

4.4 Foamglas® PFS – Test 8A/B

The experiment was conducted in the largest pit at the Brayton Fire Training Field's LNG training facilities. It measures 10 m x 6.7 m x 1.2 m with a surface area of 65 m^2, as shown in Figure 24. There were ten gas detectors placed inside the pit to measure the methane concentration above the Foamglas® PFS. Additionally, 23 gas detectors were positioned outside the pit, faced in downwind direction at three different heights (low, middle, and top), to see the LNG vapor dispersion and the cloud movement. Thirty thermocouples were located inside the pit to measure the three-dimensional temperature profile in the pit after Foamglas® PFS application, and during LNG vapor dispersion and pool fire. The thermocouples were located at five different heights (z-direction of 0.6m, 0.9 m, 1.2 m, 1.8 m and 2.4 m above the ground), with three different columns in y-direction and 2 different locations in x-direction, as shown in Figure 33. This was due to the fact that this experiment was designed to measure z-direction temperature, which is the LNG vapor and pool fire movement direction, and to study the effects of Foamglas® PFS. In addition, ten thermocouples were provided outside the pit at the same location as the gas detectors in order to measure the gas temperature and the methane concentration at the same time. Those thermocouples were placed at three different heights above the ground (0.4 m, 1.1 m, and 2.2 m). Figure 34 summarizes the placement of gas detectors in detail. Gas detectors and thermocouples located outside the pit were placed on poles. These poles were colored bright orange to ensure visibility while being recorded with the regular video camera.

LNG was spilled on top of the Foamglas® PFS from the LNG truck through a 53 m pipe. To ensure a smooth spill, and to reduce turbulence, there was an aluminum plate placed at the end of the pipe, as shown in Figure 33.

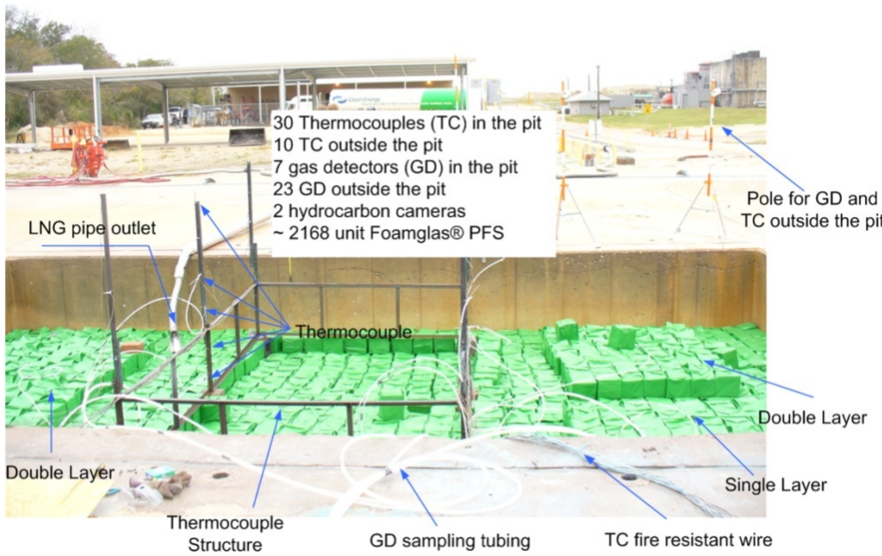

Figure 33. Placement of equipment in the pit

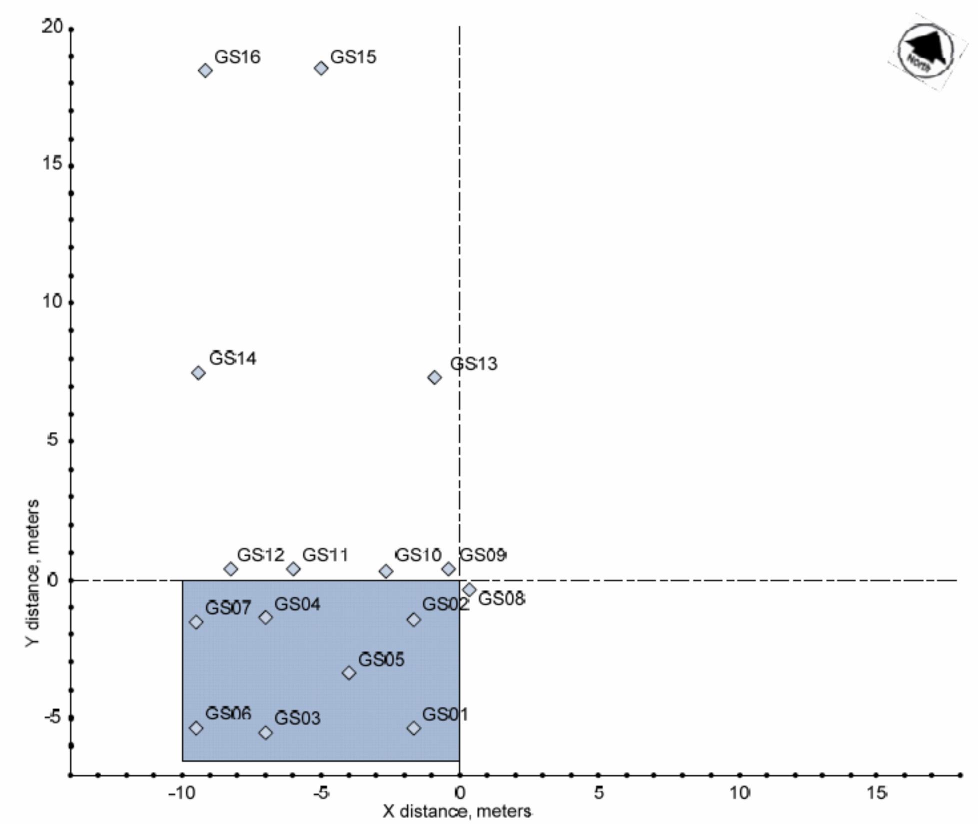

Figure 34. Gas detectors and thermocouples placement

As illustrated in Figure 35, two hydrocarbon cameras (H-1 and H-2) were placed at exactly 90 degrees to each other in order to obtain two different views of the LNG (methane) vapor cloud; concurrently, one regular camera (C-1) was used to record the visible cloud and was located at the same point as H-1 hydrocarbon camera. This setup helps to distinguish the methane cloud from the visible cloud (visible white color of condensed water from air). As a result, the real effect of Foamglas® PFS on an invisible methane cloud can be studied. Data acquisition was located 100 ft from the pit. All sensors were connected to it, and Ethernet cable from data acquisition system helped to transfer the data into the computer, which was located at the safe location about 60 m from the pit. This assignment is shown in Figure 35.

Four radiometers were placed on two crosswind directions which were R-P1 at and South-South East (SSE) and R-P2 at North-North West (NNW), as shown in Figure 35. Each location consisted of two radiometers placed 4 ft with separation distance of 1 ft.

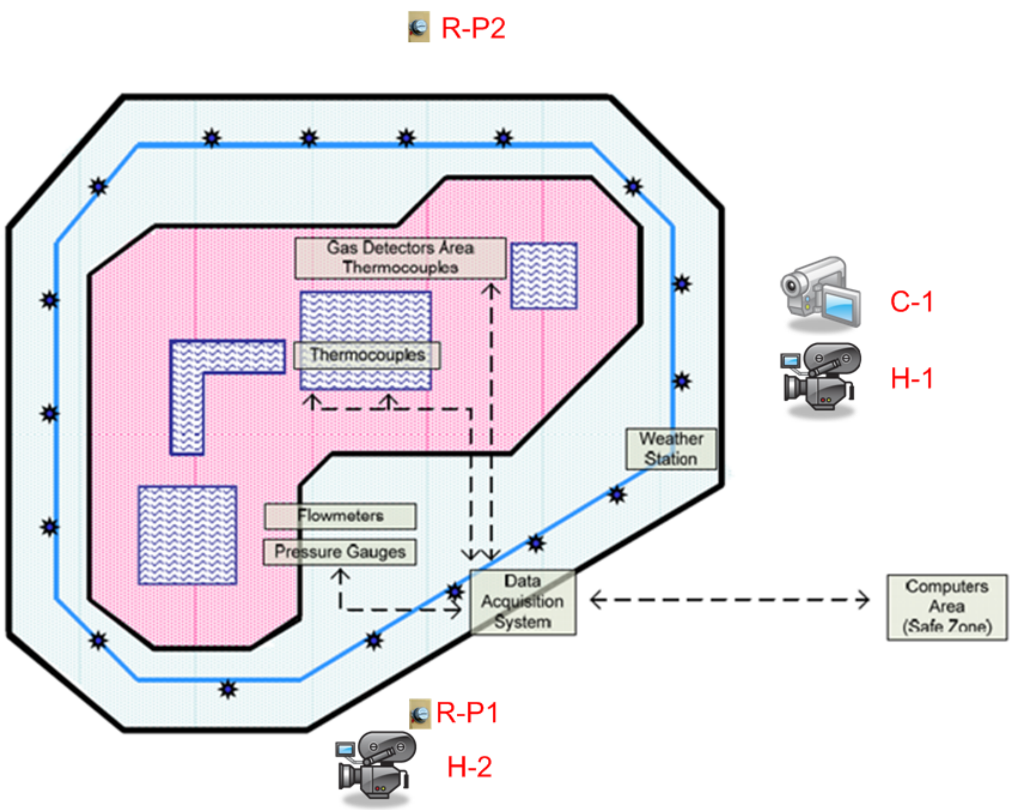

Source: Texas Engineering Extension Service (TEEX)

Figure 35. LNG pit layout and equipment placement

Foamglas® PFS was arranged as described in Figure 36. As estimated 17% of the area was covered by two layers of Foamglas® PFS, while the rest of the area was covered by single layer of Foamglas® PFS. It was estimated that 1860 units of Foamglas® PFS were used to cover the whole pit surface with a single layer of Foamglas® PFS, while it required 310 units of Foamglas® PFS to provide the second layer. The double layer around the thermocouple structure was provided with consideration to the fact that the structure created an opening that might have reduced the effectiveness of Foamglas® PFS.

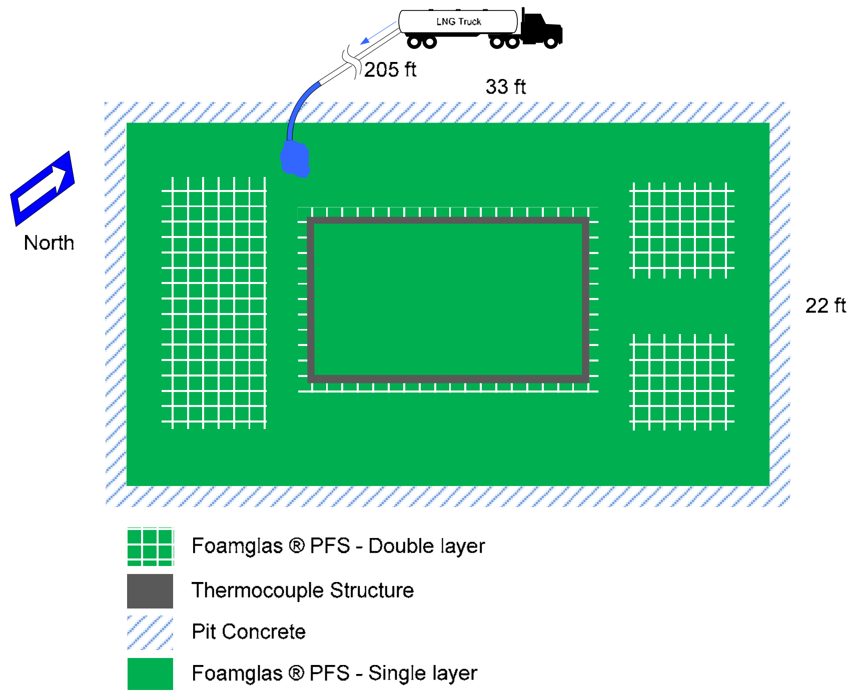

Figure 36. Foamglas® PFS experimental setup - top view

The experiment began with the placement of Foamglas® PFS in the pit when the pit was completely empty. This process was completed in one hour and concluded the first phase of the experiment.

The second phase was to evaluate the Foamglas® PFS effectiveness on LNG vapor dispersion mitigation. Once the Foamglas® PFS arrangement was completed, the LNG was spilled on the top of Foamglas® PFS single-layer-block at 125 GPM for 60 minutes until reaching 12 inches (5233 gallon of LNG) of LNG pool in the pit. The estimated amount of LNG spilled was 7477 gallons. During the course of the LNG controlled-spill, the thermocouples and gas detectors recorded data into the data acquisition system.

The next phase tested was the effectiveness of the Foamglas® PFS on LNG pool fire mitigation. Prior to ignition, all thermocouples located outside the pit and the gas detectors were moved to a safe distance. The LNG was then ignited and allowed to burn for a total of 12 minutes. Data was recorded by the thermocouples in the pit and also on radiometers.

The last phase was the extinguishing of LNG pool fire after being controlled, or suppressed, by Foamglas® PFS. This phase was completed by applying dry chemical for a few seconds until the LNG pool fire was completely extinguished. The LNG was then re-ignited to replicate the third and the fourth phase. Dry chemicals were re-applied to extinguish the LNG pool fire, and the experiment was completed. This procedure is illustrated in Figure 37.

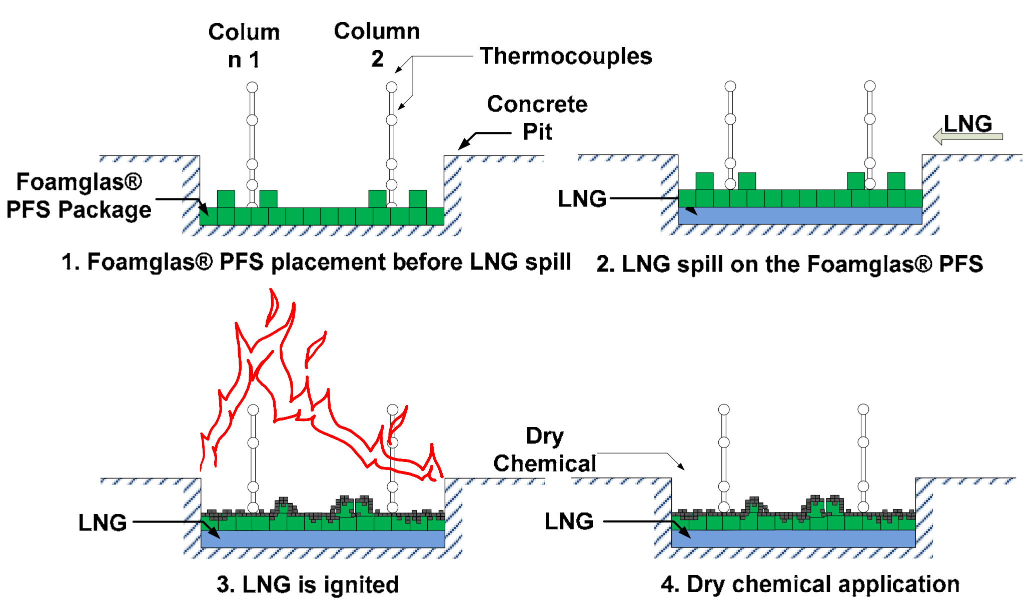

Figure 37. Foamglas® PFS experimental procedures

4.5 Data Collection System and Equipment

This document describes and discusses the equipment that will be required onsite for any LNG field experiment for data measurement and collection. The list of equipment is based on the experiments that have been conducted by Mary Kay O'Connor Process Safety Center, as listed in Table 5.

Table 5. List of equipment

Equipment	Provider
Pressure gage	Omega
Differential pressure transmitter	Omega
Volumetric flow rate	Omega
Temperature	Omega or Newport Electronics
Gas detectors	Honeywell Analytics
Weather data	Davis or Campbell Science Inc
High speed camera	Graftek Imaging
Hydrocarbon camera	Leak Surveys Inc
Heat flux transducer	Medtherm Corporations

4.5.1 Introduction

This document explains the equipment used for data measurement and collection for LNG field experiment. While additional equipment and specific installation might be required depending on the LNG field experiment scenario, this equipment list is generic and is applicable for most of the LNG field experiment.

4.5.2 Gas Concentration Measurement

Two types of gas detectors can be used to measure methane gas concentration in the air during the experiment, portable gas detectors and point gas detector.

4.5.3 Point Gas Detectors

"Searchpoint Optima Plus" model manufactured by Honeywell Analytic can be used as the point gas detector. It produces output signal of 4 – 20 mA with power requirement of 5 watts per detector. It is an infrared point flammable hydrocarbon gas detector certified for use in potentially explosive atmospheres [24]. The features of this type of gas detector include [24]:

- Failsafe operation that reduces the need for maintenance.
- Immunity to catalytic poisons allows monitoring in atmospheres not suitable for bead type detectors.
- Self check routines run constantly ensuring stable operation.
- Wide range of detectable gases including heavy Hydrocarbons and solvents.
- Range of accessories including Storm Baffle and Duct Mounting Kit.
- Infrared detection principle provides the fastest speed of response.
- IR principle allows detection without background oxygen required for bead type detectors.
- Plug-in handheld device allows fault diagnosis, change of gas type, and event log access.
- The placement and number of gas detectors per portable tripod varied with the experimental plan for each specific test.

Originally, the "Searchpoint Optima Plus" is designed for industrial application where detecting methane leak and its concentration in the range of 0% volume by volume (v/v) to 5% v/v (Low flammability level, LFL) is important. Since the experiment is to measure the methane concentration up to 100 % v/v, "Searchpoint Optima Plus" should be modified to measure a range of 0% v/v to 100% v/v of methane. This modification can and should be performed by Honeywell Analytics as the manufacturer. The application of the modified “Searchpoint Optima Plus” require the suction of methane gas sample by using vacuum into the cell of the gas “Searchpoint Optima Plus. This cell is able to measure high concentration methane gas.

While it is possible to install the gas “Searchpoint Optima Plus” directly at the field for the experiment, this configuration is not very flexible due to the size and the weight of “Searchpoint Optima Plus”. LNG vapor dispersion movement is very dynamic depending the wind speed and direction. Thus it is important to set up the gas detector in a way that relocation is easy. It is recommended to gather all “Searchpoint Optima Plus” in one place then connect the measurement cell with tubes up to at least 100 ft or to an adjusted length to the size of the experiment. To reduce the uncertainty, each “Searchpoint Optima Plus” should be connected with the same type and length of tubing. Figure 38 shows the example of 40 “Searchpoint Optima Plus” located in a box with vacuum tubing coming out and methane gas sample tubing coming in. To cover a wide range of application and area in order to obtain sufficient methane concentration profile. Placing them in the containment pit, above the pit, downwind distances, and at different heights is recommended.

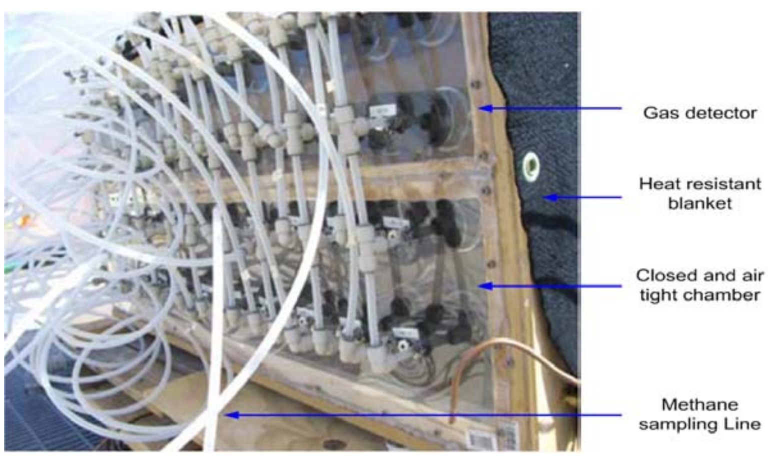

Figure 38. Gas detector closed and air tight chamber

4.5.4 Portable Gas Detector

MiniMax X4 portable gas detectors manufactured by Honeywell Analytics can be used as the portable gas detectors. The application of this includes measuring gas detector at a certain point where the point gas detectors are not available as well as for the safety of the person conducting the experiment. MiniMax X4 has the capability to store data using a regular memory card. By using the free software, the data can later be retrieved.

4.5.5 High Speed Camera

High speed camera of Bassler A311fc with video Lens-Varifocal 4.0-12.0 mm produces up to 659 x 492 pixels at 73 frame per second (fps) color video/images. The camera is connected to the computer with IEEE 1394 type of cable. Some of the installation equipment includes the following:

1. Cable, IEEE-1394, 6 pin to 6 pin
2. Cable, IEEE-1394, 4 pin to 6 pin
3. Optical Repeater Pair, 1394a-to-1394a
4. Cable, 1394b, fiber optic, 30 meter(100ft)
5. Laptop or desktop with IEEE 1394 connection available
6. Power cable

Different types of connections are illustrated in Figure 39, long connection and short connection with laptop or desktop computer. Laptop does not provide power supply the camera while desktop connection does. Therefore, item (3) is used to provide power to then camera in addition to item (2) cable that is utilized to provide short connection from the camera to laptop. On the other hand, short connection to desktop computer requires only item (1) without providing power supply. Long connection for both laptop and desktop computer requires the same configuration.

Video data is recorded to computer by using software from National Instrument (NI), Vision Acquisition Software and Vision Development Module, and Labview. The software are capable of providing driver for the camera, record video/images, and analyze the images/video data later on.

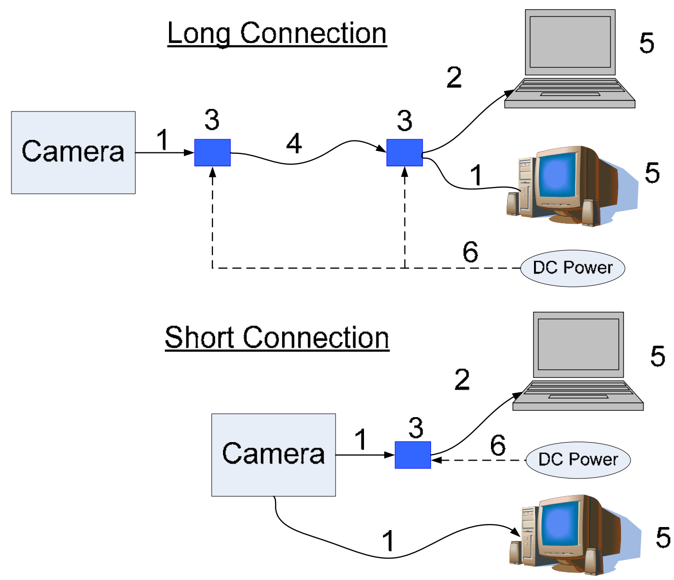

Figure 39. High speed camera connection

Some of the applications of high speed camera in LNG field experiment include recording the movement of the gas dispersion, water curtain characteristics, LNG spreading (on any substrate such as concrete and water), and expansion foam spreading. These types of application do not require a higher frame rate per second (pfs). Thus, while having high speed camera with higher pfs is recommended, 60 pfs high speed camera, such as Bassler A311fc, may be enough.

4.5.6 Hydrocarbon Imaging Camera(s)

LNG vapor lowers air temperature when dispersed, condenses the water in the air, and creates visible white cloud, although the LNG vapor itself is not visible. The hydrocarbon camera is able to capture the methane cloud; thus, enabling the observation of the cloud movement and measuring of the cloud size.

The camera utilized was the ThermaCam® Gas FindIR, manufactured by FLIR system Inc. This infrared camera was designed to spot leaks such as methane, and any other volatile organic compounds (VOCs), which appear as “black smoke” on the screen. This camera records 30 images per second and the output (NTSC/RS-170, S-video) can be recorded to any video recorder data storage [25]. The camera can be rented as well at Leak Surveys Inc.

During the experiment, two cameras should be used and placed at 90 degrees (e.g. East and South direction) to each other at distance of between 50 ft to 100 ft depending on the type of observation. This kind of placement is aimed to capture and record three dimensional images or video of the methane cloud.

4.5.7 Thermocouples

Temperature measurement is conducted by using thermocouples. The selection of thermocouples depends on the application and the possibility of exposure to high temperature. The thermocouples used were type K thermocouples that are able to measure temperature in the range of -270 °C to 1300°C. Because it could measure a large range of temperatures, it means that the thermocouple was able to handle the experiment condition during or without the fire occurrence. To withstand the heat from the fire during the LNG pool fire, the cable is protected with Nextel® ceramic fiber that could handle up to 1090 °C.

N type thermocouples are used to measure cryogenic temperature as this type of thermocouple is more stable at extreme temperature. The application includes the measurement of LNG pool spreading on water. The installation of thermocouples requires cables and particular type of connections to match data acquisition system connection.

Gas temperature measurement requires the protection of the thermocouple from the surrounding, e.g. heat from the sun, wind, etc. Thus, partial enclosure should be installed together thermocouples.

4.5.8 Radiometer(s)

Heat flux from LNG pool fire can be measured by using heat transducer (radiometer). Heat transducers model 64-10-21/ZnSeW-2C-XX ("XX" is maximum heat flux) manufactured by Medtherm Corporation can be used. This type of heat transducers is water-cooled to maintain the temperature of 400 F to ensure accurate reading. However, when low heat flux is measured, natural cooling system can be used as well. There are two radiometers facing each direction separated at 1 ft distance, as shown in Figure 40. The radiometer produces output signal of 0-12mV.

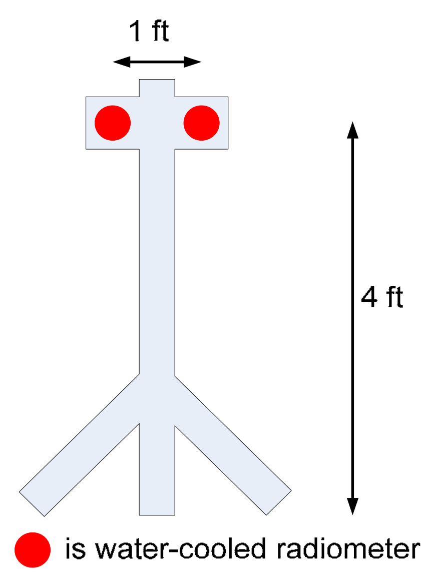

Figure 40. Radiometers placement on portable tripod – example

4.5.9 Data Collection Equipment

The whole experiment utilized one data acquisition system (DAS) with the exception of the weather station and hydrocarbon imaging cameras that have built-in data acquisition system. It is recommended to install DAS with the ability to handle a high number of channels (sensors). In addition, computer is placed at safe location which is at long distance from DAS and sensor. Thus, the chosen DAS should able to send data to computer from a long distance. The DaqScan 2005 manufactured by IOTECH is an Ethernet based system. It is able to handle up to 896 thermocouple channels or up to 256 channels when used with other cards. For example, DAS setup is capable of managing:

- Up to 168 thermocouples for temperature profile with 3 DBK 90.
- 40 point gas detectors (4 – 20 mA input) with DBK 15 card.
- Flow meters and pressure gages data for LNG (4 – 20 mA input) with DBK 15 card.
- Radiometers (0 – 12 mV input) with 5B-30-1 modules that were placed in DBK 42.

4.5.10 Flow Meter

There are two types of flow meters should be used, cryogenic flow meter to measure LNG volumetric flow meter and generic liquid flow meter. Pipe size decides the size of the flow meter size.

4.5.11 LNG Volumetric Flow Measurement

A cryogenic flow meter FTB-911 turbine meter was installed on the LNG discharge line from the LNG truck or source. The 3 inch FTB-911 turbine meters with male NPT end fittings that can be used for measuring LNG volumetric flow. This unit is supplied with a mating 2-wire connector and can be supplied with FLSC-60 Series integrally mounted signal conditioners to provide 4-20 mA output to data acquisition system. The flow meters temperature range of -268 to 232°C (-450 to 450°F) make sure this flow meter works at LNG liquid temperature.

Recommended placement is at the beginning of the pipe connected to the discharge line of the LNG source (LNG tanker truck, etc). Some of the LNG release from the truck might flash at the end of the pipe and produces two phase flow. Installing it at the end of the pipe may cause the measurement of both liquid and vapor thus giving incorrect reading.

4.5.12 Non-cryogenic Liquid Volumetric Flow Measurement

This type of flow meter is used to measure non-cryogenic liquid volumetric flow rate, e.g. water supply for water curtains and foam system and foam solution supply volumetric flow rate. FP-2540 stainless steel flow-meter can be used. Unique internal circuitry eliminates the need for magnets in the process fluid, enabling lower flow measurement while maintaining the advantages of insertion-type sensor design. The sensor's unique rotor/bearing design offers low flow measuring capability with increased reliability [26]. A conditioner was installed at each flow-meter to obtain a 4-20 mA output.

4.5.13 Wind Speed Measurement

The wind speed field measurements were obtained using commercially available three axis cup and vane anemometers located in several areas. This product is available at Davis Instruments or at Campbell Science Inc. This type of anemometer measures the wind speed directly without any signal conditioning. Signal is then sent to computer using cable or built in wireless system.

The application of this includes measuring wind speed at several different heights and locations in the field. In addition, air entrainment for water curtain experiment can be measured with this type of anemometer as well.

4.5.14 Weather Stations

Weather stations manufactured by Davis Instruments can be used to measure temperature, humidity, solar radiation, etc, as shown in Figure 41. Data is sent to computer using wireless system.

Figure 41. Weather station

4.5.15 Pressure Measurement

There are two types of pressure measurement with different objectives. Pressure gage is utilized to measure flowing liquid pressure and differential pressure transmitter to indirectly measure LNG liquid level in the pit by measuring pressure difference.

4.5.15.1 Pressure Gage

Generic liquid pressure gauge is used to measure liquid pressure, i.e. water pressure at water curtain and water and foam solution pressure and expansion foam system. DPG1000 series pressure gage is capable to measure up to 1000 psig, it produces 4-20 mA output signal, and it provides a digital display.

If the pressure gage will be exposed to high temperature, i.e. pressure gage at foam generator during LNG pool fire, General Purpose Pressure Transmitter PX305 with 4-20 mA output signals should be used. It is a welded-stainless-steel pressure transmitter and does not have digital display. Therefore, it is able to handle high temperature.

4.5.15.2 LNG Level Measurement

Differential Pressure Transmitters with 4-20 mA output signals is used for measure LNG level in the pit by measuring the pressure difference between two locations. The first location is the nitrogen source which is flowed at a relatively constant pressure. Another location is the end of the pipe placed at the bottom of the pit where the pressure is LNG pool hydrostatic pressure. Hydrostatic pressure of LNG differs according to the LNG pool liquid level. Changing in liquid level will change the pressure. Differential pressure transmitter will compare the pressure difference associated with changing in LNG liquid level and convert it into milliamps signal that is recorded to data acquisition system. This arrangement is illustrated in Figure 42.

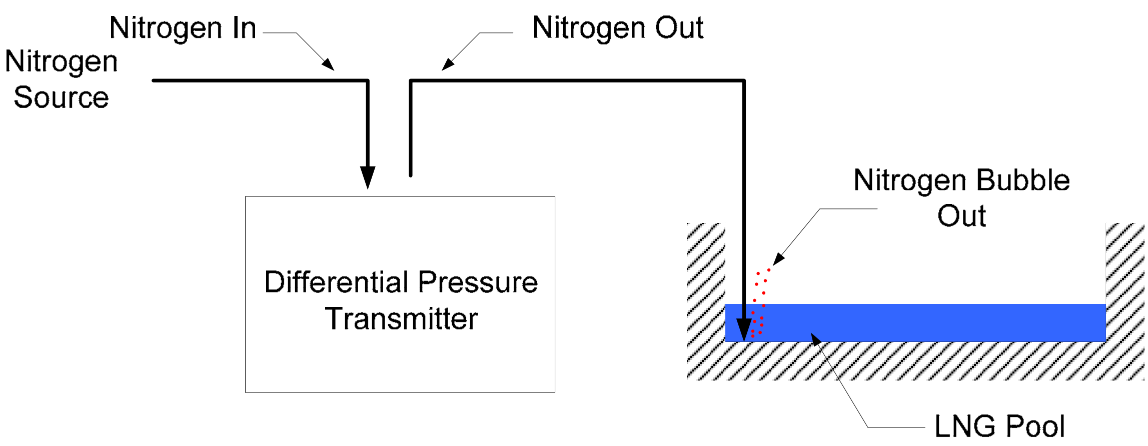

Figure 42. LNG pool level measurement with differential pressure transmitter

4.5.16 Bunker Gear(s)

LNG experiment should be conducted in safe manner. Thus, it is required for all personnel involved to wear bunker gear in any types of LNG experiment even though fire is not expected. Bunker gear and its accessories include bunker gear (coat and pant), helmet, boot, gloves, and suspenders.

4.5.17 Other Logistics

Other logistics includes:

- Cables

Cables are required for thermocouples and data and power supply for each sensor. Depending on the number of thermocouples, it is estimated 13,000 ft of thermocouple cables required and 5,000 ft of data and power cables.

- Tripod

Tripod is utilized to place the gas detectors tubing, thermocouples, and weather station. It is estimated of 30 tripods should be used.

- Fire resistant insulation

If the LNG experiment involves fire, some of the cables and equipment should be protected. Fire resistant sleeve manufactured by Firesleeve can be used. It is design to protect cables and wires to up 1200°C for short application.

- Quick disconnect

Quick disconnect for each of the sensor connection should be used to make sure the installation and un-installation is easy.

5 EXPANSION FOAM FINDINGS/RESULTS

5.1 Introduction – Purpose of the Study

This section details the findings results of all experiments conducted in this research. The test summary is explained in the following Table 6:

Table 6. Test summary

Test ID	**1**	**2**	**3**	**4A**	**4B**	**5**	**6**	**7**	**8**
Date	**04/06**	**04/06**	**04/06**	**04/06**	**10/06**	**10/07**	**11/07**	**03/08**	
Pit size (meter)	45	65	65	65	65	9.5	65	65	
Vapor Dispersion (VD), Pool Fire (PF)	PF	PF	PF	PF	PF	VD PF	VD PF	VD PF	VD PF
Mitigation	HEX	HEX	HEX	HEX	HEX	EF	EF	HEX	Foamglas® PFS
Application rate (L/minutes m^2)	10	3.5	7	10	10	10	10	10	NA
Radiometer location for pit edge (meter)	30	30	30	30	27	NA	NA	35ft 43ft 55ft 59ft	NA

Table 6 Continued

Test ID	1	2	3	4A	4B	5	6	7	8
Radiometer location for pit edge (meter)	30	30	30	30	27	NA	NA	35ft 43ft 55ft 59ft	NA
Initial LNG pool depth (meter)	0.13	NA	0.10	0.15	0.15	12	6	6	12
Average wind speed (meter/second)	3.7	NA	1.2	2.2	3.7				
Air temperature (°C)	15.8	NA	26.7	24.5	28.7				
Relative humidity (%)	83	NA	74.8	81.3	71				

5.2 HEX Application Rate and Containment Pit Effect

The following Table 7 summarizes the experimental results. There was only one experiment conducted in 45m^2-pit while there were four experiments performed on 65m^2-pit. In addition, there were two experiments performed in 65m^2-pit the same application rate, 10 Liter/minutes m^2. This was to confirm that this particular application rate is the practical application rate. While recognizing the maximum heat flux reduction achieved by HEX application is important, in the discussion, the fire control time is defined as the time required by the HEX to reduce 90% of the heat flux, as specified by NFPA 11 [27].

Table 7. Foam application experiment on LNG pool fire in 2005 and 2006

Test ID	**1**	**2**	**3**	**4A**	**4B**
Pit area (m^2)	45	65	65	65	65
Radiometer distance (x Pool Diameter)	4.0	3.3	3.3	3.3	3.0
Maximum heat flux ($kW/meter^2$) (95% confidence level)	3.88 ± 0.14	7.01 ± 0.70	3.78 ± 1.11	6.85 ± 0.55	4.07 ± 0.92
HEX Solution Application Rate (Liter/minutes m^2)	10	3.5	7	10	10
Maximum Heat Radiation Reduced (%)	91	94	95	97	93 75.64
Time to reach 90 % Heat Radiation Reduction (minutes)	3.5	2.45	1.7	1	0.85 NA
Time to reach Maximum Heat Reduction (Minutes)	3.6	4.5	2	1.2	1.5 0.79
Equivalent Pool Diameter (meter)	7.57	9.10	9.10	9.10	9.10

In addition, it is essential to understand that in current technology, LNG pool fire extinction can only be achieved by Dry Chemical Powder above the HEX blanket. Thus, as expected, the HEX did not extinguish any fire during the experiment. Generally, HEX and dry chemical can be used together to fight LNG pool fire state Zuber [16] and White [17]. The following section discusses the results and observation on:

- LNG Spill Containment Pit Design Effect on Fire
- HEX Application Rate of 3.5 $L/min/m^2$ on the 65 m^2 Pit

- HEX Application Rate of 7 L/min/m^2 on the 65 m^2 Pit
- HEX Application Rate of 10 L/min/m^2 on the 65 m^2 Pit (2 experiments)
- HEX Application Rate of 10 L/min/m^2 on the 45 m^2 Pit

5.2.1 HEX Application Rate

The summary of fire control time at tested application rate is shown in Figure 43. There are two observations that can be made and will be discussed in the following section:

- It is clearly demonstrate that higher application rate reduces fire control time
- The two different types of containment pit applied in the experiment gives different results. HEX application rate of 10L/min/m2 operated at 45m^2 pit presents a lower fire control time compared to the HEX application rate of 3.5 L/min.m^2 utilized at the larger pit, 65 m^2 pit.

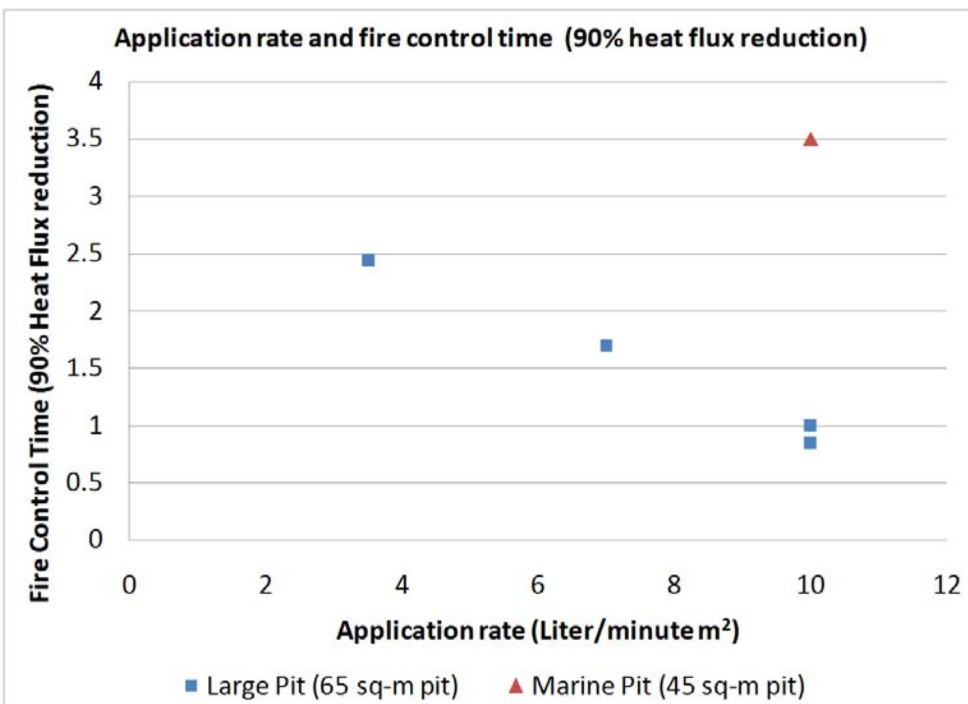

Figure 43. LNG pool fire control time (90% heat flux reduction) at tested application rate

5.2.2 Application Rate of 3.5 L/min/m^2 in the 65 m^2 Pit

This experiment was conducted on October 6, 2005. Fire control time was 177 seconds and maximum heat reduction at 94% was achieved after 270 seconds. As shown in Figure 43, this low application rate has higher pool fire control time compare to a foam application rate of 7 and 10 L/min/m^2. With a lower application rate, it takes significantly more time for the foam to cover the LNG pool but took 5 minutes to nearly fill the pit although the application rate was not high enough to overcome the foam breakdown by the fire, which was considered unacceptable for operational use as there was insufficient foam application to deal with ideal conditions. All of the pool fire surfaces were not covered to the required depth in an adequate time frame to ensure reduced heat radiation could be achieved.

Another observation is that HEX re-topping is important to maintain HEX coverage. HEX or expansion foam in general, breaks down due to the heat, as illustrated in Figure 44. On the other hand, HEX work effectively when the effective depth is reached and maintained. Thus, HEX re-topping is important.

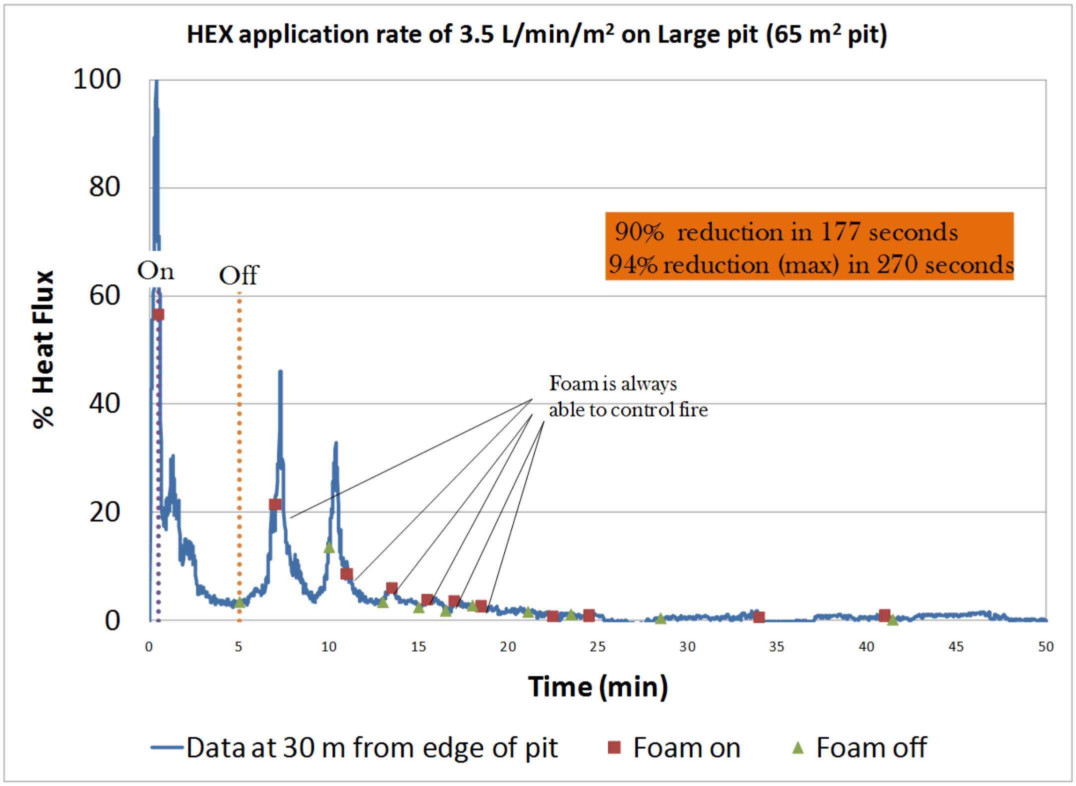

Figure 44. Fire control time for pool fire in the 65 m^2 pit with foam application rate of 3.5 L/min/m^2

5.2.3 Application Rate of 7 L/min/m^2 in the 65 m^2 Pit

From the data gathered on the foam application at 7 L/min/m² in the 65 m^2 pit, it is shown that the maximum heat radiation reduction by HEX application is 95 % within 120 seconds at a distance of 30 meters where radiometer was placed. The 90% heat radiation reduction is achieved in 100 seconds, which seems quick but this was achieved in ideal conditions, with no allowance for adverse factors of higher wind speeds drifting foam off the pit or preventing all the foam entering, and no allowance for cooling sprays drifting water into the pit on the wind, or rain storms increasing the fire intensity.

During the heat reduction comes from the fire size reduction. While fire size should be measured in the length of fire, Figure 22 shows the reduction of fire size by comparing the vertical heights. This is acceptable approach since this only represents fire size reduction and the wind speed did not change significantly during the free burn to the 107 second after HEX application.

The actual pool fire before and after the foam application is shown in Figure 45 while experiment results are presented in Figure 46. As demonstrated in Figure 45, the HEX is only intended to control the fire and permit a burn off of the LNG liquid pool through the foam blanket under controlled conditions and is not intended to extinguish the fire.

Figure 45. Pool fire on the 65 m^2 pit before and after foam application rate of 7 $L/min/m^2$

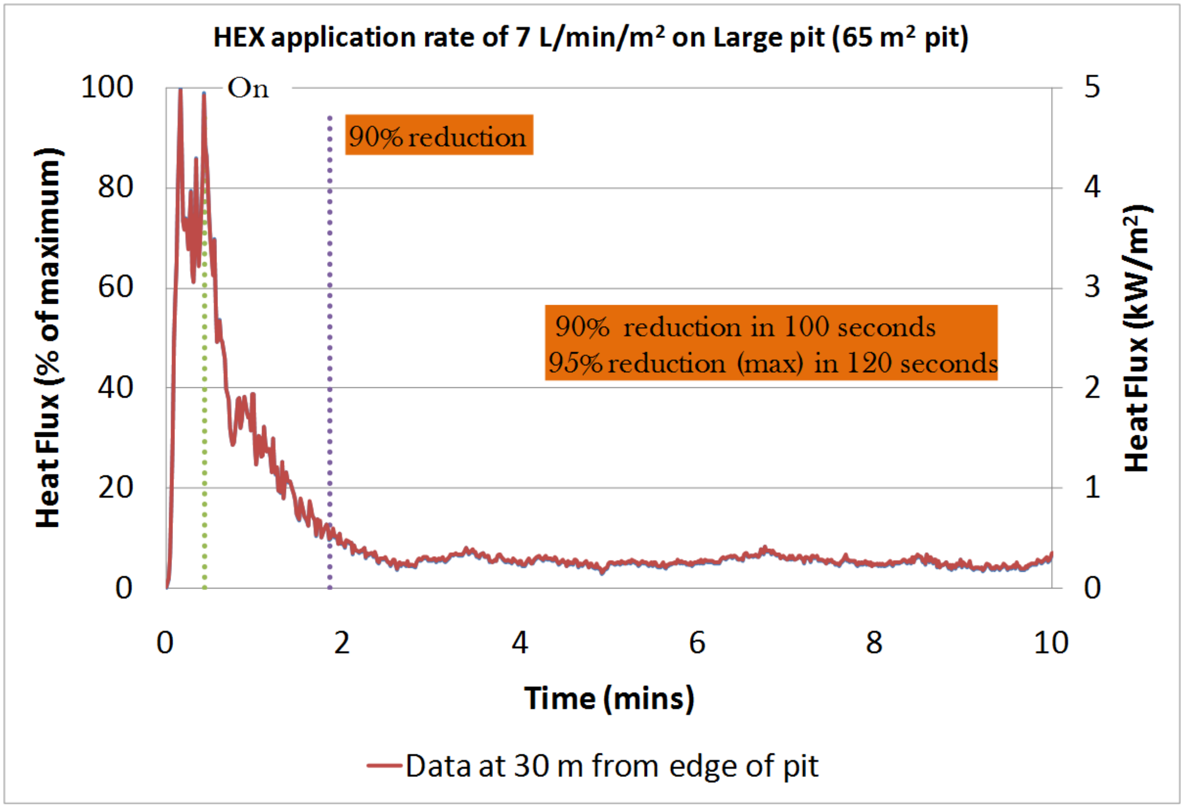

Figure 46. Fire control time for pool fire in the 65 m^2 pit with foam application rate of 7 L/min/m^2

5.2.4 Application Rate of 10 L/min/m^2 in the 65 m^2 Pit – Test 4A

The result for the foam application at 10 L/min/m² in the 65 m^2 pit is presented in Figure 47. The 90 % of heat reduction is achieved within 60 of HEX application while maximum heat reduction is achieved after 70 seconds. This is significantly improved over the 7L/min/m² HEX application rate and allows a safety margin so it will still give an effective result even under adverse conditions.

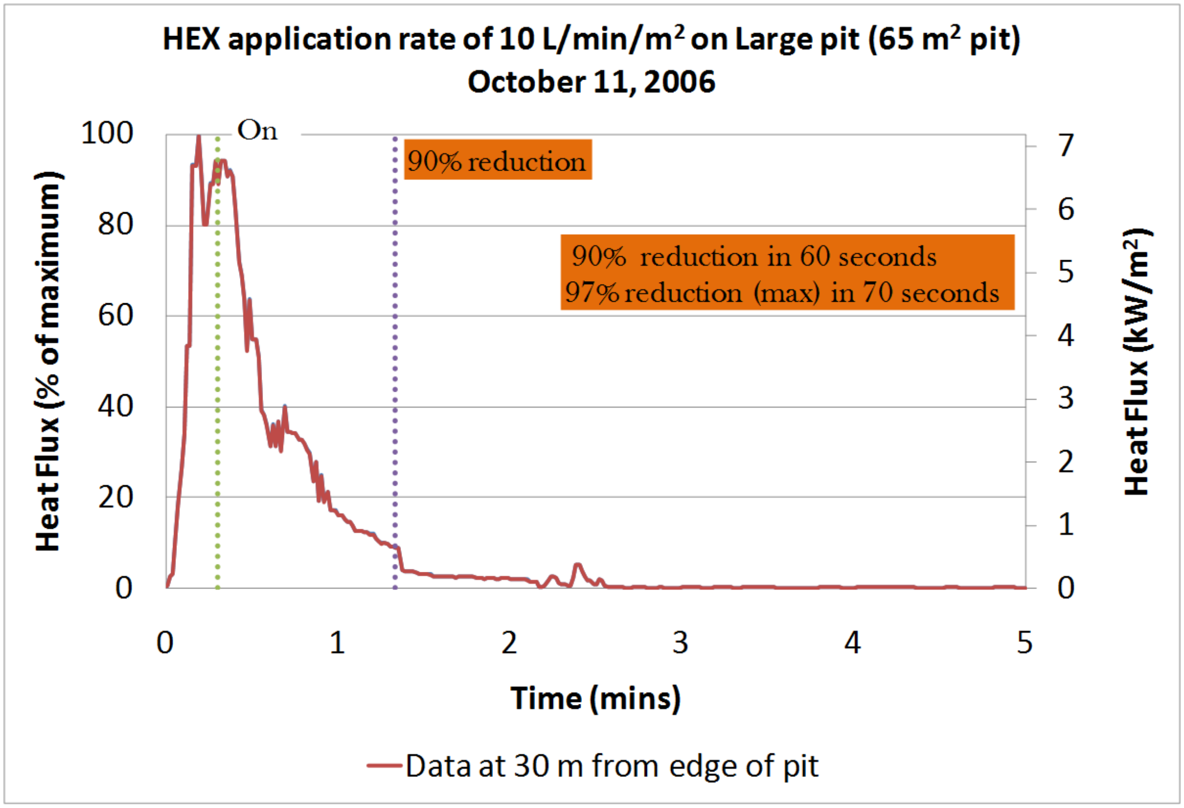

Figure 47. Test 4A - fire control time for pool fire in the 65 m^2 pit with foam application rate of 10 L/min/m^2

5.2.5 Application Rate of 10 L/min/m^2 in the 65 m^2 Pit – Test 4B

Test 4B was conducted on April 20, 2006. The foam generator was turned on and off twice. The fire size reduction is shown in Figure 48. As shown in Figure 49, the first cycle was between 26 and 120 seconds when the pit was full, while the second cycle was between 227 and 275 seconds. In the first cycle, foam is able to reach 90% heat reduction with the maximum reduction of 93 %. It was found that maintaining a full pit was the best way to maintain maximum radiation reduction and also add sufficient water to provide controlled vaporization to safely burn off the residual pool. This practical 10L/min/m^2 application rate coincides with the NFPA 11:2005 international standard recommendations of the National Fire Protection Association [27], which confirms under section A6.14.2.1 that "discharge rates per unit area shall be established by test" and section A6.14.2 that "tests often give minimum application rates, as conducted under ideal conditions with no obstructions or barriers to control. The final design rates are generally 3-5 times the test rates. This recommended practical rate is also 3 times the minimum effective experimental test rate of 3.5L/min/m².

Between the first and second cycle, the heat radiation is increasing but not as high as without the foam, so even the residual frozen foam layer is having an impact, while the pit is topped up with fresh foam. This shows that while foam is still covering the LNG surface, it does provide a level of control on the fire. And when the second cycle starts, the combination of the newly sprayed HEX and the first cycle HEX reduces the heat radiation faster and further.

Figure 48. Fire at 65m^2 pit

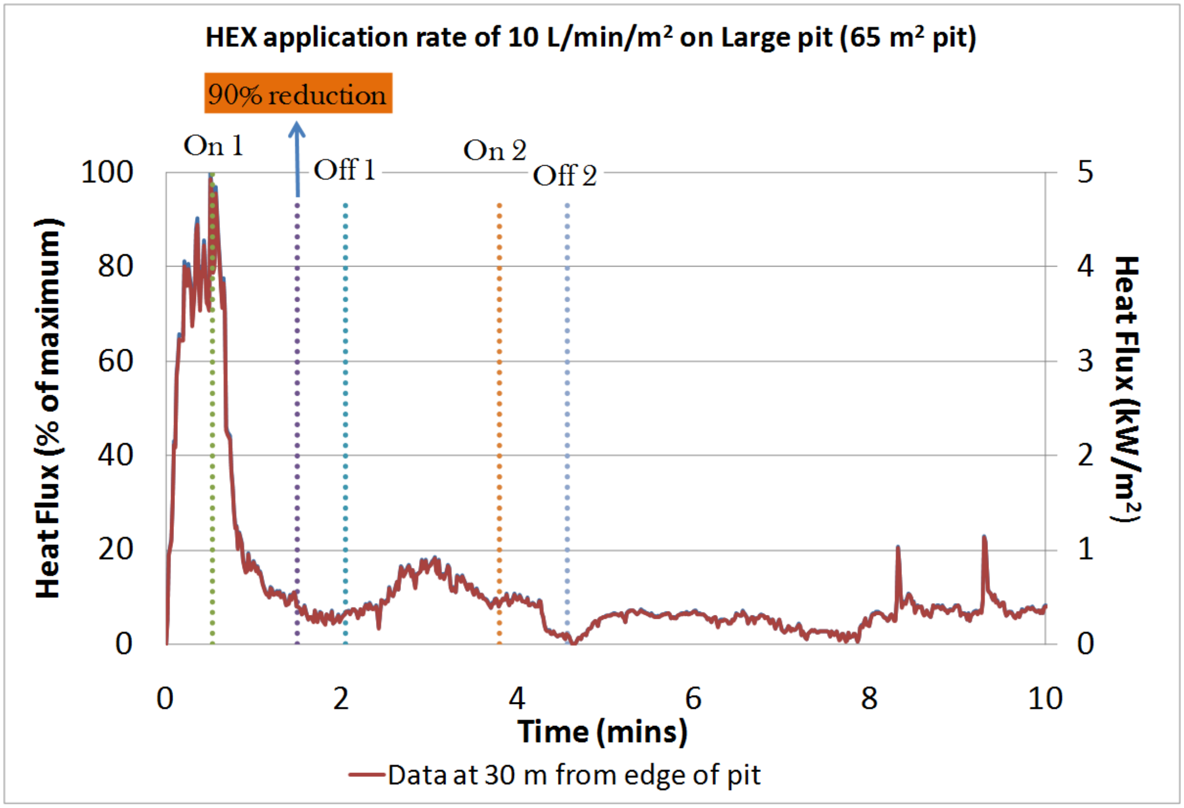

Figure 49. Test 4B - fire control time for pool fire in the 65 m^2 pit with foam application rate of 10 L/min/m^2 – Test 4B

5.2.6 Experiment on the 45 m^2 Pit

Two foam generators were provided, one as back-up knowing that a low rate was probably going to be insufficient on this tough pit. One foam generator the LNG Turbex FT1 unit was located downwind and another LNG Turbex FT2 unit was located perpendicular to the wind direction. Both units were fed by fire hoses for flexibility and ease of providing water, although in operational installations rigid metal piping would be used to supply foam solution to each LNG Turbex foam generator. The plan was to use only one foam generator, the FT1 to achieve a 5L/min/m² application rate.

However, between 16 second to 1 minute after the FT1 was turned on, its hose continued flowing foam solution even though it caught light with direct flame impingement. The flames created a small burst in the hose and it slowly burned away and fell onto the ground while still discharging the foam solution. To continue the experiment it was necessary to open the control valve to allow foam solution to the FT2 unit. At t = 1.3 to 2.4 minutes, the FT2 was operating but due to existing open ended flow at FT1, FT2 did not have enough pressure to reach 7 barg. line pressure and deliver the expected 10L/min/m^2. At t = 2.4 minutes, the valve on FT1 was closed and FT2 achieved an application rate of 10L/min/$m^{2,}$ which controlled the intense fire despite the long pre-burn time.

The observed fire size reduction is shown in Figure 50. The effectiveness of foam application is therefore analyzed starting from the data of t = 2.4 minute, as shown in Figure 51. 90% heat reduction was achieved after 3.5 minutes while the total heat reduction before fire was extinguished by using dry chemical is 91% after 3.6 minutes.

Figure 50. Fire at 45 m^2 pit

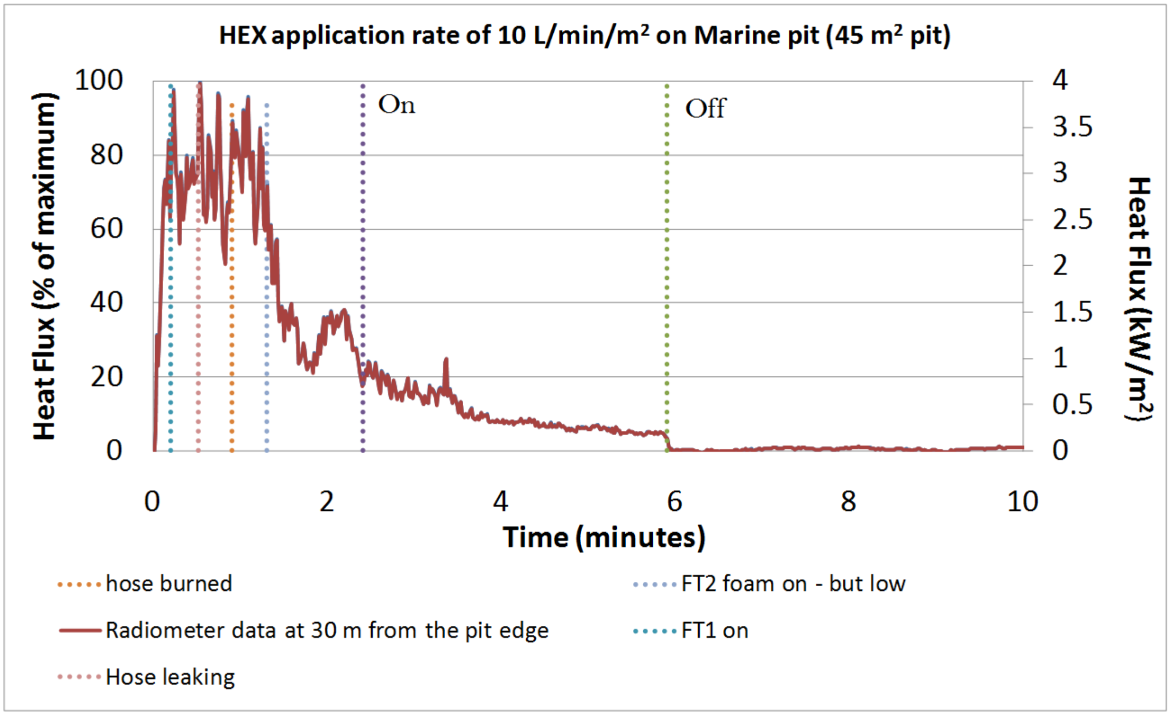

Figure 51. Fire control time for pool fire in the 45 m^2 pit with foam application rate of 10 L/min/m^2 – test 1

Slightly different results were recorded for both experiments conducted on the 65 m^2 pit with a foam application rate of 10 L/min/m^2. Different wind speed and slightly longer pre-burn time could have contributed as the wind could disturb the foam blanket thus preventing it from blanketing the pool fire surface and reducing its effectiveness.

5.2.7 LNG Pool Fire Characteristics on Different Types of LNG Spill Containment Pit

Three experiments have been conducted with the foam application rate of 10 L/min/m^2 on the 65 m^2 pit (Test 4A and 4B) and the 45 m^2 pit (Test 1). The results are then compared. The data shows that heat radiation reduction for the 65 m^2 pit is higher and fire control time is lower than that at 45 m^2 pit. This contradicts the common sense that smaller LNG pool surface area is easier to control compare to the bigger ones.

There are several explanations behind these phenomena. The fire control time on $45m^2$ pit does take into account the extra heated concrete area attacking the foam, and the "chimney effect" of the raised walls, and the amount of un-burn LNG rich vapor in the pit, as follows:

- The time is higher compared to 65 m^2 pit because although the LNG or pit surface area is smaller, the $45m^2$ pit has larger area of concrete (61 m^2 compared to 35 m^2 on $65m^2$ pit). Thus, more heat had built up in the concrete walls, which destroyed the initial HEX application for time longer before it started to work effectively.
- It estimated that ignition occurs at the top of the pit. This is due to the fact that LNG vapors in the pit do not meet enough oxygen to sustain the combustion process while at the same time the LNG vapor is not within its flammable region. Thus, the pit is filled with hot vapors that are ready to burn. There are estimated of 103 m^3 of hot vapor in $45m^2$ pit which is 1.4 times more compared to $65m^2$ pit which has 72 m^3 of hot LNG vapor. This leads to two things: chimney effect and foam damage. Higher walls at $45m^2$ pit create chimney effect that happens when hot vapor is forced to move upward. This means that 45m2 pit provides more fuel to burn outside the pit faster. At the same time, the volume of hot vapors represents the amount of heat that the HEX must endure during its travel from the top of the pit to the LN pool surface to create blanket. Contact with hot vapors breaks or damage some of the HEX thus it requires more time to build HEX blanket ion $45m^2$ pit.
- It took more time to reach the required depth to cover all surfaces. In addition, the distance travelled by the foam, which was 7.5 feet, was doubled compared to the one at $65m^2$ pit, which was 3.5 feet. During the travel, HEX was exposed to the hot vapors longer than in $65m^2$ pit. Thus, longer contact time with fire broke down the HEX by evaporation of water content in HEX and the bond between HEX solution and air in the HEX.
- As mentioned above, LNG pool fire is heavily affected by the wind. Wind tilting is when the fire is sloped by the wind creating angle between the fire and the ground. One of the results of this phenomenon is the flame drag. Flame drag is a well known

phenomenon in which some part of the fire is dragged outside the pit, as shown in Figure 52.

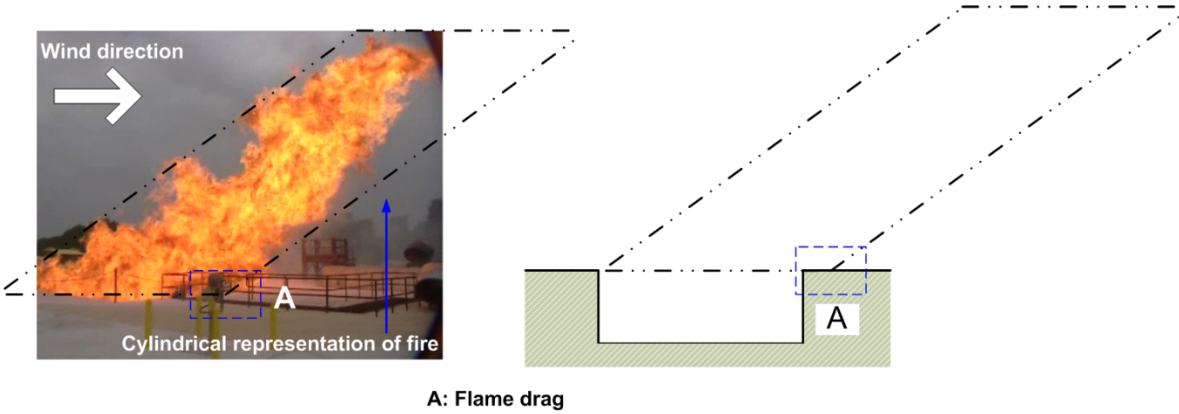

Figure 52. Flame drag at below the ground pit

Marine pit showed different behavior of flame drag, as shown in Figure 53. This type of pit has 1.2 meter-of-above-the-ground wall. As a result, the flame drag effect drags some part of the flame outside the pit and the flame falls down to the ground level. At the same time, fire warms the surrounding air and creating air entrainment and large eddies, as shown in Figure 53.

Combination of flame falling down to the ground level and air entrainment in limited volume space in the between the ground and pit wall creating fire turbulence, as illustrated in Figure 53. While this fire turbulence becomes smaller when the fire size is smaller during HEX application, this part itself is not covered by HEX. It becomes ignition source for the hot vapors moving outside the pit forced by the chimney effect. In addition, it freely emits radiant heat to the surrounding object. Any object in the down wind direction might be affected by the intensity of this fire turbulence. HEX foam generator (FT1) was engulfed in flame all the time solution hose was burn by this effect during the experiment. This part of the experiment shows that a different type of containment pit provides different fire behavior thus requires special attention when placing object or mitigation system.

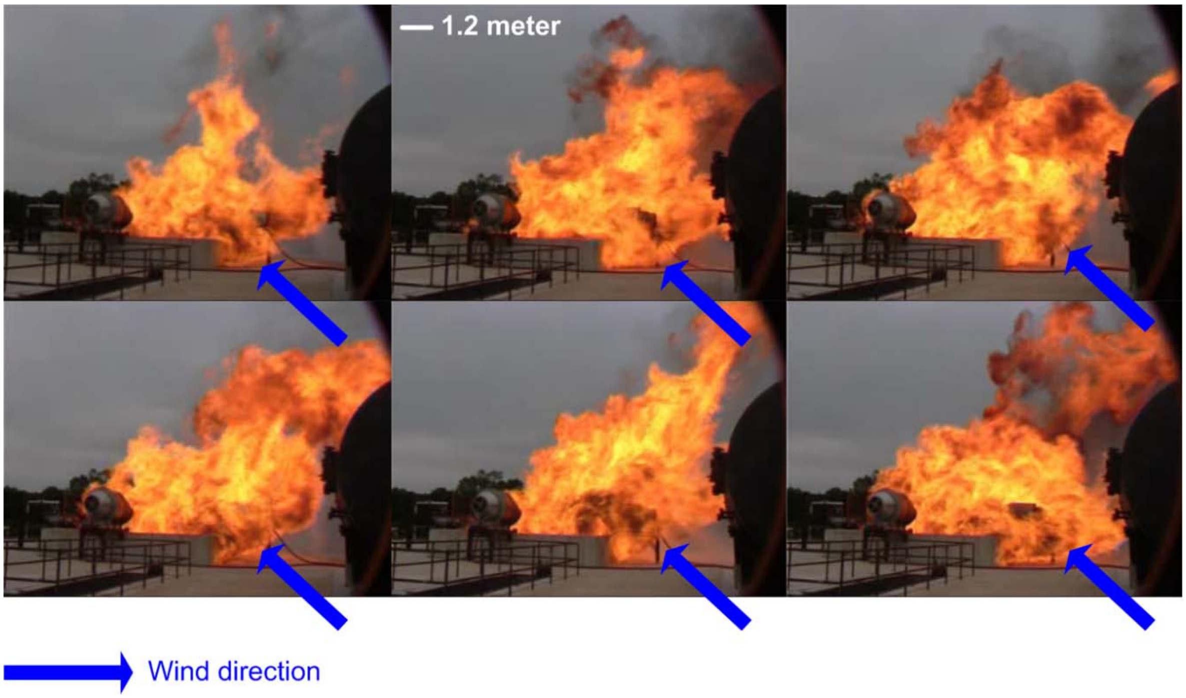

Figure 53. Fire turbulence at 45 m^2 containment pit

Had the foam application rate been lower, it is questionable whether it would have achieved effective fire control, as there reaches a point where the generator is producing foam non-stop, but the foam is being destroyed faster than it is building up so radiation levels do not drop to acceptable levels, the pit never fills with foam and the resulting extra radiant heat can cause a danger to personnel and plant structures. Additionally there is an increased risk of incident escalation. It is therefore vitally important that a safety margin is built in to the designed system application rate to cover unexpected factors and adverse operating conditions should an incident occur.

In summary, those phenomena are illustrated in Figure 54 and do not happen during HEX application in 65m^2 pit. It is also interesting to see that in Figure 51 above, the limited foam application from the LNG Turbex FT1 unit has had a significant effect at reducing radiation despite operating pressure problems, but very quickly when foam application stops the foam is being destroyed by the heat and flames, reflected as the radiation level starts climbing again up to 40%, before new foam from the FT2 unit operating correctly reverses this trend and regains fire control.

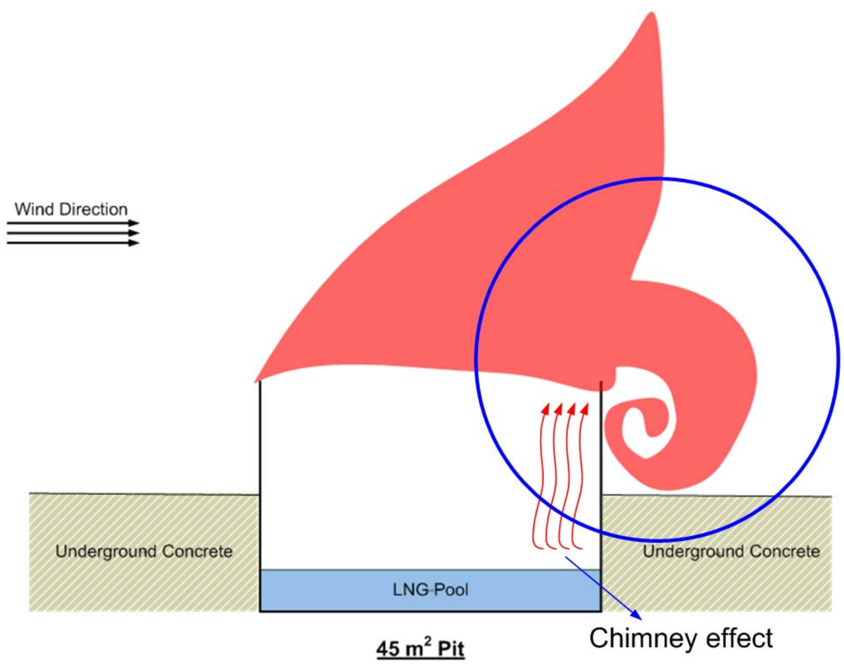

Figure 54. LNG fire phenomena in the 45 m^2 pit

5.3 Expansion Foam

Tests 6, and 7 were performed to assess the internal phenomena that happen in the expansion foam during its application on LNG surface during and without fire occurrence. Test 5 was performed to test the procedure and equipment as part of preparation for tests 6 and 7. Fortunately, usable results were obtained during test 6 and can be used for comparison with larger size of experiment. The list of experiments and its conditions are shown in Table 6. The following results and discussion are discussed in this section:

- Temperature profile based on the thermocouple measurement during both vapor dispersion and LNG pool fires.
- Evaporation rate based on the temperature profile and LNG pool level measurement throughout the experiment (with and without fire occurrence).
- Gas concentration based on the gas detector measurement during LNG vapor dispersion.
- Heat flux based on direct measurement with heat flux transducer during LNG pool fire.

5.3.1 Temperature Profile

Temperature profiles observations were performed based on temperatures measured on tests 6 and 7, which was performed on October 2007 and November 2007. While both tests has LNG vapor dispersion and pool fire, in this dissertation, test 6 temperature profile data analysis is focused on LNG vapor dispersion while test 7 is focused on temperature profile during LNG pool fire occurrence.

5.3.1.1 LNG Vapor Dispersion

For analysis on LNG vapor dispersion, test 6 can be divided into two sections, continuous spill and free vapor dispersion, during which both was not mitigated with expansion foam. Then, the temperature profiles at those two different sections are compared with the foam temperature profile when in contact with LNG pool surface. Continuous spill section is where the LNG is spilled onto the containment pit until it reached 6 inches of LNG pool. Free vapor dispersion section is when 6 inches of LNG was already reached, LNG discharge was stopped, and the vapor dispersion occurred freely from the boiling pool only. Temperature profile inside the pit is shown in Figure 55.

During continuous spill, the temperatures at 5 different thermocouple positions were lower from ambient temperature. Thermocouple placed at the lowest measure the lowest temperature as the thermocouple location is closer to the LNG pool surface. The measured temperatures were then increased along with the increase of distance from the LNG pool surface. It means the LNG vapor receives heat from the surrounding to increase its temperature to a certain temperature. However, the heat is not enough for the LNG vapor to become positively buoyant.

Once the expansion foam was applied, the temperatures measured by all thermocouples were increased instantaneously, even after the flow of expansion foam was stopped. It took 70 seconds for the expansion foam to fill and overflow the containment pit used in the experiment. As shown in Figure 55, the thermocouples at 2ft, 2.9ft, 3.9ft, and 5.9ft measures an instant increase of temperature even though at 7.9ft, the increase is not as significant as at other thermocouples. This can be explained by the fact that the heat transfer between LNG and expansion foam (water and air) occurred. LNG releases its heat to warm both air and water at the same time. The temperature reached its peak in the range of -40°C and 0°C. When the expansion foam flow was stopped, the heat transfer still occurred until the heat transfer reaches steady state and thermocouples measured the decrease of the temperature. However, the final temperature was higher than when expansion foam was not applied. During this time, based on the recorded low temperature, there was a possibility of ice formation in the expansion foam layer.

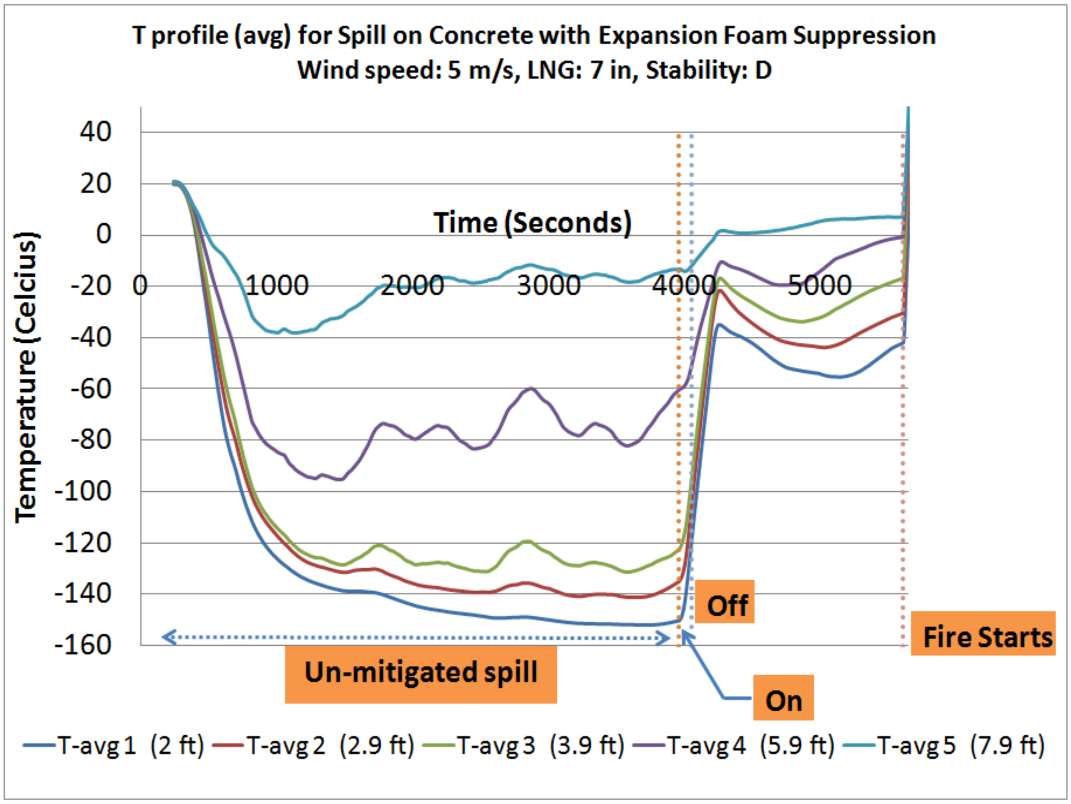

Figure 55. Foam temperature profile during vapor dispersion on test 6

The relation between the measured temperature profile and the LNG/air mixture density can be determined by having a simplified assumption that the mixture is only an LNG/air mixture and the mixture density is proportional to its concentration. It is shown in Figure 56 that the expansion foam increased the temperature of the mixture thus increasing the mixture density at the same time. This explains that expansion foam works as the heat provider to warm LNG vapor and help to reach or to have density close to air density while LNG vapor is still in the expansion foam. While it is not necessary for the expansion foam to warm LNG vapor enough to reach density higher than air density, the warm LNG vapor will reach that faster once it flows out of the expansion foam layers.

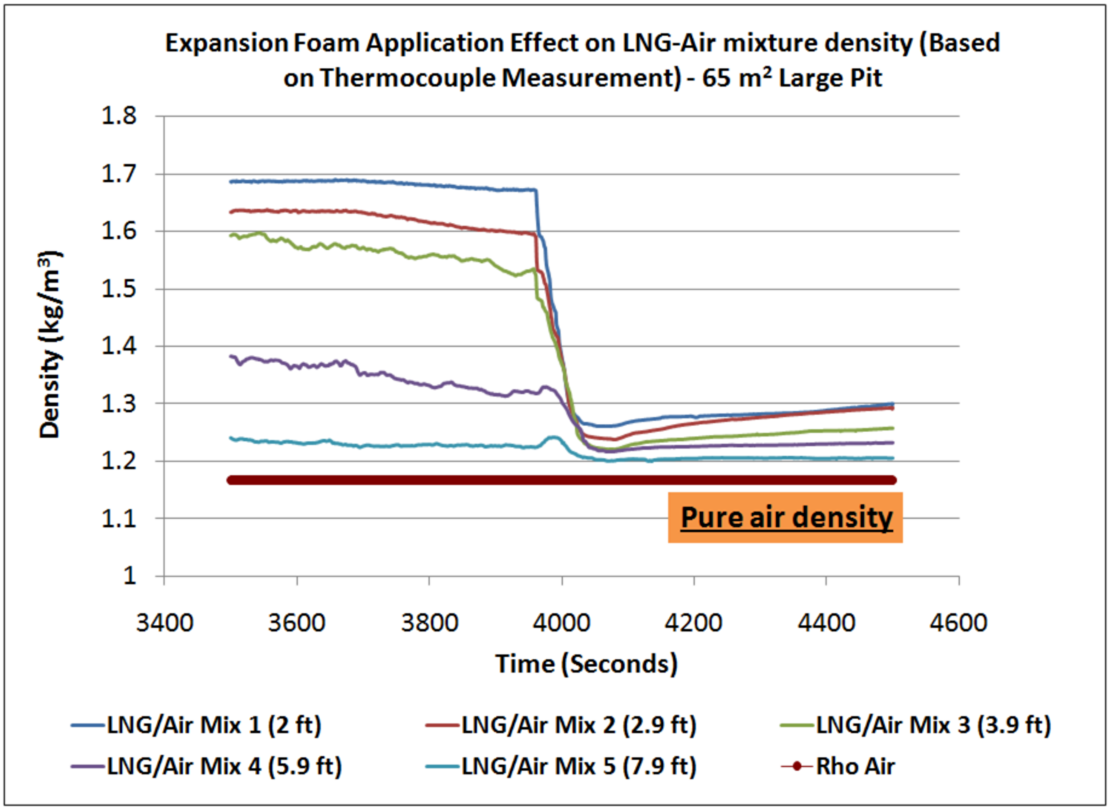

Figure 56. LNG vapor density reduction during expansion foam application – test 6

In addition to the temperature profile measurement, the hydrocarbon camera was also used to study the character of methane vapor cloud and to confirm the phenomena described above. As shown in Figure 57, the free (unsuppressed) LNG vapor dispersion when spilled on concrete produces dark and dense methane cloud that moves towards downwind instead of moving upward. This shows that the LNG is still cold and its density is lower than surrounding air density hence heavier than air. Figure 58 shows the LNG vapor characteristics once the expansion foam is applied. At the beginning of the application, during instantaneous temperature increase, the LNG evaporation rate is increased significantly as well. This phenomenon is shown as the large dark cloud on Figure 58. After one minute of the expansion foam application, the dark cloud disappear over time and warm methane cloud (shown as less dark cloud moving upward on Figure 58) occurs. This phenomenon is still going on even after 10 minutes (estimated at 9 minutes after expansion foam was stopped). This gives clear indication that expansion foam warms the LNG vapor during its travel from the LNG pool surface to the top part of the expansion foam.

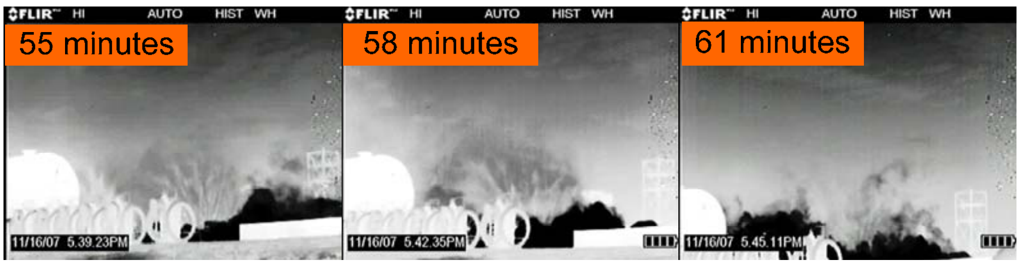

Figure 57. LNG vapor dispersion shown by hydrocarbon camera before expansion foam application during test 6

Figure 58. LNG vapor dispersion shown by hydrocarbon camera after expansion foam application during test 6

Another temperature profile measurement was conducted by installing thermocouples starting from the bottom of the pit. Thus, some of the thermocouples were located inside the LNG pool and the results are shown in Figure 59 and Figure 60. Both level temperature measurement shows that the initial LNG pool depth was less than 6 inches. In addition, both temperature measurements provides the time for the LNG to reach each of the inches of LNG pool. While evaporation rate seems can be predicted using this measurement, the result is not accurate. Thus, this can be improved in the next experiment where the thermocouple placement can be decreased to 0.5 inch distance between thermocouple.

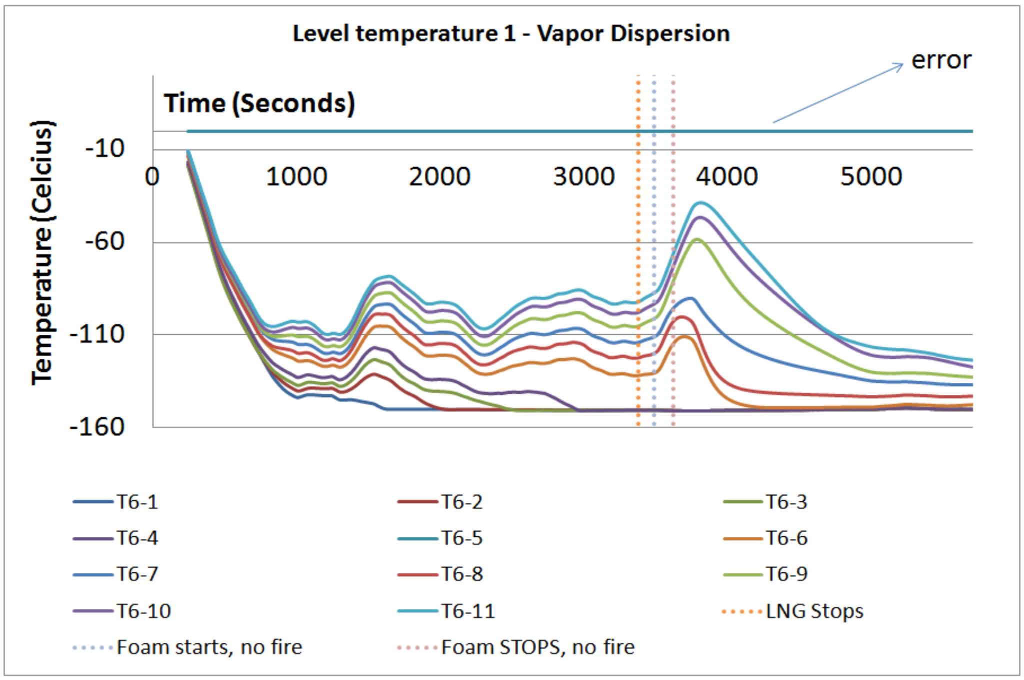

Figure 59. Temperature profile during vapor dispersion on test 7 measure by level thermocouple 1

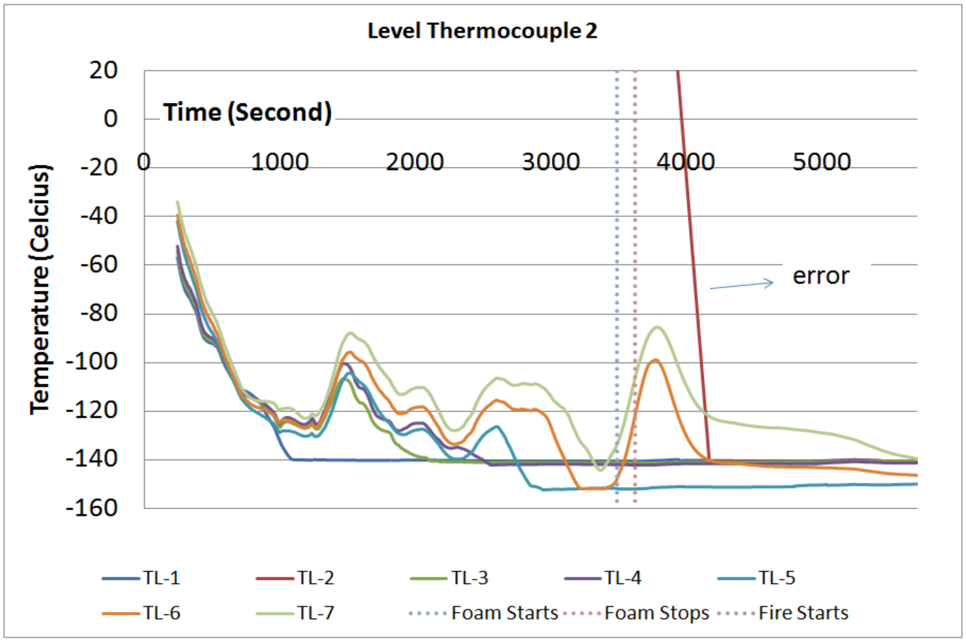

Figure 60. Temperature profile during vapor dispersion on test 7 measure by level thermocouple 2

5.3.1.2 LNG Pool Fires

Temperature profile measurement during the LNG pool fire was conducted following the completion of the vapor dispersion experiment on test 6 and test 7. The wooden walls were removed prior to the ignition thus only the first three thermocouples were inside the expansion foam while the remaining thermocouples were outside the expansion foam layer and directly exposed to the flame.

The fire during expansion foam application can be seen in Figure 61. The fire starts from the very top of the expansion foam instead of in it. Fire turbulence can be seen as part of the expansion foam was flown upward by the turbulence and at the same time the expansion foam looks "boiling" as the water inside it boil off due to the fire heat effect. During experiment, expansion foam was never overfilled the containment pit as it did on during LNG vapor dispersion experiment. This shows that fire breaks down expansion foam layer much faster than that during LNG vapor dispersion. Thus, the expansion foam was continuously applied to maintain the expansion foam layer up to 4 ft.

Figure 61. LNG pool fire with foam – test 6

As shown in Figure 62, Test 6 shows two different zones that can be analyzed, expansion foam temperature profile measured by thermocouples at 2ft, 2.9ft and 3.9ft and flame temperature profile measured by thermocouples at 5.9ft and 7.9 ft. The maximum measured flame temperature was in between 800 to 900 □C which occurs at the beginning part of fire at the very top of expansion foam layer and measured by thermocouple at 5.9 ft. Lower temperature measured by thermocouple at 7.9ft compared to the one at 5.9 ft was due to the fact that fire size decreases as being further to the top (away from the fire base). Since both thermocouples were in the flame, there is no temperature decrease throughout the fire until the fire was extinguished using dry chemical.

Expansion foam temperature profile shows different phenomenon. Once the thermocouples are covered by the expansion foam layer, the measured temperature was decreased to a temperature slightly less than 100°C. All thermocouples show the similar final temperature. This describes the behavior of expansion foam suppressing LNG pool fires. The water in the foam (which continuously supplied by continuous supply of expansion foam this experiment) receives heat from fire and starts to boil and evaporates. Thus much of the heat emitted by the fire onto the LNG pool surface was absorbed by water to create steam. The fire suppression can be maintain as long as this layer of temperature below 100°C can be maintain by providing enough expansion foam layer.

During expansion foam application at the beginning of the fire, heat from the fire destroy the expansion foam easily while at the same time expansion layer was developed. Due to this, thermocouples were covered by the expansion foam layer at different time. This is shown in Figure 62 as the first three thermocouples reached temperature below 100°C at three different times. This effect was not seen in Figure 55 where instantaneous temperature increase applied to all thermocouples during LNG vapor dispersion.

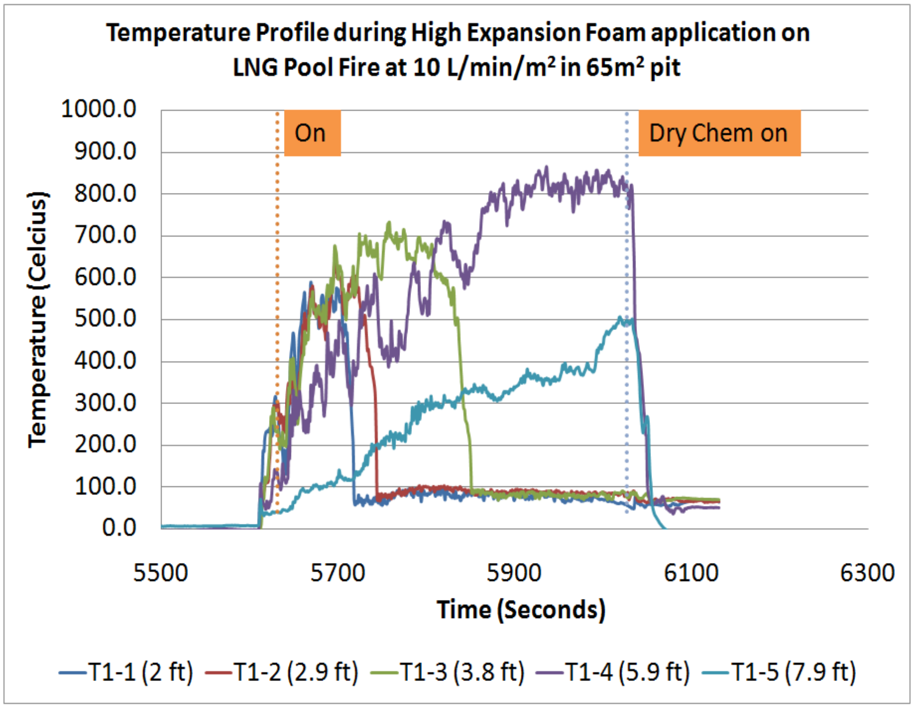

Figure 62. Temperature profile during fire in test 6

This phenomenon was also observed during Test 7, as shown in Figure 63. The first three thermocouples shows similar behavior and measured temperature of 100°C at different times. Additional information that is shown is that thermocouple at 5.9ft show similar temperature. This could be due to the fact that:

- Fire during expansion foam suppression is not homogeneous. Thus, not the entire surface is covered by the flame.
- The steam or boiling water flows upward with thermocouples was in it. This happens at location with no flame occur.

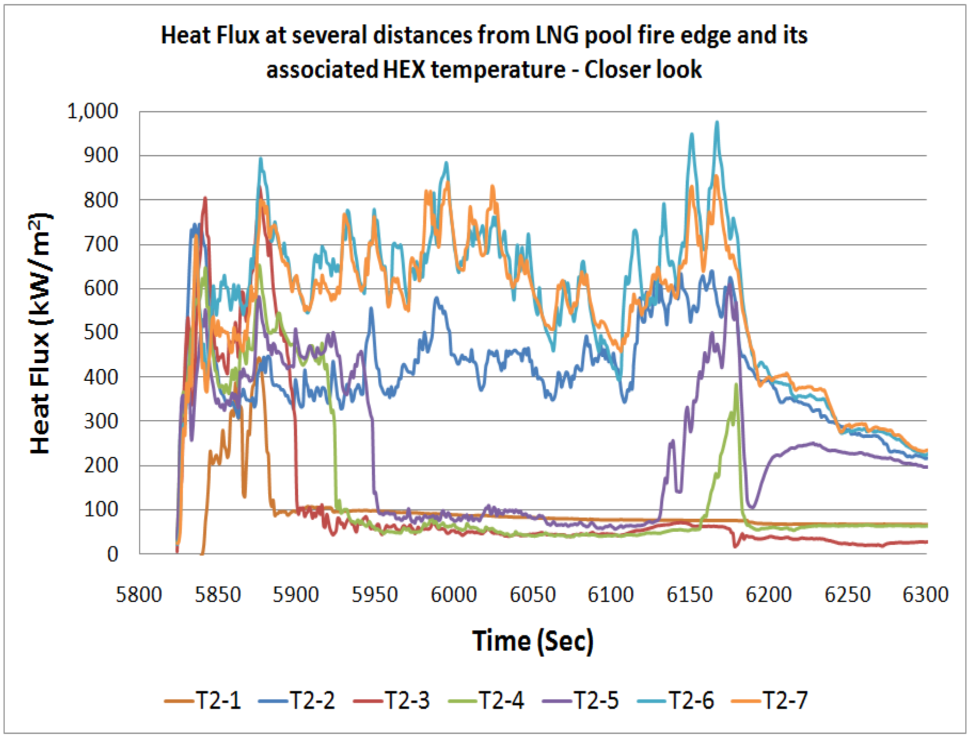

Figure 63. Temperature profile during fire in test 7

An attempt to study the scaling effect was performed on test 5. The surface area on this test was 100ft^2 compared to 760ft^2 on test 6 and 7. With the pit depth of 4ft and 2ft of LNG inside the pit, the foam was only at maximum of 2ft layer. Temperature profile shown in Figure 64 shows that similar water boiling effects were occurred. The difference lies in the fact that the fire size was smaller for the smaller pit area thus the maximum flame temperature was different. The measured maximum temperature was 450^{o}C. The lower flame temperature is based on the fact that smaller fire size has lower emissivity thus lower flame temperature.

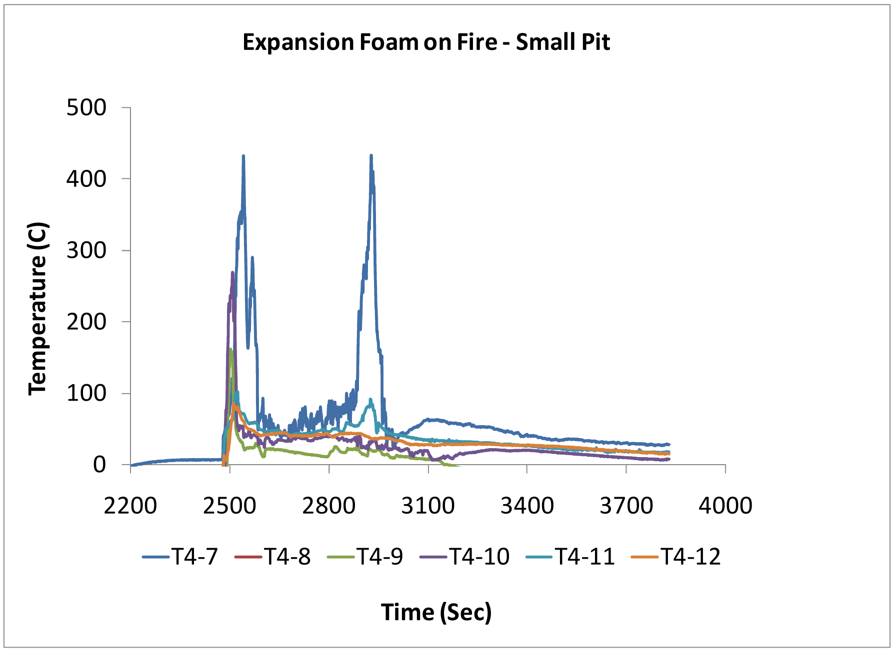

Figure 64. Test 5 temperature profiles during fire occurrence

A closer look at the temperature profile close to LNG pool surface is investigated as well. While the setup was intended to measure the evaporation rate during the experiment, the temperature profile can be studied as well. Both Figure 65 and Figure 66 show 3 inches of LNG left after experiment. This shows that total average evaporation during the whole experiment was 0.16 kg/m^2.s.

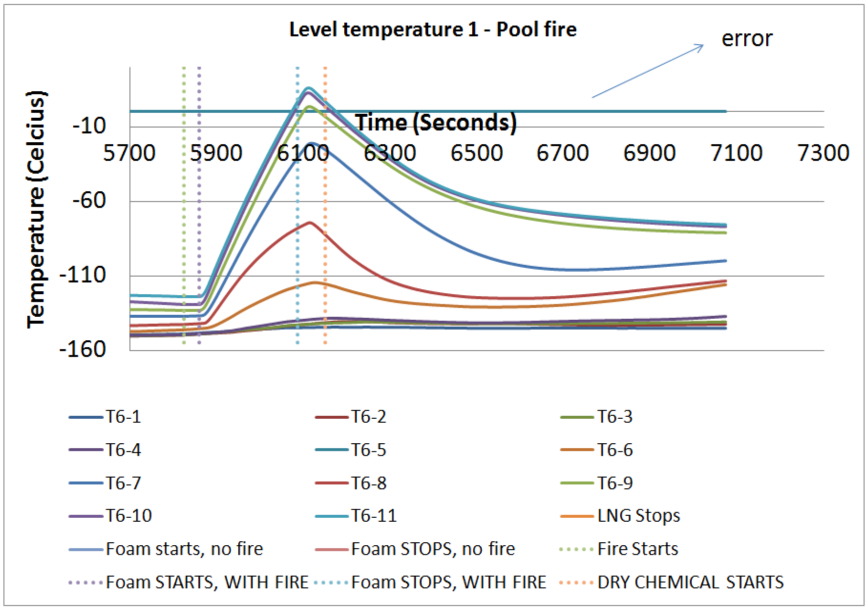

Figure 65. Temperature profile during fire on test 7 measure by level thermocouple 1

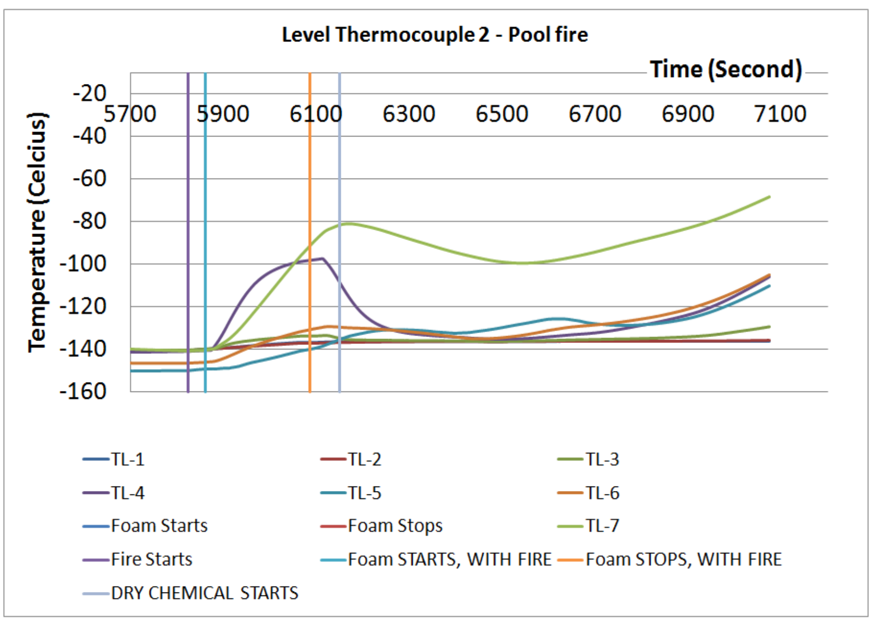

Figure 66. Temperature profile during fire on test 7 measure by level thermocouple 2

The pit condition after the fire is controlled using expansion foam and extinguished using dry chemical is shown in Figure 67. Ice layer was formed but not in the form of a block of ice. Instead, it was in the form of honeycomb ice layer.

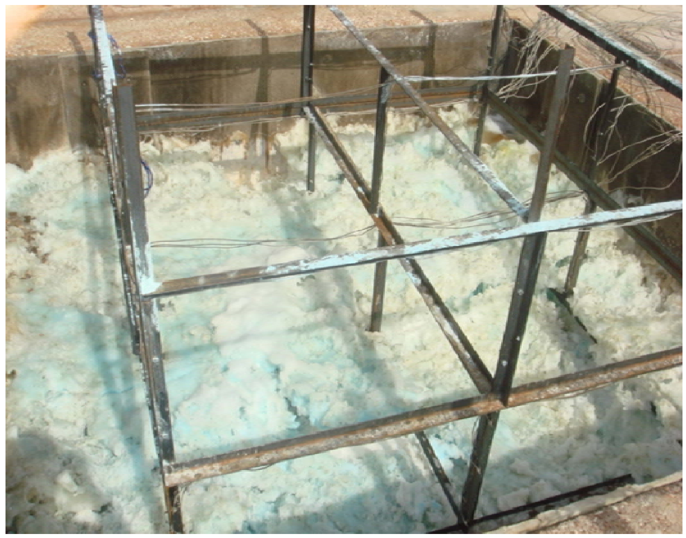

Figure 67. Pit condition after expansion foam application – test 5

5.3.2 Evaporation Rate

There were several methods applied to measure the evaporation rate:

- Pressure differential (test 7)
- Liquid thermocouples (test 7). As shown in the previous section, LNG evaporation rate for the whole experiment was 0.16 $kg/m^2.sec$
- Heat transfer calculation based on heat transfer phenomena illustrated in Figure 10

Figure 68 is obtained from the pressure differential measurement. Basically, the LNG pool liquid level was measured by using liquid hydrostatic principle. There are several finding in this as follows, as shown in Figure 68:

- LNG started at 5 inches. This measurement is different than the one measured when LNG was discharged onto the containment pit. This is due o the fact that the pit bottom is arranged in a way that water will go to the sewer system. Thus, the floor has an angle and results in different depth in different area.
- During LNG vapor dispersion and HEX was already applied, the level reduction represents the mean LNG evaporation rate of 0.15 kg/m^{2}s. This evaporation rate is based on the evaporation due to the heat from HEX and other source such as atmosphere and concrete bottom.
- LNG evaporation rate can also be based on total LNG consumed throughout the experiment (during both vapor dispersion and pool fire). It represents a reduction of 3.5 inches of LNG pool which represents an evaporation rate of 0.13 kg/m^{2}s.
- It was not easy to measure the LNG pool level using pressure differential. HEX from the vapor dispersion, ice formation, and dry chemical could affect the measurement.

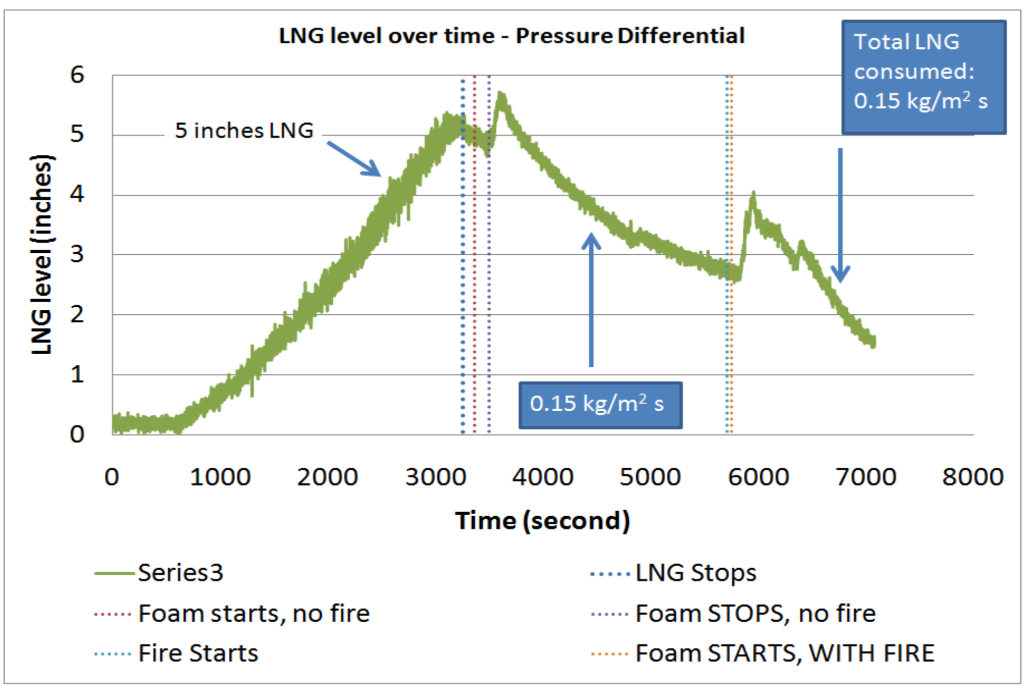

Figure 68. Evaporation rate based on pressure differential measurement on test 7

Another attempt to estimate the LNG evaporation rate was performed by using the approached presented in Figure 10. It was predicted that initially during expansion foam application; the LNG evaporation rate was instantaneously increased up to 0.7 kg/m^2.sec and then decreased to 0.17 kg/m^2.sec. During LNG pool fire, it is estimated that the LNG evaporation rate (or burning rate) before expansion foam application is 0.3 kg/m^2.sec which then lowered to 0.19 kg/m^2.sec. The evaporation rate profile for this approach is shown in Figure 69.

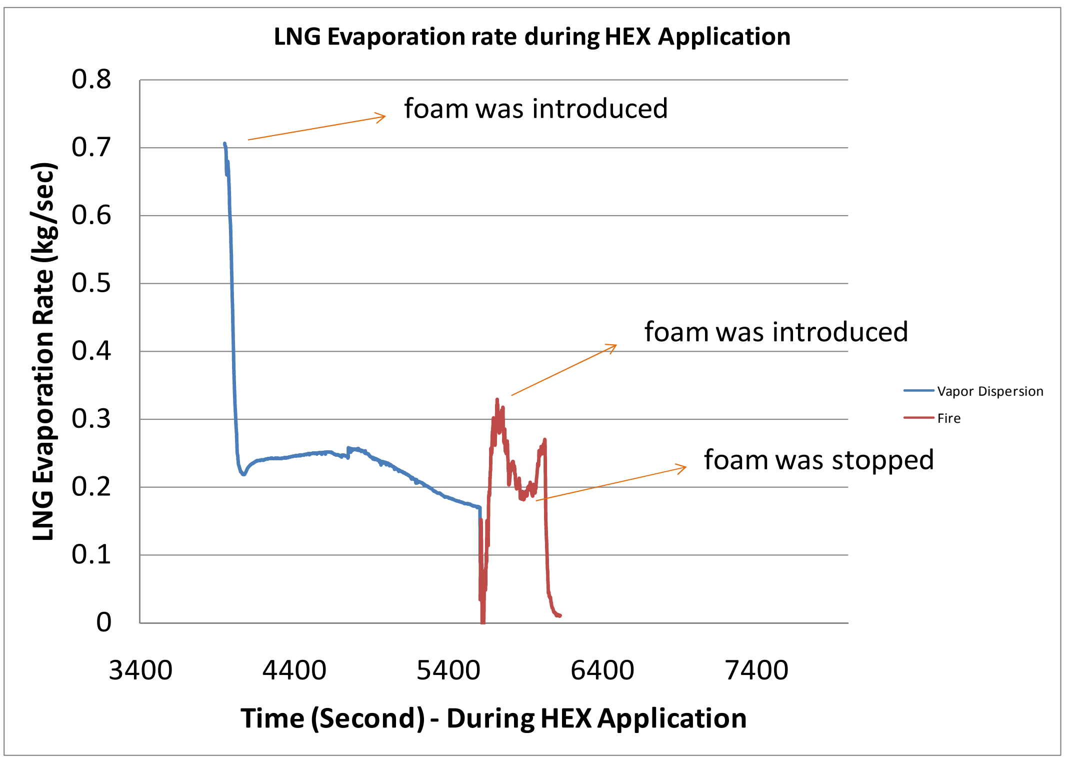

Figure 69. LNG evaporation rate based on heat transfer calculation

5.3.3 Gas Concentration

Gas concentration measurement was conducted to measure methane concentration before and after HEX application. This data is based on test 7. From many gas detectors, due to the wind changes and experimental procedures, only 6 gas detectors placed above the containment pit presented results that can be analyzed. As shown in Figure 70, the range of concentration reduction is between 6.6% to 29% concentration reductions. While this data is not enough to quantify the concentration reduction, the experiment was very useful to setup the base for the future work where concentration profiles should be captured.

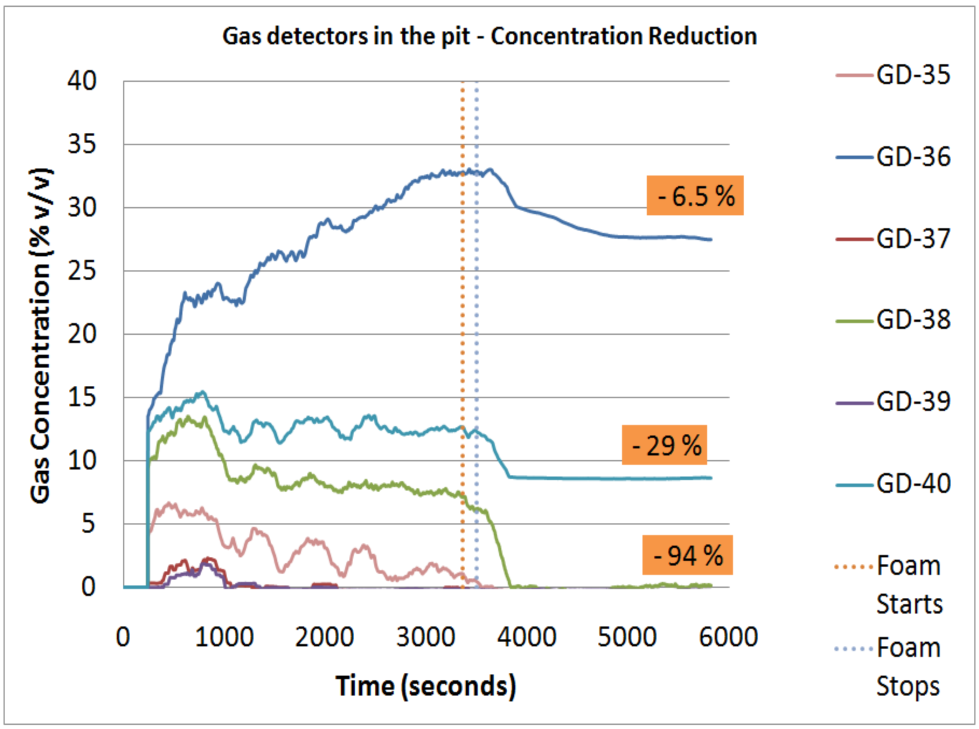

Figure 70. Gas concentration reduction shown during test 7

5.3.4 Heat Flux

This data was obtained from the test 7. Heat flux was measured using five heat flux transducer (radiometer) purchased from Medtherm corporation. The heat fluxes measured were the incidental heat flux. Thus, only the radiations from the fire that were measured. Figure 71 shows the heat radiation at several radiometer placements and measured during the experiment. The distance is measured from the edge of the pit at crosswind direction. Without HEX application, it was measured that the maximum heat flux was 35 kW/m^2 occurred at 35ft from the edge of the pit. When HEX was applied, the heat flux was reduced to 5 kW/m^2.

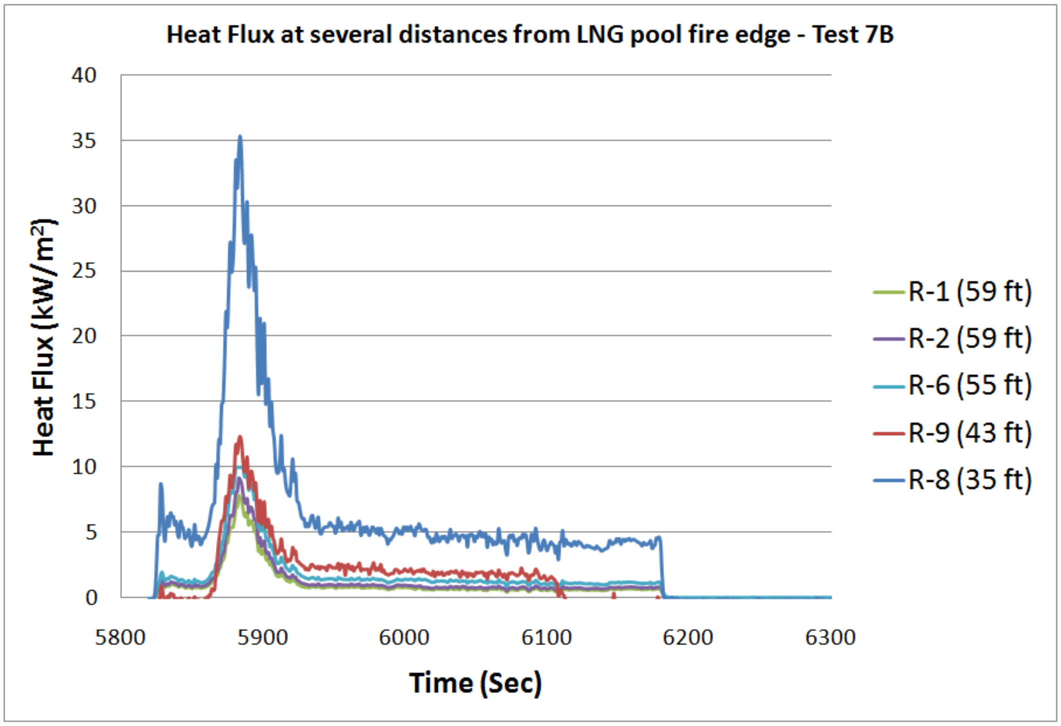

Figure 71. Heat flux measurement from test 7B

Heat flux reduction was clearly shown in this experiment and the results are shown in Table 8. The heat reduction was in the range of 87% to 91%. This heat reduction leads to the reduction of exclusion zone area. By having 5kW/m2 as the threshold for human injury, free burn (without any mitigation system) emits 5 kW/m^2 at estimated of 62ft. The same heat flux was measured at 35ft when LNG pool fire has been suppressed by HEX. This shows a reduction of 56% of the initial heat flux. This results is illustrated in Figure 72.

Table 8. Heat flux reduction during HEX application on test 7

Location from Edge of pit (ft)	w/out Foam	w/ Foam	% Reduction
60	7.8	0.7	91%
59	9.2	0.8	91%
55	10.0	1.2	88%
35	35.4	4.4	87%
43	12.4	1.2	91%

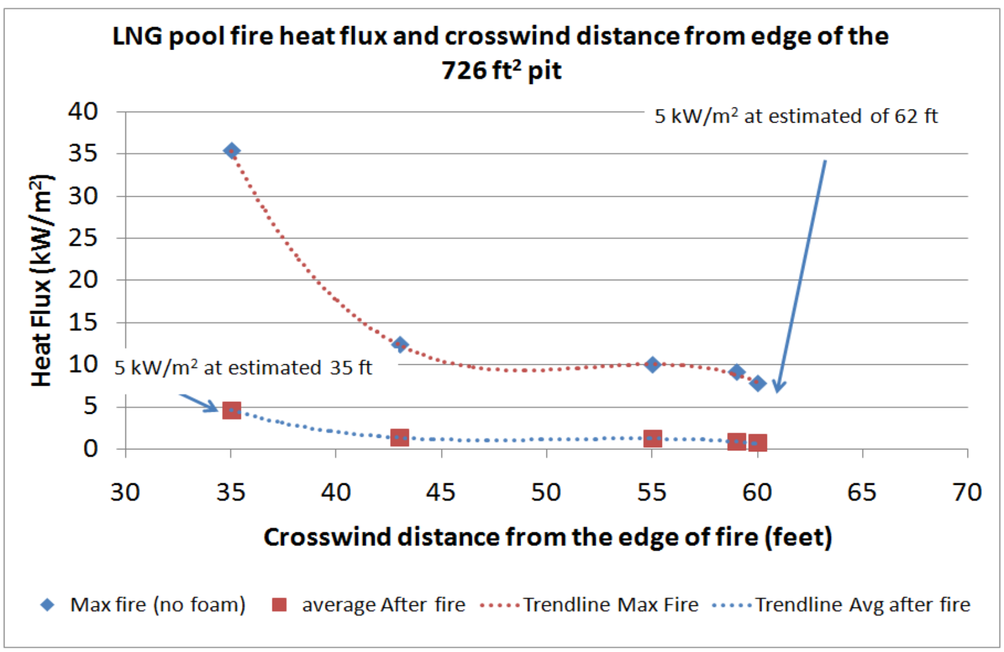

Figure 72. Heat flux at several distances before and after HEX application on test 7

One of the significance in this experiment is it is able to relate phenomena occurs in the foam with the heat reduction. This is clearly shown in Figure 73 where the radiant heat at 35ft was plotted together with the temperature profile when HEX was controlling the

LNG pool fires. It is clearly seen that during the increase of heat flux, the measured temperature was also increasing. The heat flux reduction begins when the first layer of HEX was developed and the reduction continues while the HEX layer is growing in depth. This clearly indicates that the water boiling effect affects the heat flux reduction.

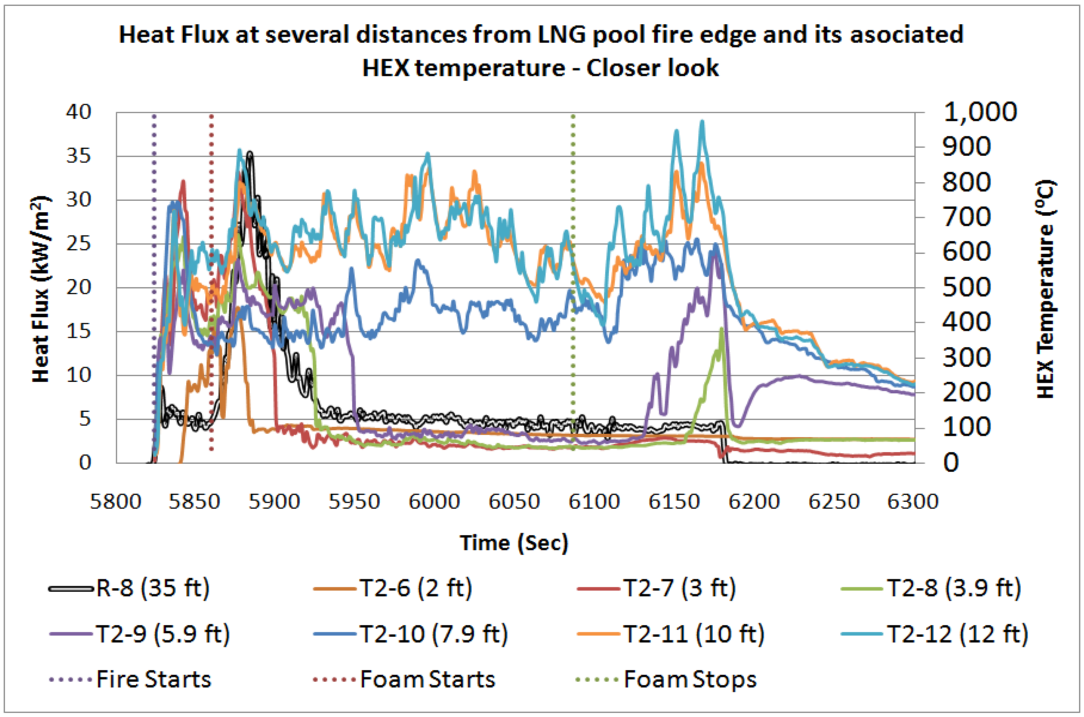

Figure 73. Heat flux at 35ft with its associated HEX temperature profile – test 7

6 FOAMGLAS®PFS RESULTS AND FINDINGS

Although Foamglas® has been used as insulation in pipelines and in storage tanks, industrial application experience has been limited in the area of suppressing LNG vapor and pool fire suppression. The following are several important characteristics of Foamglas® PFS that builds confidence in having Foamglas® PFS as a potential alternative for LNG vapor and fire mitigation [10]:

- It is "solid foam" that acts as a floating barrier to insulate a burning liquid surface.
- It is a nonflammable material.
- Its density is less than one third of LNG's density (Foamglas® PFS's density is 130kg/m^3), and thus floats on LNG pool surfaces when LNG spills. It remains independent of the amount of LNG pool depth, and creates constant coverage during the spill when applied correctly. Current Foamglas®PFS technology is able to reduce the density to less than 120kg/m^3 without compromising the performance.
- It has a completely closed-cell structure; as a result, no LNG liquid is absorbed during contact.
- Its softening temperature is 730 °C hence the structure is stable at flame temperature, and the effectiveness is not reduced; thus, no re-application or further coverage maintenance is required.
- It is waterproof, impervious to water vapor, acid resistant, and is easily cut to shape. It has high compressive strength, and is also dimensionally stable.

Foamglas® PFS can be easily arranged to take the shape of the spill containment pit. Generally, it is packed as block within a UV-resistant polyethylene bag to facilitate installation and protect the Foamglas® PFS from various weather conditions, as shown in Figure 74. When the LNG pool fire starts, the polyethylene cover is burned, and small cubes are distributed to cover the liquid surface. A LNG pit, bund, or trench can be fully covered by FOAMGLAS® PFS.

There has been only one previous experiment with Foamglas® for suppression of LNG pool fires, which was performed by Shell Research [10]. LNG pool fire radiant heat with and without Foamglas® were measured and recorded, but did not include other important data such as the effectiveness Foamglas® in suppressing LNG vapor dispersion, LNG burning rate or LNG pool evaporation rate during the application of FOAMGLAS®. The proposed experiment is expected to add more understanding of the effectiveness of FOAMGLAS® as an alternative mitigation measure.

Figure 74. FOAMGLAS® PFS block

This research aims to measure the performance of Foamglas®PFS in suppressing both LNG vapor dispersion and pool fire thermal radiation. This experiment was performed in collaboration with the Pittsburgh Corning Corporation, which was the Foamglas® PFS technology provider.

This experiment was part of a series of LNG medium field experiments conducted by MKOPSC of TEEX of Texas A&M University on November 16-17, 2007. Thus, some of the data such as LNG free burn and LNG free vapor dispersion was shared with the Foamglas® PFS Experiment.

6.1 Foamglas® PFS Application on LNG Pool Fire

Once the LNG vapor was ignited, the fire conditions were observed to study the phenomena. The fire was stable without much fluctuation, illustrating that the coverage is maintained by Foamglas® PFS without any need to apply additional materials.

6.1.1 Foamglas Temperature Profile

Figure 75 (A) and (B) show the temperature profiles in one pole where five thermocouples were placed. There were two different peaks representing two different LNG pool fires, and the valley in-between illustrating the temperature after dry chemicals (DC) were applied to extinguish the fire. LNG pool fire Solid Flame model states that [13]:

$$q = EF\tau$$

Where q is the radiative heat flux received by the object, an average value of thermal radiation flux emitted by the fire surface, F is the view factor and τ is the atmospheric transmissivity. It is very clear that view factor is important in determining the heat flux received by the object. In this experiment, as shown in Figure 75, it is important to understand that the first three thermocouples (0.6 m, 0.9 m, 1.2 m above the pit floor) were inside the pit; thus, the radiation emitted by flame temperature of 590°C to 790°C was not received by the object outside the pit and the view factor became lower. Only the top part of the fire, (temperature of 200°C to 500°C) where the radiation was lower, can be "viewed" by the object. This phenomenon helped reduce the radiant heat received by the object.

Even though the maximum temperature achieved in the experiment was comparable to the one obtained from the expansion foam application on the LNG pool fire experiment (for the same type of experiment pit), the main difference lies in the view factor of the fire. Since the surface of Foamglas ® PFS was only 7.5 inch above LNG, the fire starts in the pit (at approximately 2 feet below the ground level) while expansion foam was applied to fully fill the pit, and the fire starts from the top. Thus, with the same size of fire, the view factor of the LNG pool fire after being suppressed by Foamglas® PFS was lower.

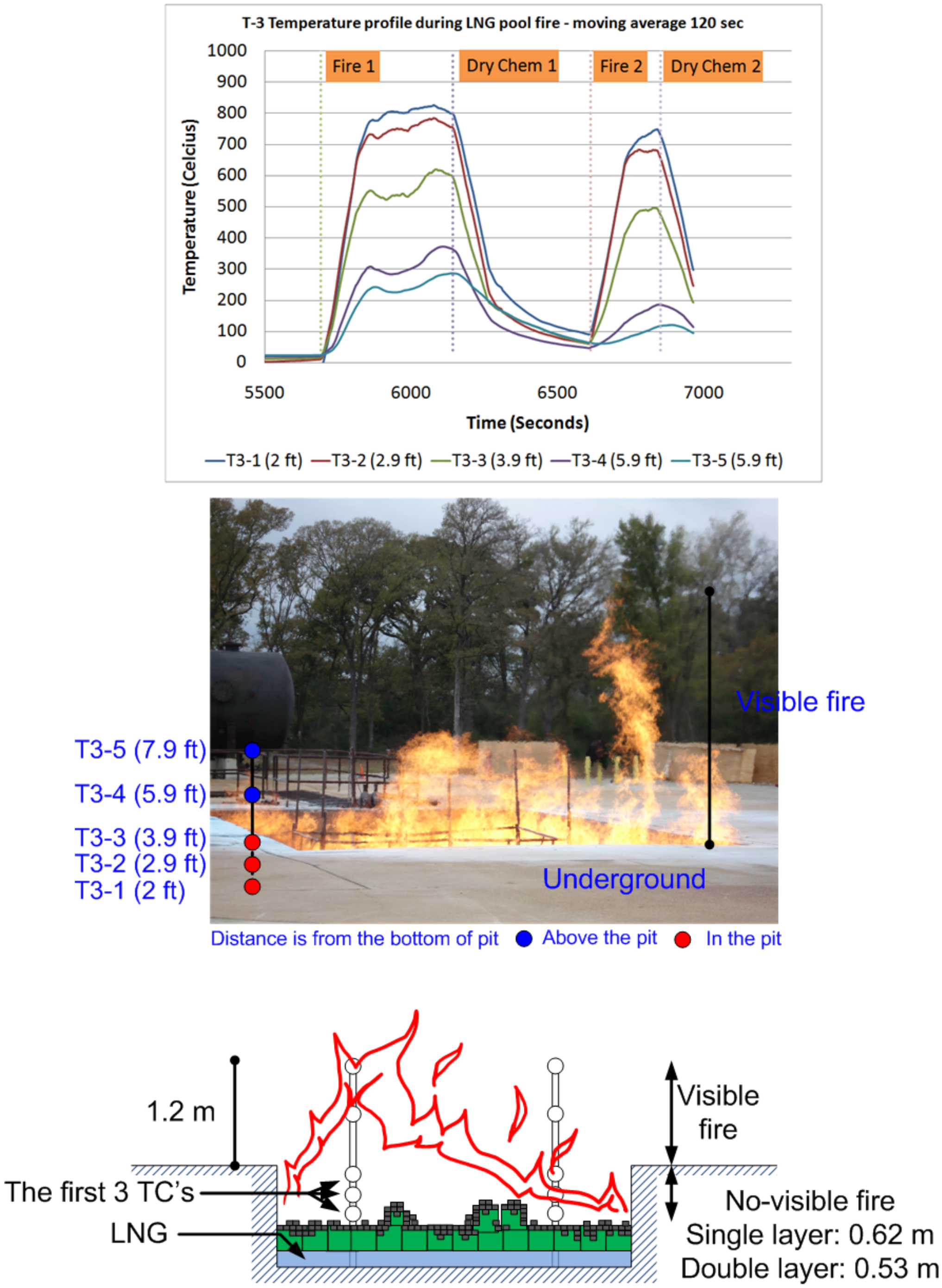

Figure 75. Fire temperature profile (A), fire and thermocouple location (B), and fire illustration (C) during Foamglas® PFS application

As shown in Figure 76, during the first few seconds of LNG ignition, the fire was large. This was due to the fact that LNG vapors that are already in the pit burn during this phase (approximately 75% of the pit filled with LNG vapor). However, after 11 seconds, the visible fire (above the pit) becomes stable and stays not much higher than four feet high above the pit. Thus, heat radiation comes only from this part of the fire.

The LNG pool fire was then extinguished by applying dry chemical for ten seconds from a 120 lb dry chemical system (wheeled-unit). The maximum flame temperature of 790 °C did not burn the lower portion of the polyethylene bags. This was observed in several locations. Additionally, after 12 minutes of fire, only the exposed outer portion of the Foamglas® PFS cubes were discolored and damaged; therefore, the system continued to perform as designed. Figure 77 illustrates the condition of Foamglas® PFS after the experiment.

Figure 76. LNG pool fire during Foamglas® PFS application

Figure 77. Foamglas condition after the experiment

6.1.2 Temperature Profile at Different Locations in Visible Fire

In this section, the comparison of temperature profile during LNG pool fire when Foamglas® PFS and expansion foam are applied is presented based on results shown in Figure 78. There are five thermocouples were placed in different locations from the bottom of the pit, which are 2ft, 2.9ft, 3.9ft, 5.9ft and 7.9 ft. While the first three thermocouples showed different temperature profile, the results cannot be compared as Foamglas® PFS and expansion foam provides different mechanism in suppressing LNG pool fire. Expansion foam creates insulation in between LNG pool fire and the LNG pool surface. The radiant heat reduction is caused by the heat absorbance by the water in the foam to create steam. Thus, the first three thermocouples, which are in the foam layer, show temperature of less than 100^{o}C, which is a boiling point of water to become steam. As long as this temperature is maintained, the insulation works. This phenomenon does not occur during Foamglas® PFS. The insulation layer is the 0.2 m above the LNG pool surface. Thus, all thermocouples are in the fire. This results in higher temperature of the first three thermocouples. However, please note two things:

- Fire in this region is inside the pit and invisible fire thus does not emit fire to the object outside the containment pit, as shown in Figure 75.
- Flame maximum temperature (at 2 ft from pit bottom) during Foamglas® PFS application is almost similar to flame maximum temperature during expansion foam application, which is measured at 5.9 ft from pit bottom and approximately 2 ft from the top of expansion foam layer where the flame is visible.

The other thermocouples that were placed at 5.9 and 7.9 ft can be compared as well. During Foamglas® PFS application, thermocouples shows a maximum temperature of 300^{o}C to 400^{o}C respectively. In overall, flame temperature goes down along with the increase height. On the other hand, during expansion foam application, the fire starts at 4 ft from the pit bottom, which is right above expansion foam top part layer. Thus, the maximum measured flame temperature was 800^{o}C at 5.9 ft and decrease to 300 to 400^{o}C at 7.9 ft.

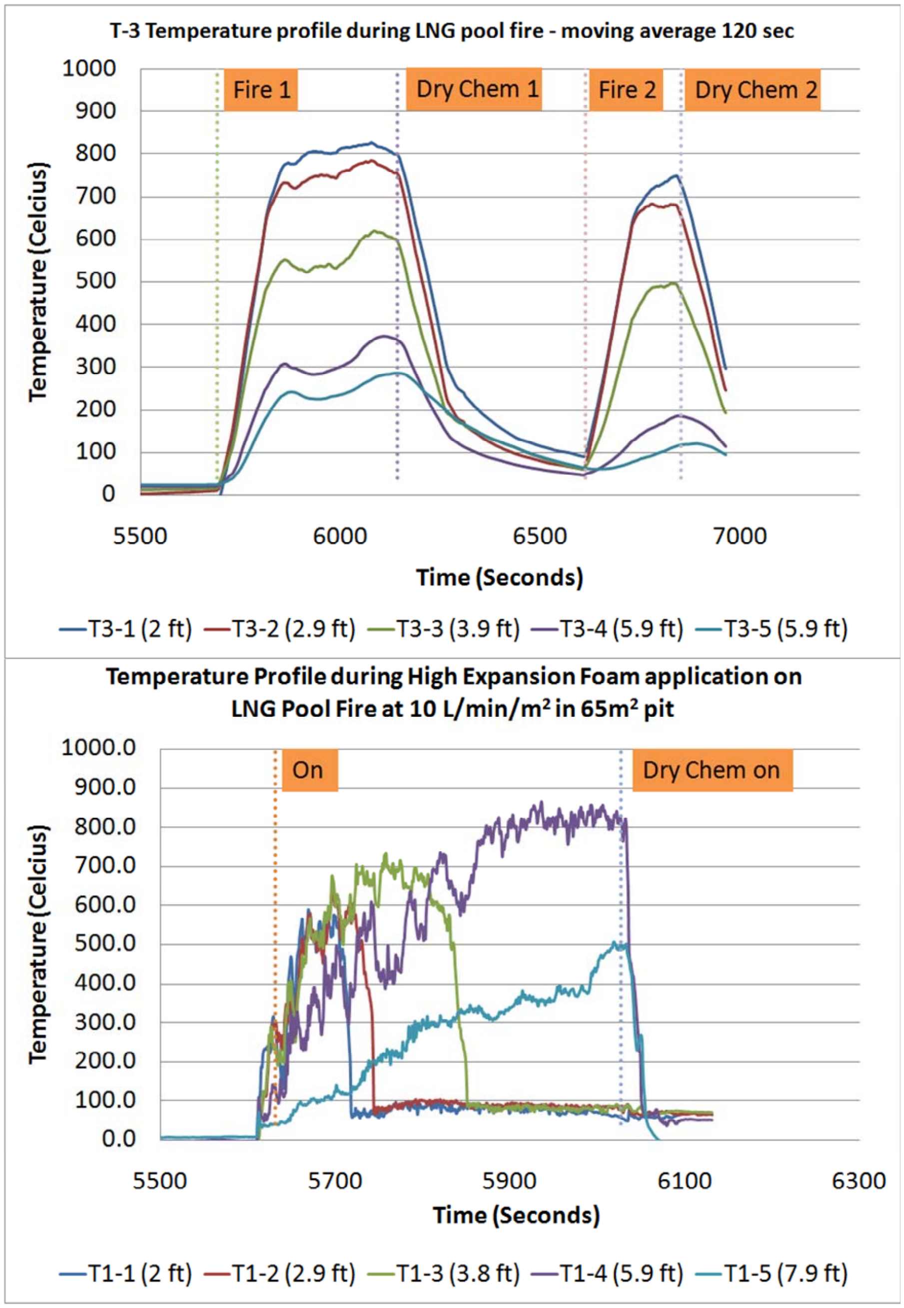

Figure 78. Temperature profile : Foamglas(R) PFS and expansion foam application

Based on temperature profile, conservative assumption can be taken. During Foamglas® PFS and expansion foam application, maximum measured flame temperature can be the same. The main difference is the visible and invisible fire locations. The visible flame maximum temperature during Foamglas® PFS application is lower than the flame temperature during expansion foam application.

6.1.3 View Factor

Based on the experiment data shown in Figure 75, view factor plays important role in explaining the difference between Foamglas® PFS suppression and expansion foam. Comparison of view factor and its associated effect on the LNG pool fire radiant heat during the suppression can describe the effectiveness of Foamglas®PFS. The view factor calculation can be performed by using the following equation [28]:

$$F_{d1-2} = \frac{1}{\pi H}\mathrm{Tan}^{-1}\left(\frac{L}{\sqrt{H^2+1}}\right) + \frac{L}{H}\left[\frac{X-2H}{H\sqrt{XY}}\mathrm{Tan}^{-1}\sqrt{\frac{X(H-1)}{Y(H+1)}} - \frac{1}{H}\mathrm{Tan}^{-1}\sqrt{\frac{H-1}{H+1}}\right]$$

$$L = \frac{h}{r} \qquad H = \frac{R}{r} \qquad X = (1+H)^2 + L^2 \qquad Y = (1-H)^2 + L^2$$

The view factor calculation could also be used to calculate the radiation heat flux based on both view factor and flame temperature. Rew Et al. [29] suggests that for LNG, the following equation can be used for estimating flame surface emissive power, as follows:

$$E = E_{\infty}\left(1 - e^{k_m D}\right)$$

Tien et al. [28] suggest the following equation to predict the estimate the total heat flux:

$$q = \varepsilon_m E_b \sum_{j=1}^{3} F_j$$

With [28]:

$$\varepsilon_m E_b = E$$

$$E_{\infty} = \sigma T_f^4$$

$$\sigma = 5.67\,E - 11$$

And [30]

k_m for LNG = 0.452 m^{-1}

Based on the spectral data obtain during the Montoir 35m-diameter LNG pool fire experiment, the LNG is basically a gray-body emitter. It corresponds to a black body at temperature (radiative) of 1547 K and with a mean emissivity of 0.92 [31]. Based on equations and data obtained from the experiment, the following calculation can be illustrated in Figure 79. Please note that the calculation is conducted to study the effect of view factor and flame temperature to the flame surface heat flux.

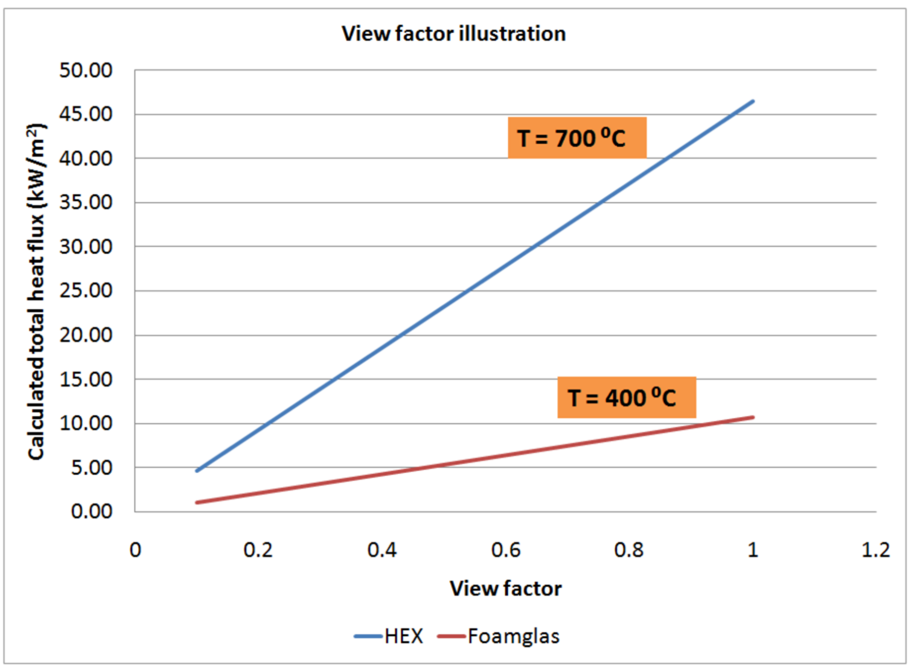

Figure 79. View factor

Flame temperature at 5.9 ft is used, where flame temperature during Foamglas® PFS application was 400°C while flame temperature during expansion foam application was around 700°C. Figure 79 illustrates that with the same view factor, lower flame temperature has lower surface emissive power. At the same time, the increase of view factor increases the heat flux as well. The calculation is performed by taking conservative assumption of flame height during Foamglas® PFS application was 2 feet lower (this part of the flame is in the fire). The total flame height during application of both mitigation systems is considered the same to see the view factor. View factor during Foamglas® PFS application is 0.61 compared to 1 for expansion foam. By incorporating the flame temperature, this represents a heat flux of 6.6 kW/m^2 during Foamglas® PFS application and 46.7 kW/m^2 during expansion foam application. While this could be different if the heat flux would have been measured by radiometer, this calculation shows that Foamglas® PFS application is effective in reducing the view factor when the pit height is less than the fire height.

6.2 Foamglas® PFS Application during LNG Vapor Dispersion

The effectiveness of Foamglas® PFS to suppress LNG vapor dispersion was studied. Foamglas® PFS experimental data were compared to the experimental data from expansion foam experiment conducted the previous day. The following experimental data were analyzed:

- Temperature profile
- Hydrocarbon camera video
- Gas concentration

6.2.1 Temperature Profile with Foamglas®PFS Application

Thermocouples at 0.6m, 0.9m, and 1.2m measures temperature in between -100°C and -150°C, as shown in Figure 80. This is due to thermocouples locations that were located closer to the LNG pool surface. However, this situation changed when the LNG controlled-spill was stopped and the gas temperature in the pit was increased. As, illustrated in Figure 81, this might be due to the fact that there were two LNG vapor sources:

- The first source was the LNG flashed from the LNG discharge line during the continuous spill. The LNG vapor is heavier than air vapor and was therefore naturally filled the pit above the Foamglas® PFS surface.
- The second source was from the evaporating LNG pool underneath Foamglas® PFS layer. The space between Foamglas® PFS units may be the only avenue for LNG vapor to disperse into the atmosphere. While in an unmitigated spill, vapors are generated and move upward over the entire LNG pool surface area. Foamglas® PFS on the LNG pool surface blocks the vapor flow and creates channeling (space between blocks) for LNG vapor to flow, as described in Figure 81. A non-homogeneous vapor pocket occurs and establishes “Venturi Effect” where large area of vapor space above LNG pool surface becomes smaller when moving upward through the channel with higher speed. This following was observed:
    - The thermocouples were not located in the cloud; therefore a higher methane and air mixture temperature was measured.
    - Less gas dispersion in the pit compared to outside the pit and compared to continuous spill, creates less mixing between methane and air which results in lower temperature.

Another analysis was conducted to study the effect of Foamglas® PFS as the heat source to warm the LNG. Before proceeding, the possible heat sources were identified. Briscoe and Shaw [32] illustrated the variation of heat flux into evaporating LNG pool. Heat from solar radiation and the atmosphere accounts for less than 5% (if heat transfer from the ground is 30 kW/m^2 and heat transfer from solar radiation and atmosphere is 1 kW/m^2). Insulating the LNG pool from solar radiation and atmosphere might not provide significant vapor suppression.

Foamglas®PFS does not provide additional heat to the pool except, possibly, at the beginning of the spill when the temperature difference is high. The evaporation rate may not be increased. However, no direct measurement on evaporation rate was conducted but the experimental results shows there is no effect on the LNG vapor temperature.

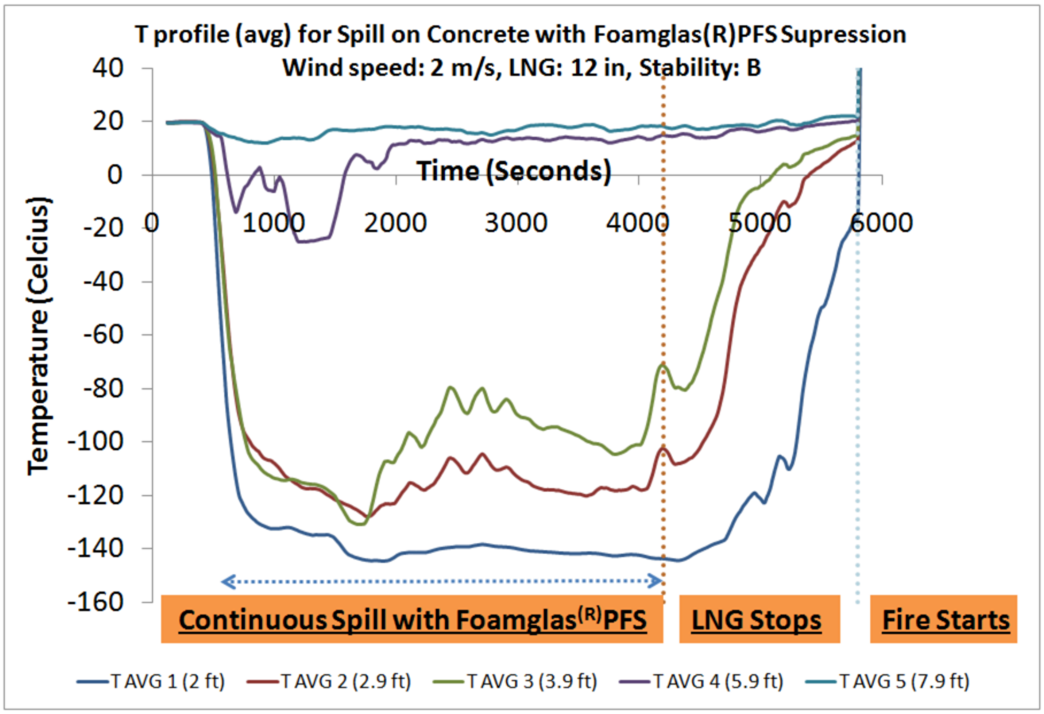

Figure 80. T average temperature profile at 240 seconds average

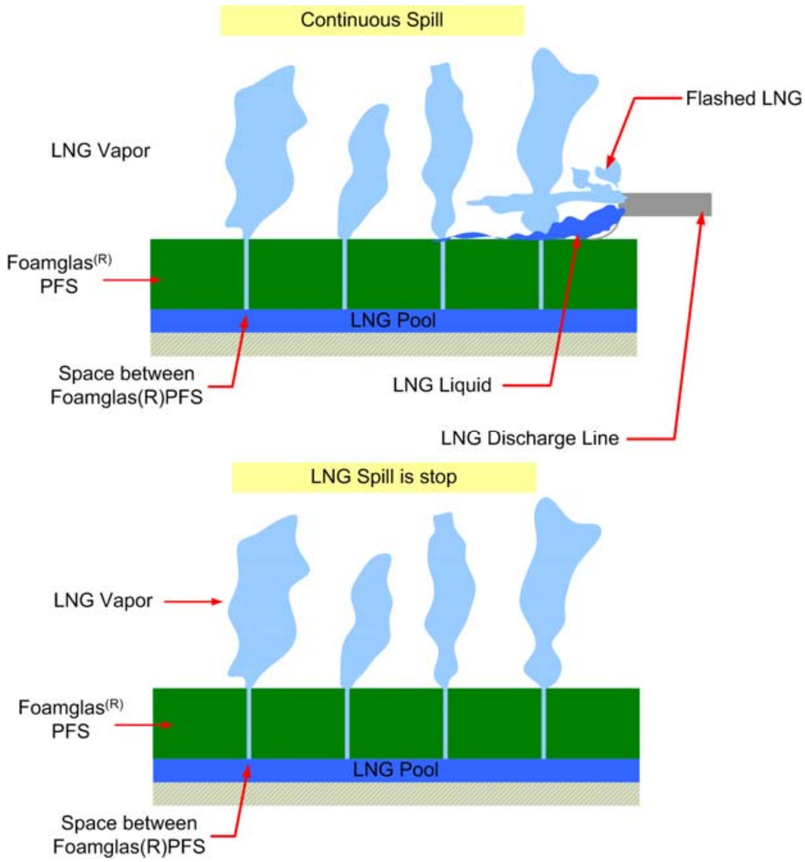

Figure 81. Gas movement in the pit - illustration

Comparison with unmitigated continuous spill and other methodologies, (e.g. expansion foam), was also performed. The experiment procedures and setup are described Figure 82. The same pit was used in this experiment. The difference was that an additional four feet of height was added using wooden walls in order to reach a height of eight feet ft of containment. The equipment was the same for both experiments. The first step consisted of a continuous LNG spill for 60 minutes to reach six inches of LNG pool in the pit. During the course of the spill, there was no mitigation system applied. Therefore, this may be a good reference for free LNG vapor dispersion.

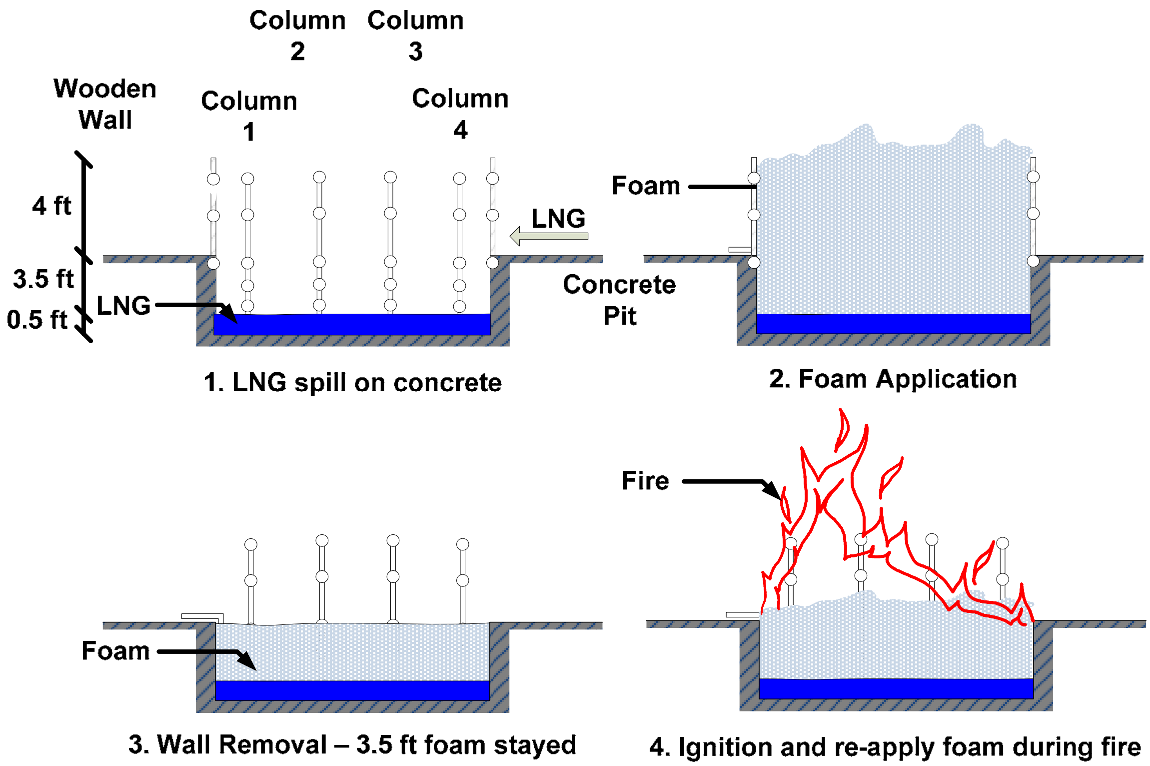

Figure 82. Expansion foam experiment

The next step of this experiment was to stop the LNG spill and apply expansion foam at 10L/min/m^2. This experiment provided comparison between the two different methodologies in suppressing LNG vapor dispersion. The walls were removed and the LNG vapor was ignited to create the LNG pool fire. This part of experiment was used to compare the performance of expansion foam with the Foamglas® PFS for the suppression of LNG pool fire.

6.2.2 Comparison with Unmitigated Continuous Spill

Figure 83 provides the temperature profile during the Foamglas® PFS experiment and the expansion foam experiment in suppressing LNG vapor dispersion. During the continuous spill, both the reference and Foamglas® PFS had similar profiles. Thermocouples that were placed at the lower location measured lower temperature as well. The difference is shown on two thermocouples placed at the height of 5.9 ft and 7.9 ft where Foamglas® PFS showed higher temperatures. This is due to the fact that the reference experiment had wooden walls installed while the thermocouples in the Foamglas® PFS experiment were placed open to air. Thus, dispersion is reached faster. Comparison of pit temperature profile in Figure 83 shows that Foamglas®PFS might not provide enough vapor mitigation and the methane cloud was still of negative buoyancy after it was dispersed outside the pit.

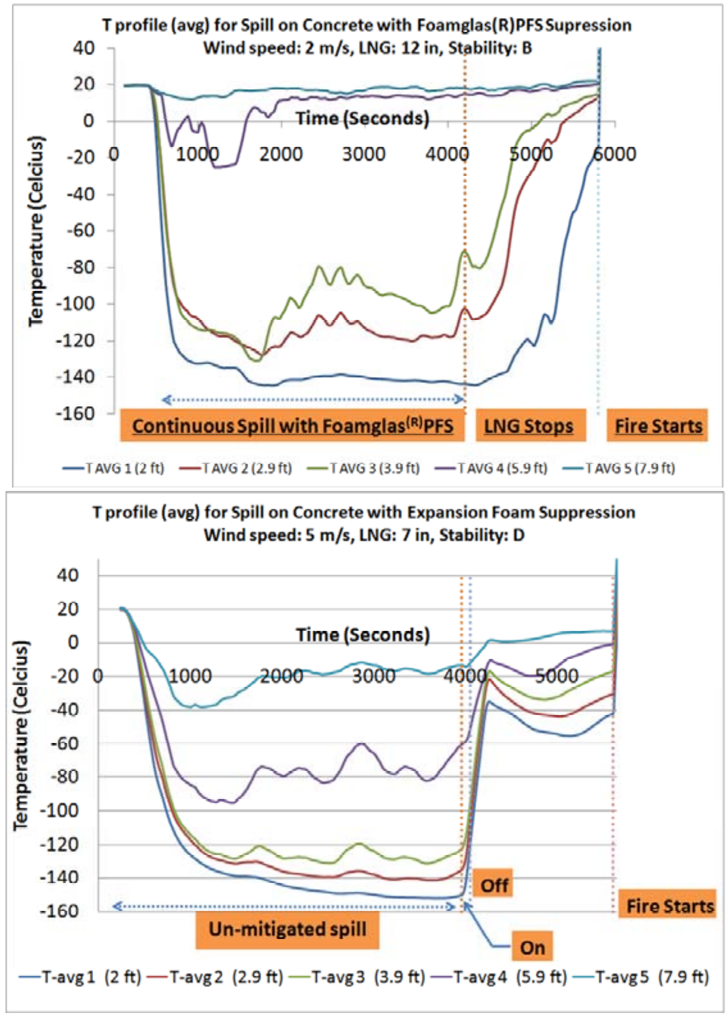

Figure 83. Temperature (average) comparison: Foamglas®PFS vs expansion foam

6.2.3 Comparison with Expansion Foam

Comparison with expansion foam confirms the results stated above. Figure 83 demonstrates that the expansion foam increases the temperature in the pit significantly. This leads to the decrease of the density of the LNG vapor mixture in the air to reach density closer to the air density. Once the mixture density was lower than the air density, the LNG vapor became more buoyant and moved upward.

Figure 84 shows the density of LNG vapor in the pit decreasing when expansion foam is applied. This may lead to a shorter amount of time and distance for the LNG vapor to reach positive buoyancy compared with unmitigated spill.

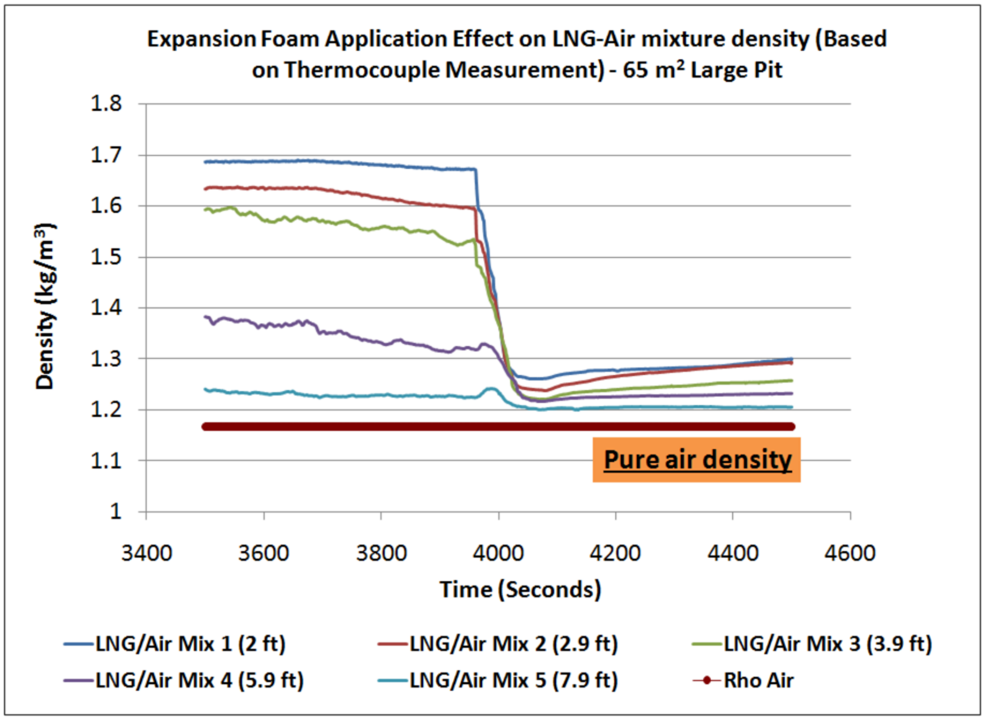

Figure 84. LNG vapor density reduction during expansion foam application

6.2.4 Hydrocarbon Camera

Using hydrocarbon camera imaging technology, a methane cloud can be captured and appears as “black smoke”. Darker color shows a colder temperature in the cloud. While the temperature profile provides some insight regarding the effectiveness Foamglas® PFS for LNG vapor dispersion suppression, there was a need to confirm this observation. Therefore, hydrocarbon cameras were used to capture the methane cloud movement and sizes during the experiment. Then, the video was compared with the video captured during the un-mitigated LNG continuous spill onto concrete and expansion-foam-mitigated LNG vapor dispersion (Spill is stopped).

Figure 85 shows that without any suppression, the methane cloud was visible as dense-dark-cloud. Most of the methane cloud moved downwind and there was no sign of an increase in temperature of the methane cloud. The cloud was still in negative buoyancy and heavier than air. A suppression system is intended to reduce the hazardous distance, which is the downwind distance passed by the vapor to reach 5% v/v concentration. Therefore, the typical suppression method is introduced as a heat source that is able to warm the vapor and reach positive buoyancy faster. This kind of phenomenon is clearly not shown by Figure 85.

Figure 86 illustrates the methane cloud when Foamglas® PFS is deployed. The Foamglas® PFS for LNG vapor dispersion experiment can be divided into two phases, a) continuous spill on the top of the Foamglas®PFS and b) vapor dispersion from LNG pool underneath the Foamglas®PFS layers. As shown by the hydrocarbon camera snapshots, the methane cloud remained dense and move downwind with no sign of significant vapor warming process. However, during continuous spill, the cloud appeared bigger compared to when the LNG spill was stopped. This occurred when LNG was released and a fraction of the discharged LNG was vaporized or flashed directly without creating the pool. Thus, the LNG vapor came from the evaporated LNG pool and the flashed LNG. This did not happen when LNG spill was stopped, and the source of the vapor was only from the evaporating LNG pool. This analysis was confirmed by the temperature measurement shown in Figure 83 where the temperature was lower (more vapor cloud) when LNG was spilled.

High expansion foam is recommended by NFPA 59A as the LNG vapor dispersion suppression method. Hence, comparison of expansion foam with this methodology characterized effectiveness of Foamglas® PFS methodology. Figure 87 illustrates the behavior of LNG vapor during deployment of expansion foam. When applied, expansion foam acts as the heat source, increasing the LNG vapor temperature and buoyancy. This phenomenon is clearly explained with temperature profile analysis. Figure 87 also shows that at the beginning, expansion foam increase the evaporation rate shown by the increased of cloud size. Then, after ten minutes, a significant amount of methane cloud was moving upward (becoming positive buoyant) while other are warmed by the expansion foam.

Theoretically, Foamglas® PFS likely provides insulation to reduce heat from solar radiation and atmosphere on LNG vapor dispersion. However, heat from solar radiation and atmosphere accounted for less than 5% in heating the LNG, while most of the heat comes from the pit surface. Thus, Foamglas®PFS likely reduces the heat from the atmosphere but the total heat reduction is not significant.

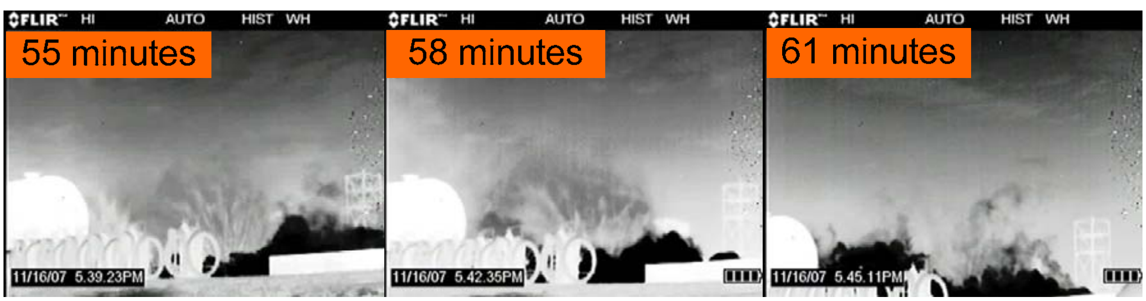

Figure 85. Un-mitigated continuous spill - hydrocarbon camera snapshots

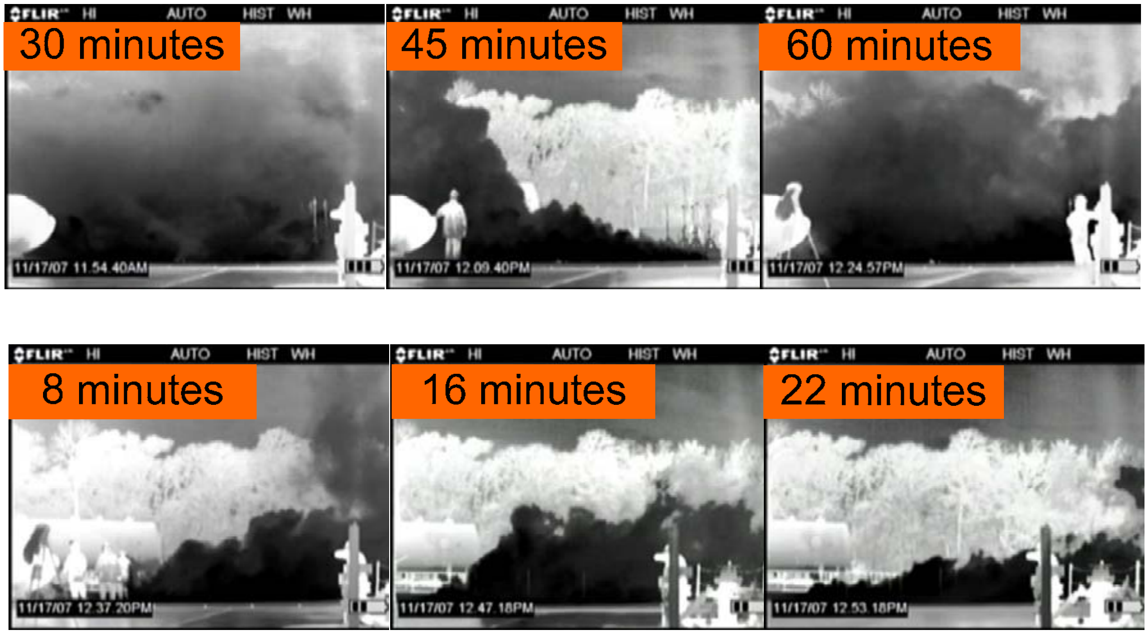

Figure 86. Foamglas hydrocarbon camera snapshots

Figure 87. Methane cloud characteristics - no suppression and with expansion foam

6.2.5 Gas Concentration

Methane concentration is measured using gas detectors. The data from Foamglas®PFS Experiment during LNG continuous spill was compared with un-mitigated continuous spill.

While other figures showing gas concentration at different placements are shown in Appendix B. Figure 88 and Figure 89 show examples of the methane concentration. Figure 88 clearly showed that the methane concentration was low at the beginning and then increased dramatically to reach a maximum value of 62% CH_4 volume by volume (v/v). Lower concentrations were observed is when the wind direction changed and moved away from the gas detectors (moving from north to south while gas detectors were placed on North). Once the wind direction shifted to the North from the South, the gas detectors were able to measure the methane concentrations. Figure 89 shows the gas concentration inside the pit; the maximum methane concentration reached 85% CH_4 v/v.

In addition to temperature profile and hydrocarbon camera data, gas detectors data were utilized to assess the effectiveness of Foamglas®PFS in suppressing the LNG vapor dispersion. The comparison was conducted by comparing the maximum value at each gas detector. Methane concentration contours were creates to see the maximum methane concentration at different placement for both experiments.

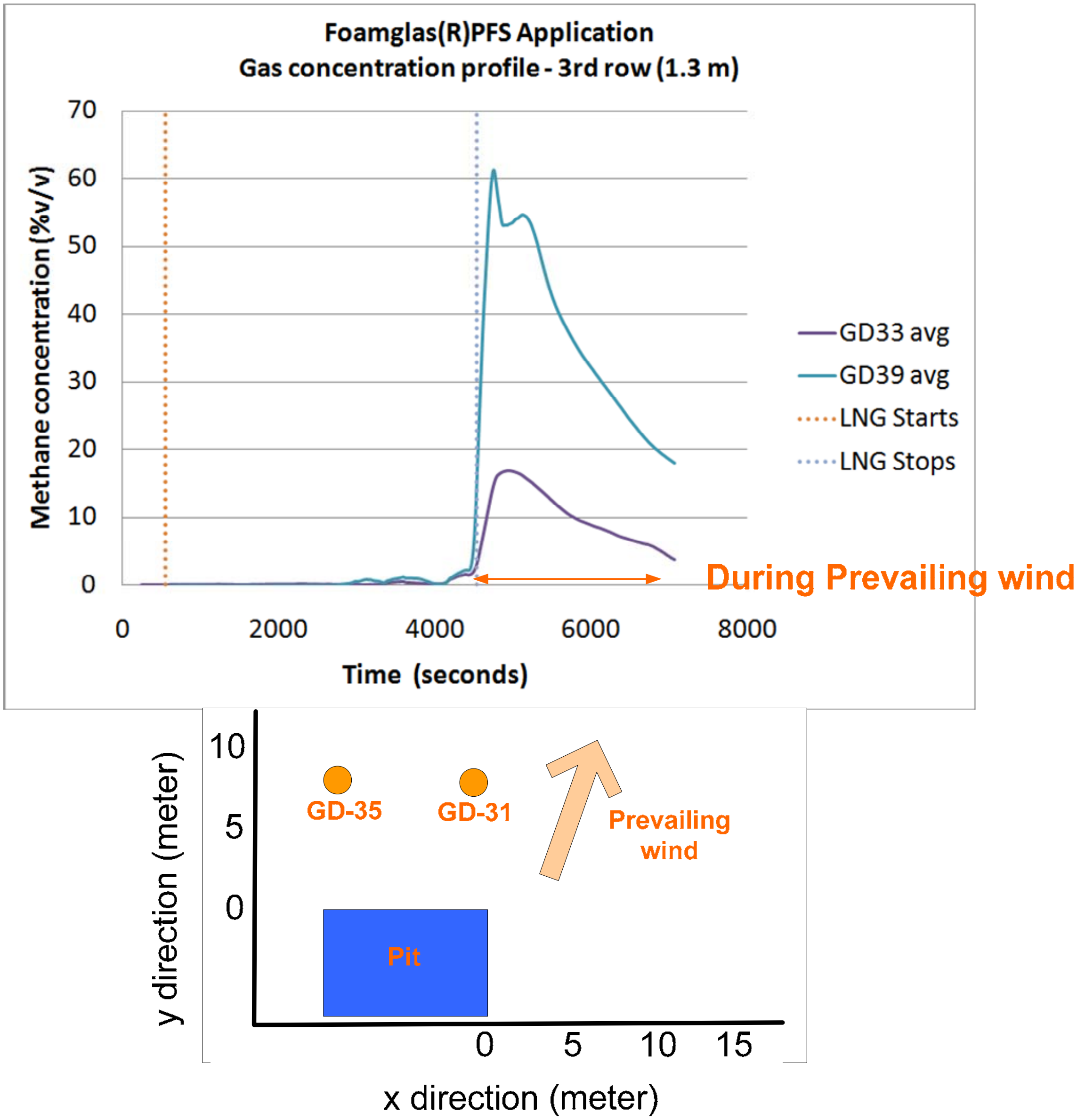

Figure 88. Methane concentration profile in the 65m^2 pit during Foamglas®PFS application

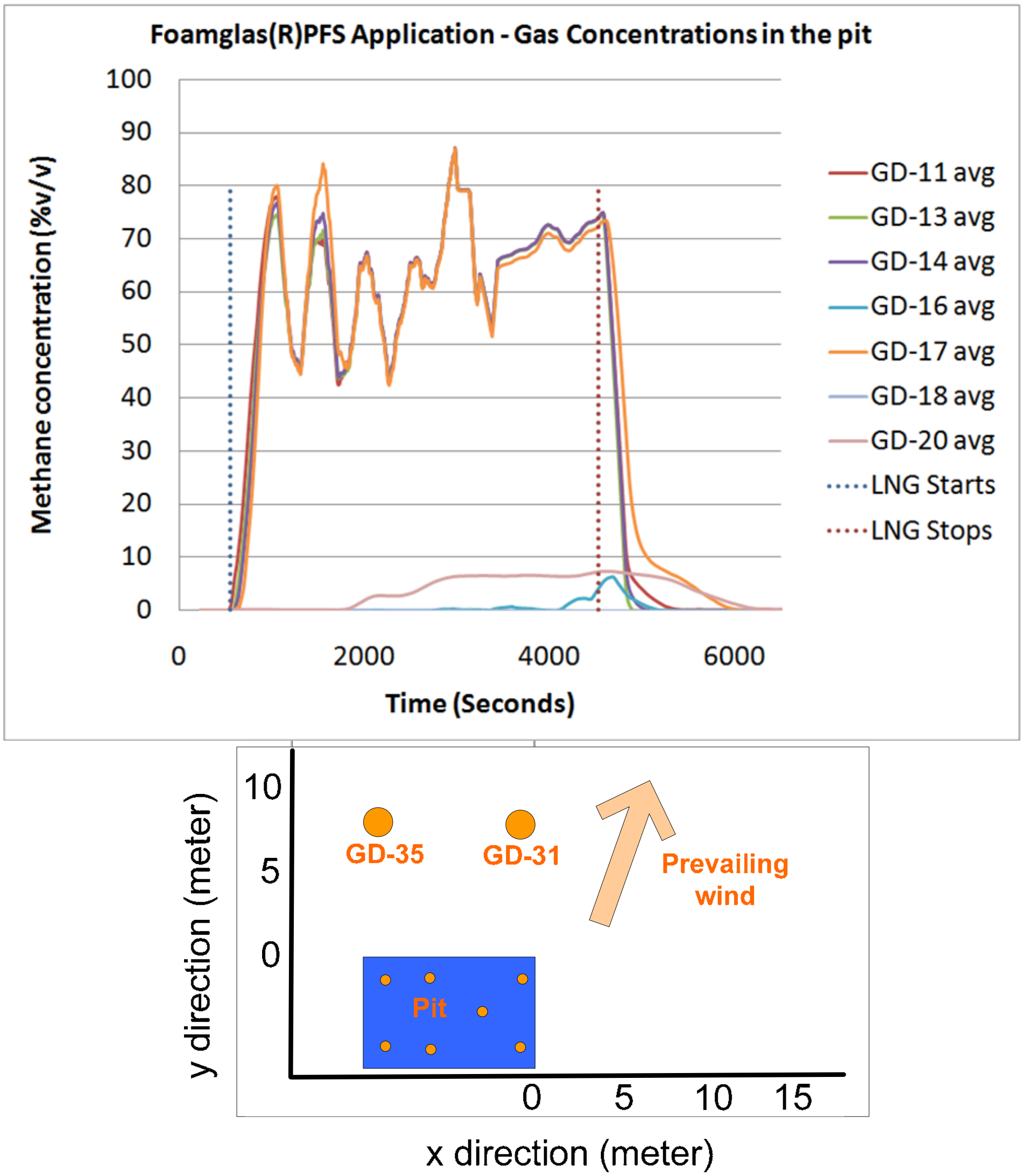

Figure 89. Methane concentration profile inside the 65m^2 pit during Foamglas®PFS application

The maximum methane concentration is shown in Figure 90. The contour shows where the gas was moving while illustrating how it was dispersed. The maximum concentration of the un-mitigated continuous spill was less than 35% CH_4 v/v. While this did not prove conclusive, at distance of x=11.4 m and y=13.4 m from the origin of the coordinate, the methane concentration of 13 to 16 % CH_4 v/v (GD-7 and GD-9) was reached using Foamglas® PFS. This did not happen during the un-mitigated spill, where the maximum concentration was 33% CH_4 v/v.

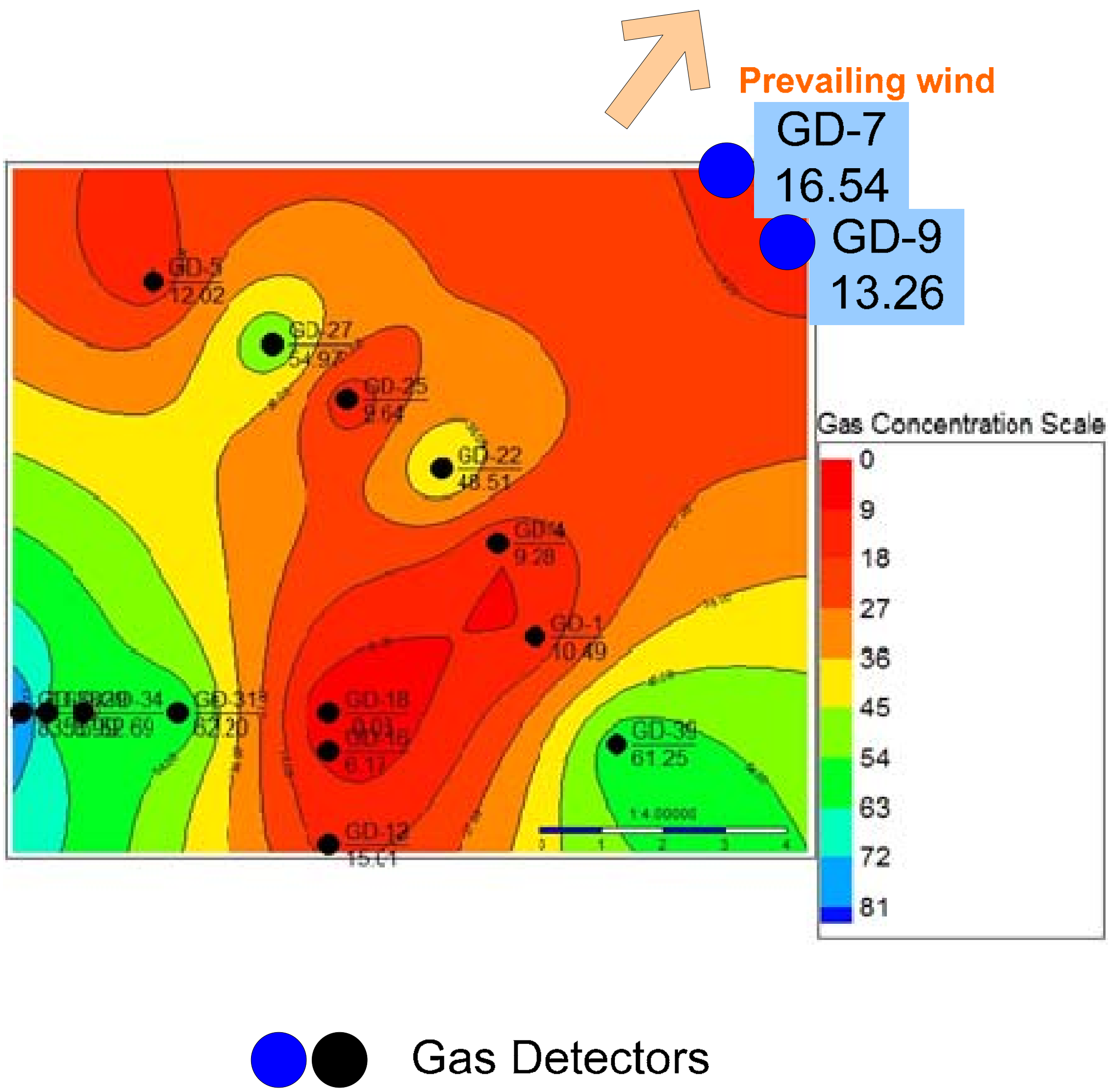

Figure 90. Foamglas maximum concentration contour at several gas detectors

7 CONCLUSIONS AND RECOMMENDATIONS

This section summarizes what findings that closed the gaps, and what new findings with regards to the application parameters.

7.1 HEX Application Rate and Containment Pit Effect

Forms the above experiment results discussion, the following conclusions are made:
NFPA 11:2005 international standard recommendations of the National Fire Protection Association, which confirms under section A6.14.2.1 that “discharge rates per unit area shall be established by test”. In addition, NFPA 11:2005 section A6.14.2 that “tests often give minimum application rates, as conducted under ideal conditions with no obstructions or barriers to control. The final design rates are generally 3-5 times the test rates” [27]. This detailed testing on LNG in association with BP and Texas A&M Emergency Services Training Institute has established that practical foam application rates of 10L/min/m² are effective on modern concrete LNG containment pits when LNG Turbex foam generators and Expandol high expansion foam concentrate at 3% induction rates are used on the tested containment pits. This is obtained based on the results that shows HEX application rate of 3.5L/min/m² under ideal (experiment) condition. This recommended practical rate of 10L/min/m² is 3 times the minimum effective experimental test rate of 3.5L/min/m².

The fire control time in Figure 43 has been defined as the time required achieving the 90% heat radiation. Figure 43 shows that the pool fire control time is reduced with increasing HEX application rate as expected, but this provides an important built in safety factor against unexpected adverse conditions at the time the systems are activated in an incident. It is clear that the foam controls the fire by blanketing the LNG pool surface thus the faster the blanketing time, the faster the foam controls the pool fire.

The 45 m^2 pit at twice the depth of the 65 m^2 pit (2.64 m versus 1.32 m) with no significant difference in LNG pool height of 6 inches in both pits showed different fire control behavior at the same 10L/min/m^2 application rate. The 45m^2 pit has significantly more hot concrete and hot LNG vapors to attack the foam and a seemingly more intense fire from the chimney effects which made it harder to control. Experiment results shows that it required more time for the foam to form an adequate depth, thus increasing the time to reduce heat radiation on the 45m^2 pit.

The location of foam generators around larger pits and relative to the wind direction is very important as big flames and excessive heat intensity may burn the generators and cause units to fail unless the foam generators have been specifically designed and tested to withstand these tough conditions. Develop a fence of foam generator could be a good solution to reduce foam transit distance, travel time, and time to achieve required depth.

Foam will stay on the surface of pool fire for a certain time (depending on the foam break down) so that even the foam flow is stopped, foam is still functioning and later foam addition will help reducing heat radiation further until maximum heat radiation reduction achieved.

It is important to design the LNG pool fire suppression system as one system. Containment dike should be designed to maximize the HEX application and vice versa. Separate design involving the two might bring drawbacks.

7.2 Expansion Foam

Expansion foam characteristics and behavior during its applications to suppress LNG vapor dispersion and pool fire are identified and studied. Vapor warming, ice formation, water boiling effects, and temperature profile are some of the fundamental parameters that could be used in future research in order to close the gaps. In addition, future experiments can be well prepared based on the experiences, equipments, and setups obtained from this research.

In addition, the following are concluded based this research:

- Expansion foam is able to suppress LNG vapor dispersion by increasing the temperature of the LNG vapor moving upward from the boiling LNG pool. However, some of the LNG vapor are warmer and reach the positive buoyancy after expansion application but not all. Thus, conservative assumption should be used in applying this principle.
- Expansion foam is able to suppress LNG pool fire by providing insulation above LNG pool surface and water content in the foam absorbed the heat from the fire. The required effective depth is determined by the layer in which the temperature is at water boiling temperature.
- Expansion foam-controlled LNG pool fire can be extinguished by using dry chemical.
- The 65m^2 containment pit requires 10 L/min/m^2 of application rate and expansion depth of 7.5 ft is sufficient to warm LNG vapor thus increase the LNG vapor density.
- Expansion foam application not only increases the density but also reduce the amount of vapor coming out of the expansion foam layers. The experiment shows 6% to 29% of concentration reduction. This information should be studied in more detail with another field experiment.

- The $65m^2$ containment pit requires 10 $L/min/m^2$ of application rate with continuous application to reach an effective depth of 3.5 ft.
- Expansion foam reduces the heat flux by 90% and reduced the 5 kW/m^2 distance by 43%.

7.3 Foamglas® PFS

Based on the detailed experiment setup, procedures, analysis, and comparison with other suppression methods, the following conclusions and recommendations are obtained.

Foamglas® PFS is able to suppress LNG pool fire. The system provides the following benefits:

- Foamglas® PFS was rapidly installed. During the experiment, installation required one $minute/m^2$ when done by up to four people (in the pit and outside the pit).
- Foamglas® PFS was effective in suppressing LNG pool fire. The performance of Foamglas® PFS is comparable, if not superior, to continuous application of expansion foam at an application rate of $10L/min/m^2$ when suppressing LNG pool fire in a 65 m^2 pit. These conclusions are based on the use of one layer of PFS units, with an additional 17% distributed in a second layer of coverage suppressing a pool fire with eleven inches of LNG, compared to expansion foam covering five inches of LNG. The second layer protected the polyethylene green bag on the first layer of Foamglas from burning. Therefore, intuitively, double layers of Foamglas®PFS (15 inches) will likely provide superior results. This may also help maintain its effectiveness (as additional safety factors when used in industry) during inclement weather (rain, etc).
- Consistent coverage provided by Foamglas® PFS stabilized the fire with no fluctuations observed during the suppression. It does not depend on any additional procedure or supplemental application during the fire.

- The experimental data shows that the fire control time on the 65 m^2 pit was less than ten seconds. An additional ten seconds were required to completely extinguish the LNG pool fire with a 1200 lb wheeled-unit dry chemical.

As expected, Foamglas®PFS may not be ideal for the control of LNG vapor dispersion. This was based on the data shown by the pit temperature profile, hydrocarbon camera, and gas detectors data and comparison with un-mitigated LNG continuous spill and expansion foam suppression method data. While the suppression method should be able to create positive buoyancy for LNG vapor, Foamglas® PFS did not provide enough heat to warm the LNG vapor. Foamglas® PFS may reduce heat from solar radiation, but it was not significant enough to suppress LNG vapor dispersion.

It is recommended to install both expansion foam and Foamglas® PFS in order to achieve maximum protection during LNG vapor dispersion and LNG pool fire.

7.4 Future Works

This section explains the limitations on the measurement, validation, and statistical problems that are encountered. While some of the gaps are identified, some of the findings in this research provide a stepping stones for the future results in order to close the gaps. There are several limitations in these experiments, as follows:

- Due to the gas detectors setup with time lag of around 3 minutes, the time to measure the gas concentration should be increased.
- More gas detectors should be installed above the expansion foam layer and above the pit. This is to create a gas concentration profile before and after expansion foam application. This information is useful for expansion foam effectiveness analysis and for future CFD simulation.
- More gas detectors with lower level concentration measurement (100% LFL) should be used in further distance from the containment pit. The modified gas detectors used in this experiment might not be good for very low concentration.

- Radiometers were successfully installed during the last experiment. Thus, future experiment must incorporate radiometers in measuring the heat flux profiles. In addition, the maximum heat flux of the fire can be measured with the same system setup as well.
- LNG level measurement with thermocouples is one of the best ways to measure evaporation rate of LNG. This research employs two sets of thermocouples level measurement (total of 12) with a distance of 1 inch in between thermocouples. Future experiment should have at least 0.5 inch or less to measure the LNG level more accurately.
- Foamglas® PFS experiment should use radiometers to ensure the heat flux reduction is quantified based on experiment.

One of the gaps in expansion foam research is that expansion foam application cannot be simulated as it is a complex phenomenon. Currently, computational fluid dynamics (CFD) is increasingly applicable in LNG safety area. Thus, the application of CFD to predict the LNG vapor dispersion and pool fire exclusion hazards is inevitable. While simulating the free vapor dispersion and pool fire without mitigation system is important, it is also necessary to simulate the hazards when the mitigation is applied. Thus, some of the characteristics of the LNG vapor after expansion foam application should be identified.

This research identifies that evaporation rate during vapor dispersion and pool fire is reduced. While evaporation rate measurement was attempted and experimental setup is identified, there is a need to improve the experiment to determine the evaporation rate. The data is very helpful to characterize the LNG characteristics in detail then being used as input to the simulation tools such as CFD.

This research produces many data that could be analyzed in many different ways as well. Heat transfer calculation or modeling has not been done in this research. Thus, future works must include more thorough measurement by improving the experiment. Then, heat transfer in the expansion foam is modeled so it can be used for industrial scaling up where the possible release is larger than release used in this experiment. Heat transfer is also useful in determining the minimum required depth to reach effective suppression.

In the end, this research is expected to help LNG industry by advancing the current guidelines in suppressing LNG vapor dispersion and pool fire.

REFERENCES

[1]. Center for Liquefied Natural Gas, Filling the supply/demand gap, www.lngfacts.org, accessed on June 9, 2008.

[2]. C.D. Zinn, LNG codes and process safety, Process Safety Progress, 3(2005), 158-167.

[3]. Y. Qiao, H.H. West, M.S. Mannan, D.W. Johnson, and J.B. Cornwell, Assessment of the effects of release variables on the consequences of LNG spillage onto water using FERC models, Journal of Hazardous Materials, 1-2 (2006), 155-162.

[4]. J. Alderman, Introduction to LNG safety, Process Safety Progress, 3(2005), 144-151.

[5]. National Fire Protection Association, NFPA 11 Standard for low-, medium-, and high-expansion foam, (2002).

[6]. University Engineers Inc, Control of LNG spill fires on land, (1973).

[7]. University Engineers Inc, LNG fire control, fire extinguishment and vapor dispersion tests, (1972).

[8]. K. Takeno, T. Ichinose, K. Tokuda, R. Ohba, K. Yoshida, and K. Ogura, Effects of high expansion foam dispersed onto leaked LNG on atmospheric diffusion of vaporized gas, Journal of Loss Prevention in Process Industries, 2(1996), 125-133.

[9]. A.L. Bror Persson, Henry Perrson, Dave Mulligan, Antonio Lancia, Micaela Demichela, Foamspex-Large scale foam application - modeling of foam spread and extinguishment, SP Swedish National Testing and Research Institute Report 2001:13, (2001).

[10]. Y. Lev, Novel method for controlling LNG pool fires, Fire Technology, 4(1981), 275-284.

[11]. S. Fred and B. Adams, Principles of foam fire fighting. Stillwater, Oklahoma. 74078, Fire Protection Publications, Oklahoma State University, (2003).

[12]. S.P. Woodworth and J.A. Frank, Fighting fires with foam, Van Nostrand Reinhold, New York, (1994).

[13]. P.K. Raj, Large LNG fire thermal radiation - modeling issues and hazard criteria revisited, Process Safety Progress 3(2005), 192-202.

[14]. P.K. Raj, LNG fires: A review of experimental results, models and hazard prediction challenges, Journal of Hazardous Materials, 3(2007), 444-464.

[15]. P.W. Parfomak and A.S. Vann, Liquefied Natural Gas (LNG) Import terminals: siting, safety, and regulations. Congressional Research Service (CRS) report for congress, RL32205, (2007).

[16]. K. Zuber, LNG facilities — engineered fire protection systems, Fire Technology, 1(1976), 41-48.

[17]. L.E. Brown, H.R. Wesson, and J.R. Welker. Thermal radiation from LNG fires and LNG fire suppression, in: Proceeding of the 3rd Conference on Natural Gas Research and Technology, (1974).

[18]. D.P. Nolan, Handbook of fire and explosion protection engineering principles for oil, gas, chemical, and related facilities. Noyes publications, New Jersey, (1996).

[19]. H.R. Wesson, J.R.Welker, and L.E. Brown, Control LNG spill fires, Hydrocarbon Processing, 12(1972), 61.

[20]. N.F.P. Association, NFPA 11 Standard for low-, medium-, and high-expansion foam, (2002).

[21]. A.L. Bror Perrson, Henry Persson FOAMSPEX: Large scale foam application - modeling of foam spread and extinguishment, Fire Technology, (2003), 347-362.

[22]. University Engineers Inc, LNG vapor dispersion and fire tests, University Engineers Inc, Norman, Oklahoma, (1971).

[23]. J.R. Welker, H.R. Wesson, and L.E. Brown, Use of foam to disperse LNG vapors, Hydrocarbon Processing, 2(1974), 119-120.

[24]. www.honeywellanalytics.com, accessed on June 9, 2008.

[25]. www.flirthermography.com, accessed on June 9, 2008.

[26]. Omega Engineering, www.omega.com, accessed on June 9, 2008.

[27]. National Fire Protection Association, NFPA 11 Standard for low-, medium-, and high-expansion foam, (2005).

[28]. C.L. Tien, K.Y. Lee, and A.J. Stretton, Radiation heat transfer, in: P.J. DiNenno, D. Drysdale, C.L. Beyler, W.D. Walton, R.L.P. Custer, J. John R. Hall, and J. John M. Watts (Editors), SFPE Handbook of fire protection engineering, National Fire Protection Association, Quincy, Massachusetts 02269, (2002), 1-73 - 1-88.

[29]. P.J. Rew, W.G. Hulbert, and D.M. Deaves, Modelling of thermal radiation from external hydrocarbon pool fires, Trans IChem E, 75 part B(1997), 81-89.

[30]. R. Barron, Cryogenic heat transfer, Taylor & Francis, Philadelphia, (1999).

[31]. H. Malvos and P.K. Raj, Thermal emission and other characteristics of large liquefied natural gas fires, Process Safety Progress, 3(2007), 237-247.

[32]. F. Briscoe and P. Shaw, Spread and evaporation of liquid, Progress in Energy and Combustion Science, 2(1980), 127-140.

VITA

Jaffee Arizon Suardin was born in Palembang, South Sumatera, in Indonesia. He obtained his Bachelor of Science degree in chemical engineering in October 2002 from Institut Teknologi Bandung (ITB) in Indonesia. He continued his studies at Texas A&M University (TAMU) in College Station and joined the Mary Kay O'Connor Process Safety Center in January 2004 where he began conducting research under the guidance of Dr. Sam Mannan. His master degree research involved the integration of Dow's Fire and Explosion Index into process design and optimization. He graduated with a Master of Science degree in chemical engineering in August 2005. He started his Ph.D. degree in Fall 2005 with the study of LNG vapor dispersion and pool fire mitigation technology using high expansion foam and Foamglas®PFS.

In addition to conducting research in process safety area, he has been involved in several industrial projects including leading HAZOP team, developing P&ID and PFDs, and performing consequence modeling. He interned with Shell International Exploration and Production (SIEP) of Shell Oil Company in summer 2006 and 2007 where he conducted projects in fire and explosion assessment on FPSO and action tracking system. In addition, he developed Dow Fire and Explosion and Chemical Exposure Indices software which was used in senior project in a process design class at TAMU. This program was developed in collaboration with Dow Chemical and AIChE and will be published as free software in the near future. He was the instructor for AspenPlus process design software for undergraduates at Artie McFerrin Department of Chemical Engineering.

Dr. Suardin is employed with Shell International Exploration Production of Shell Oil Company located at 200 N Dairy Ashford, Houston, Texas, 77084. He may be reached at jaffeesuardin@gmail.com or Jaffee.suardin@live.com.